STUDIES IN MICROWAVE SPECTROSCOPY

Thesis by

James Nelson Shoolery

In Partial Fulfillment of the Requirements

For the Degree of

Doctor of Philosophy

California Institute of Technology

Pasadena, California

1952

ACKNOWLEDGMENTS

It is a great pleasure to acknowledge the constant friendly advice and helpful discussions of Professor Don M. Yost, with whom my association has been a never failing source of inspiration. I am also grateful to Professor William D. Gwinn of the University of California for introducing me to the field of microwave spectroscopy and for his continued encouragement throughout the course of this work.

For the enthusiastic cooperation of Dr. Robert G. Shulman in the task of recording and interpreting the spectral data I wish to express my sincere appreciation. Thanks are also due Professors W. H. Pickering and H. V. Neher and Mr. Bart Locanthi, who contributed to the success of this venture through valuable counsel concerning electronic problems.

I am deeply grateful to the Research Corporation, without whose grant in aid the construction of the apparatus would not have been possible, and to the General Electric Company for the award of a Gerard Swope Fellowship for the year 1950 - 1951.

ABSTRACT

The theory of microwave spectroscopy is first presented in some detail. Following this, sources of errors in structure determinations based on moment of inertia data are considered, and approximate equations for estimating their effects are derived.

A microwave spectroscope has been assembled and its design, construction, and operation are discussed. Microwave spectra in the region from 20 to 25 kmc have been obtained for $HN^{14}C^{12}O^{16}$, $HN^{15}C^{12}O^{16}$, and $DN^{14}C^{12}O^{16}$. A rotational constant obtained from an infrared study of HNCO by L. H. Jones is combined with the microwave data to yield the interatomic distances and bond angle. High resolution studies of the spectra of HNCO and HNCS permit evaluation of their electric quadrupole coupling constants and qualitative deductions concerning their structures to be made. The molecular species $CF_3-C\equiv C-H$, $CF_3-C^{13}\equiv C-H$, $CF_3-C\equiv C^{13}-H$, and $CF_3-C\equiv C-D$ have been observed to absorb in the microwave region, and from the frequencies of these absorptions the $C\equiv C$ and C-H distances are determined. In addition, the measured moments of inertia are employed to calculate consistent sets of the remaining three parameters in $CF_3-C\equiv C-H$. The application of the electron diffraction data of W. F. Sheehan, Jr., to this problem to determine which set of parameters actually represents the structure is described. Stark effect measurements are presented which determine the dipole moments of $HN^{14}C^{12}O^{16}$ in three vibrational states and of DNCO, OCS, H_2CO, CHF_3, and $CF_3-C\equiv C-H$ in their ground states. Finally, attempts to obtain microwave spectra for several other compounds are briefly described.

TABLE OF CONTENTS

I. GENERAL THEORY OF PURE ROTATIONAL SPECTRA.

Pure rotational spectra for only a few very light molecules had been observed prior to World War II. The development of microwave radar during the war had a profound effect on the field of spectroscopy, because it opened up a new region of the spectrum which had been reached previously only by the pioneering work of Cleeton and Williams (1), who used semi-optical methods to detect a broad absorption band in ammonia at 1.25 $cm.^{-1}$

Insofar as the term is applied to pure rotational spectra, microwave spectroscopy has come to mean the detection and measurement of a sharp line absorption spectrum due to molecular transitions from one allowed state to another, during which only the mode of rotation changes. Detection is accomplished by passing microwave energy through the substance contained in a rectangular cell and measuring the attenuation as a function of frequency. A monochromatic, single phase source of energy allows the use of a tuned detector and results in a resolving power 100,000 times better than that of the best infrared grating instrument. Frequency measurements can be made electronically to one part in 10^7.

During its brief but eventful existence, the field of microwave spectroscopy has become a beehive of activity. No less than thirty spectroscopes were in operation at the last count, and untold numbers were under construction. Spectra have been obtained for several score of compounds, and from most of these it has been possible to obtain useful structural information. A description of early work in the field is contained in two excellent reviews (2,3) of the subject. The remainder of this section will be concerned with the systematic treatment of the pure rotational spectra of molecules.

1. THE RIGID ROTOR.

Let us consider a rigid, rotating molecule consisting of two atoms a fixed distance, r, apart. For a system with no external forces, for example, a molecule suspended in free space, the axis of rotation passes through the center of mass. The kinetic energy of the molecule is given by

$$T = \tfrac{1}{2} I\omega^2 = P^2/2I \ , \qquad (1\text{-}1)$$

where ω is the angular velocity of the molecule with respect to a principal axis through the center of mass, I is the moment of inertia about this axis, and P is the angular momentum about the same axis. Since the potential energy of such a rigid rotor may be set equal to zero, the wave equation for the system is

$$\left\{P^2/2I\right\} \Psi(\theta,\phi) = E\, \Psi(\theta,\phi) \qquad (1\text{-}2)$$

in which $\Psi(\theta,\phi)$ is a probability amplitude function for finding the line joining the atoms oriented at angles θ and ϕ with respect to space fixed axes. The square of the total angular momentum may be written in operator form as

$$P^2_{op} = -\hbar^2 \left\{ \frac{1}{\sin\theta} \frac{\partial}{\partial\theta} \left(\sin\theta \frac{\partial}{\partial\theta}\right) + \frac{1}{\sin^2\theta} \frac{\partial^2}{\partial\phi^2} \right\} . \qquad (1\text{-}3)$$

Therefore,

$$\frac{-\hbar^2}{2I} \left\{ \frac{1}{\sin\theta} \frac{\partial}{\partial\theta} \left(\sin\theta \frac{\partial\Psi}{\partial\theta}\right) + \frac{1}{\sin^2\theta} \frac{\partial^2\Psi}{\partial\phi^2} \right\} = E\,\Psi . \qquad (1\text{-}4)$$

Equation (1-4) can be solved by separation of the variables and subsequent application of the polynomial method. The final result is that the series for Ψ is finite only for certain values of the energy of the rotor,

namely

$$E = \hbar^2 J(J+1)/2I . \qquad J = 0,1,2, \cdots . \tag{1-5}$$

The quantity $h/8\pi^2 cI$ is conventionally called B, and

$$E/hc\ (cm^{-1}) = BJ(J+1) . \tag{1-6}$$

The complete, normalized, rotational wave function is

$$\Psi(\theta,\phi) = \left(\frac{1}{2\pi}\right)^{1/2} \left\{\frac{(2J+1)(J+|M|)!}{2(J+|M|)!}\right\}^{\frac{1}{2}} P_J^M(\cos\theta)\, e^{iM\phi}, \tag{1-7}$$

where the $P_J^M(\cos\theta)$ are the associated Legendre functions, and J and M are quantum numbers.

Eigenvalues of P^2 and P_z are easily obtained. The square of the total angular momentum, P^2, is given by

$$P^2 = J(J+1)\hbar^2 . \tag{1-8}$$

The component of angular momentum along the space fixed Z axis is

$$P_z = M\hbar . \tag{1-9}$$

2. THE SYMMETRIC TOP.

A symmetric top molecule is one in which two of the principal moments of inertia are equal. The kinetic energy of rotation of a symmetric top is given by

$$T = P_x^2/2I_{xx} + P_y^2/2I_{yy} + P_z^2/2I_{zz} , \tag{2-1}$$

where x, y, z are the directions of the principal axes. Let us designate the x direction as the one for which the moment of inertia is unique. The projection of angular momentum along the x axis is quantized and is

$$P_x = K\hbar . \qquad K = 0,1,2, \cdots . \tag{2-2}$$

The square of the total angular momentum is given by

$$P_x^2 + P_y^2 + P_z^2 = J(J+1)\,\hbar^2 . \qquad (2\text{-}3)$$

If $I_{yy} = I_{zz}$, then

$$T = K^2\hbar^2/2I_{xx} + \left\{J(J+1) - K^2\right\}\hbar^2/2I_{zz} . \qquad (2\text{-}4)$$

The three principal axes in molecules are labeled the a, b, c axes in order of increasing moment of inertia. The quantities $A \geqslant B \geqslant C$ are defined as

$$A = h/8\pi^2 cI_{aa} \; ; \; B = h/8\pi^2 cI_{bb} \; ; \; C = h/8\pi^2 cI_{cc} .$$

If x corresponds to a, then C equals B, the rotor is prolate, and

$$E/hc = BJ(J+1) + (A-B)K^2 . \qquad (2\text{-}5)$$

If x corresponds to c, then A equals B, the rotor is oblate, and

$$E/hc = BJ(J+1) + (C-B)K^2 . \qquad (2\text{-}6)$$

By writing the Hamiltonian for the symmetric top in terms of a set of Eulerian angles defining the orientation of principal axes in the body with respect to axes fixed in space, we can solve the wave equation, $H\Psi = E\Psi$, for the symmetric top eigenfunctions. Such a calculation yields the following expression for Ψ:

$$\Psi_{JKM} = N_{JKM}\, F(x)\, x^{\frac{1}{2}|K-M|}\, (1-x)^{\frac{1}{2}|K+M|}\, \exp(iM\Psi + iK\phi) , \qquad (2\text{-}7)$$

where $x = \frac{1}{2}(1 - \cos\theta)$, and $F(x)$ and N_{JKM} are defined in Pauling and Wilson (4), p. 278. The angle θ is the angle between the space fixed Z and molecule fixed z axes, ϕ is the angle between the space fixed X axis and the line of nodes, and Ψ is the angle from the line of nodes to the molecule fixed x axis.

3. THE ASYMMETRIC ROTOR.

Molecules in which all three moments of inertia are different are

called asymmetric rotors. The energy levels of the asymmetric rotor cannot be represented by an explicit formula analogous to that for the symmetric top. Qualitatively, the energy levels of the asymmetric rotor may be considered to lie somewhere between the levels for the limiting prolate symmetric top ($B \rightarrow C$) and those for the limiting oblate symmetric top ($B \rightarrow A$). This is shown quite clearly on p. 45 of Herzberg II (5). There are $J + 1$ levels having the same value of J but with different values of K in the symmetric top, each level except $K = 0$ being doubly degenerate. This degeneracy is removed in the asymmetric rotor and $2J + 1$ levels appear for each value of J. For slightly asymmetric rotors the quantum number K still is approximately defined, and the levels appear as essentially symmetric top energy levels, each split into two levels except for $K = 0$. As the degree of asymmetry increases, the quantum number K loses all physical meaning and the $2J + 1$ levels are denoted simply by a subscript τ, which runs from $-J$ to $+J$ in order of increasing energy. τ is defined as K(prolate) minus K(oblate) and the asymmetric top levels are designated by the notation $J_{K_p,K_o;\tau}$. Thus, for $J = 3$, the level connecting $K_p = 1$ in the limiting prolate rotor with $K_o = 2$ in the limiting oblate rotor is $3_{1,2;-1}$; this is the third level from the bottom on the energy scale for $J = 3$.

In order to obtain the energy levels of the asymmetric rotor we must solve the wave equation

$$H\Psi = E\Psi. \tag{3-1}$$

The wave function, Ψ, may be expanded in terms of a complete orthonormal set of functions. The symmetric rotor eigenfunctions are such a set. Hence

$$\Psi = \sum_{JKM} a_{JKM} \Psi^{o}_{JKM}, \tag{3-2}$$

where the Ψ°_{JKM} represent the symmetrical top eigenfunctions for the appropriate limiting symmetric top. Substitution of (3-2) in (3-1) yields

$$\sum_{JKM} a_{JKM} (H-E) \Psi^{\circ}_{JKM} = 0 . \qquad \begin{array}{l} J = 0,1,2, \cdots . \\ K = 0,1,2, \cdots J . \\ M = -J \cdots\cdots J . \end{array} \qquad (3\text{-}3)$$

From the orthonormality of the Ψ°'s, multiplication by $\Psi^{\circ *}_{J'K'M'}$ and integration over the space of the function gives

$$\sum_{JKM} a_{JKM} (H_{J'K'M' ; JKM} - E \, \delta_{J'K'M' ; JKM}) = 0 . \qquad (3\text{-}4)$$

If the set of equations (3-4) is to have a non-trivial solution for the a_{JKM}, the determinant of the coefficients must equal zero. Wang (6) has given the Hamiltonian operator for an asymmetric rotor in the Eulerian angle system previously defined. On carrying out the integrals $H_{J'K'M';JKM}$ he found that the only integrals which are not zero are those for which $J' = J$ and $M' = M$; therefore, the secular equation factors into an infinite number of finite determinants, each $2J + 1$ on a side. The general form of the secular equation is

		J = 0	J = 1		J = 2	
J = 0		$H_{00}-W$	K = 1	K = 0	K = -1	
	K = 1	$H_{11}-W$	H_{10}	$H_{1,-1}$		
J = 1	K = 0	H_{01}	$H_{00}-W$	$H_{0,-1}$		
	K = -1	$H_{-1,1}$	$H_{-1,0}$	$H_{-1-1} - W$	K = 2	K = 1
				K = 2	$H_{22}-W$	H_{21} --
				K = 1	H_{12}	$H_{11}-W$ \
J = 2					⋮	⋱ .

Furthermore, Wang found that only diagonal and two off the diagonal terms

are different from zero. The energy levels of the asymmetric rotor are given by

$$E/hc = \tfrac{1}{2}(B + C)J(J + 1) + \left\{A - \tfrac{1}{2}(B + C)\right\} W_\tau , \quad (3\text{-}5)$$

where the W_τ's are the $2J + 1$ solutions to the secular determinant for the particular J value. These secular determinants have been factored still further by Nielsen (7) into algebraic equations (four for $J > 2$) and listed by Herzberg (5, p. 46) up to $J = 6$.

4. SYMMETRY PROPERTIES OF THE ROTATIONAL EIGENFUNCTIONS.

A. The Rigid Rotor.

A parity operator, R, may be introduced in quantum mechanics; it is defined as an operator that reflects all coordinates of all particles through the origin. Since the Hamiltonian is left unchanged by such a reflection for the case of rotating molecules in field free space, the operators R and H commute; consequently, the energy eigenfunctions are simultaneously eigenfunctions of R, and R is a constant of the motion. Hence

$$R\Psi = r\Psi \qquad \text{and} \qquad R^2\Psi = r^2\Psi = \Psi .$$

$$r^2 = 1 \quad ; \qquad R\Psi = \pm\Psi .$$

A reflection is obtained by replacing θ by $\pi - \theta$ and ϕ by $\pi + \phi$. The rigid rotor eigenfunctions remain unchanged if J is even and change sign if J is odd. For Σ_g^+ electronic states the total eigenfunction has the symmetry of the rotational eigenfunction, and the levels of even J are labeled $+$, while those of odd J are labeled $-$.

Symmetry selection rules for dipole radiation are obtained by calculating the matrix elements of the dipole moment. These are of the form:

$$\int \Psi_n^* M_x \Psi_m \, d\tau .$$

Since M_x, M_y, and M_z change sign upon reflection at the origin, the product of Ψ_n^* and Ψ_m must also change sign if the transition is to have a non-vanishing intensity. We obtain the selection rules: $+ \leftrightarrow +$, $+ \leftrightarrow -$, $- \leftrightarrow +$, $- \leftrightarrow -$.

In the case of a homonuclear diatomic molecule we could define an operator which interchanges only the identical nuclei. As before, the total eigenfunction either remains unchanged or changes its sign for such a symmetry operation; it is said to be symmetric or antisymmetric in the nuclei. The Pauli exclusion principle requires that the total wave function (including nuclear spin) be symmetric or antisymmetric in the nuclei, depending upon whether the nuclei follow Bose or Fermi statistics. For $\sum_g^+$ electronic states the wave function (exclusive of nuclear spin) for levels with even J is symmetric and for those with odd J is antisymmetric. In the case of spinless nuclei the nuclear spin wave function is symmetric and the nuclei follow Bose statistics; consequently, only levels of even J appear. If the nuclei have spin I, the ratio of symmetric to antisymmetric spin functions is $(I + 1)/I$; therefore, states with even and odd J have different statistical weights. A very strict selection rule prohibiting transitions between states other than those with the same symmetry in the nuclei results in an alternation of intensities of the observed spectral lines. Since homonuclear diatomic molecules do not possess a dipole moment, they do not absorb microwave or infrared radiation, so that the phenomenon would appear to be of little interest. However, an entirely analogous but more complicated situation arises in symmetric top molecules, leading to an observable intensity alternation in lines of the

same J and different K, the statistical weights of the different K levels depending upon the symmetry of the molecule and the spin of the identical nuclei interchanged by the rotation about the symmetry axis.

B. The Symmetric Top.

As in linear molecules the total eigenfunctions have the symmetry properties + or - . However, in a non-planar molecule an inversion at the center of mass produces a configuration which cannot also be obtained by a simple rotation. There are two modifications of the molecules which cannot be transformed into one another except by passage through a potential barrier. If, as in most molecules, this barrier is very high, the molecules will remain for the most part in one or the other of the configurations. However, there is a certain probability of finding a given molecule in either of the two configurations, and this gives rise to a slight splitting into two energy levels. The eigenfunctions for the system are symmetric and antisymmetric linear combinations containing equal contributions of the eigenfunctions for the left and right handed forms; therefore, the symmetric top energy levels are split into two closely spaced levels, one of which is + and the other - . This splitting is nearly always unresolved and the symmetry property is of little consequence, since there are always + and - levels nearly coincident.

C. The Asymmetric Top

Each level of the asymmetric rotor has an overall symmetry designation of + or - . The usual symmetry selection rule, $+ \leftrightarrow -$, holds but is not very important in molecules with inversion doubling. It is of interest to consider the symmetry properties of just the rotational

part of the asymmetric rotor eigenfunctions. Mulliken (8) has used group theory to obtain the following results.

There exists an internal rotation group due to the symmetry of the momental ellipsoid. Two fold rotations of the internal axis system, x, y, z, about the three principal axes, a, b, c, result in eigenfunctions which are unchanged or change sign. The character table for the internal rotation group, known as the Group V, is given below.

Table I. Character table for the Group V.

	E	C_2^c	C_2^b	C_2^a	Symmetry Operation
A	1	1	1	1	
B_c	1	1	-1	-1	
B_b	1	-1	1	-1	
B_a	1	-1	-1	1	

Here, a, b, c are the usual labels for the principal axes.

All asymmetric rotor eigenfunctions belong to one of the species of the Group V. They may be correlated with the evenness or oddness of the quantum numbers K_a and K_c in the limiting prolate and oblate rotors, as shown in Table II below.

Table II. Classification of Asymmetric Rotor Levels.

Species	K_a(prolate)	K_c(oblate)
A	even	even
B_a	even	odd
B_b	odd	odd
B_c	odd	even

The orientation of the permanent electric dipole moment with respect to the principal axes determines between which levels transitions may occur. The matrix elements of the transition will be zero unless the product of the characters for the initial and final wave functions and the component of the dipole moment be + 1 for each of the group operations. The components of the dipole moment along the axes a, b, and c belong respectively to the species B_a, B_b, and B_c of the Group V. Table III gives the direction of the electric moment permitting transitions between states belonging to the various representations of the Group V.

Table III. Symmetry selection rules

Rep.	A (ee)	B_a (eo)	B_b (oo)	B_c (oe)
A (ee)	-	a	b	c
B_a (eo)	a	-	c	b
B_b (oo)	b	c	-	a
B_c (oe)	c	b	a	-

5. SELECTION RULES FOR J, K, AND M.

The electric moment of a diatomic molecule is directed along the line joining the two atoms. If M_o is the constant dipole moment, the three components along the space fixed axes X, Y, Z are: $M_x = M_o \sin\theta \cdot \cos\phi$, $M_y = M_o \sin\theta \sin\phi$, and $M_z = M_o \cos\theta$. The matrix elements of the dipole moment for the transition $J'M' \rightarrow J''M''$ are accordingly

$$R_x^{J',M';J'',M''} = M_o \int \psi^{J',M'*} \sin\theta \cos\phi \quad \psi^{J'',M''} \sin\theta d\theta \, d\phi ,$$

$$R_y^{J',M';J'',M''} = M_o \int \psi^{J',M'\,*} \sin\theta \sin\phi \; \psi^{J'',M''} \sin\theta \, d\theta \, d\phi,$$

$$R_z^{J',M';J'',M''} = M_o \int \psi^{J',M'\,*} \cos\theta \; \psi^{J'',M''} \sin\theta \, d\theta \, d\phi.$$

The integrals involving ϕ vanish unless $M'' = M'$ for R_z and $M'' = M' \pm 1$ for R_x or R_y. This leads to the selection rule

$$\Delta M = 0, \pm 1 .$$

The integrals involving θ can be shown to vanish except when $J'' = J' \pm 1$; therefore

$$\Delta J = \pm 1 .$$

Similar considerations for the more complicated case of a symmetric top yield the result that for an accidentally symmetric top the selection rules are

$$\Delta J = 0, \pm 1 \quad ; \quad \Delta K = 0, \pm 1 \quad ; \quad \Delta M = 0, \pm 1 .$$

The quantum number K has lost its significance in asymmetric tops. However, transitions for which ΔK (prolate), ΔK (oblate), or both are greater than ± 1 generally occur with reduced intensities. The selection rules

$$\Delta J = 0, \pm 1 \quad ; \quad \Delta M = 0, \pm 1$$

still hold as in symmetric tops.

6. THE NON-RIGID ROTOR.

Molecules are capable of executing vibrations which, although not strictly a simple harmonic motion, are to a good approximation simple harmonic vibrations. A generally satisfactory description which takes account of the slight deviation from harmonicity is the Morse function (9) for the potential energy.

$$U(r) = D\left\{1 - \exp\left(-a\left[r - r_e\right]\right)\right\}^2. \qquad (6\text{-}1)$$

If the wave equation for the diatomic rotor is solved with the Morse function for the potential energy the following expression for the term values is obtained.

$$E/hc\ (cm^{-1}) = (v + \tfrac{1}{2})\omega_e - x_e\omega_e(v + \tfrac{1}{2})^2 + J(J + 1)B_e \qquad (6\text{-}2)$$
$$- D_e J^2(J + 1)^2 - \alpha_e(v + \tfrac{1}{2})J(J + 1) + \cdots\cdots$$

in which some higher terms have been neglected. The vibrational quantum number, v, may take all positive integral values including zero. The first two terms of (6-2) are the vibrational term value for a harmonic oscillator and the anharmonic correction term. We shall not be concerned with these in the pure rotation spectra. The remaining three terms represent respectively the rotation of a non-rigid rotor at the equilibrium distance, the correction for centrifugal distortion of the rotor, and the correction for the interaction of rotation and vibration. D_e can be shown to be $4B_e^3/\omega^2$, where ω is the energy of the vibration expressed in cm^{-1}. It is generally so small that its effect on the energy levels is nearly negligible. We may rewrite (6-2) as

$$E/hc = F(J) = B_v J(J + 1) - D_e J^2(J + 1)^2, \qquad (6\text{-}3)$$

where

$$B_v = B_e - \alpha_e(v + \tfrac{1}{2}), \qquad (6\text{-}4)$$

and the terms involving only vibration have been dropped.

B_v represents an average value of the reciprocal moment of inertia over a complete vibration. Even for a harmonic vibration the mean value of $1/r^2$ is not equal to $1/r_e^2$, even though the mean value of r equals r_e.

Actually, $\overline{1/r^2}$ is slightly greater than $1/r_e^2$. In addition, if the vibration is anharmonic, we must expect B_v to be slightly smaller than B_e, since the average nuclear separation will be greater. In actual physical cases the anharmonic term is greater than the harmonic one.

In a symmetric or asymmetric rotor we expect the following relations to hold to a first approximation:

$$A_{[v]} = A_e - \sum_i \alpha_i^A (v_i + d_i/2),$$

$$B_{[v]} = B_e - \sum_i \alpha_i^B (v_i + d_i/2),$$

$$C_{[v]} = C_e - \sum_i \alpha_i^C (v_i + d_i/2),$$

where we have lumped together the effect of the different vibrations, each of degeneracy d_i, and let $[v]$ stand for the value of all vibrational quantum numbers.

In a non-rigid symmetric top there are terms due to the individual effect on the B values of centrifugal stretching caused by rotation about the axis of intermediate moment and about the figure axis. Slawsky and Dennison (10) have given the following equation for the energy levels:

$$F(J,K) = B_v J(J+1) + (A_v - B_v)K^2 - D_J J^2 (J+1)^2 - D_{JK} J(J+1)K^2 - D_K K^4 . \qquad (6\text{-}5)$$

Strictly speaking, equation (6-5) only represents the energy levels of a symmetric top when it is in a non-degenerate vibrational state. For a molecule vibrating in one mode of a degenerate vibration, the rotation about the figure axis results in Coriolis forces on the atoms which tend

to excite the other component of the vibration. This results in a net vibrational angular momentum about the symmetry axis of the top. Since the vibrational angular momentum may add to the molecular angular momentum in either a parallel or anti-parallel way, equation (6-5) must be modified to include such a term.

$$F(J,K,\zeta) = F(J,K) \mp 2A_v \zeta K \; ; \; -1 \leq \zeta \leq 1 \quad (6\text{-}6)$$

For the pure rotation spectrum $\Delta\zeta = 0$.

For symmetric top molecules the magnitude of the energy shifts in consequence of the centrifugal distortions due to non-rigidity depends upon J and τ as well as the force constants of the molecule. E. B. Wilson, Jr. (11) has devised a method of introducing this dependence into the secular equation for the energy levels. For all but the simplest molecules this method requires more knowledge than is usually available. In general, a correction for centrifugal distortion will not be necessary except in very light rotors for which the velocity of rotation is high, or, in the case of heavier molecules, for very high values of J.

From equations (6-3) and (6-5) and the selection rules $\Delta J = +1$, $\Delta K = 0$, we predict transitions from $J' \longrightarrow J$ at the following frequencies:

$$\nu \text{ (mc)} = 2B_{[v]}J - 4DJ^3 \text{ (linear molecules).}$$

$$\nu \text{ (mc)} = 2B_{[v]}J - 2D_{JK}JK^2 - 4D_JJ^3 \text{ (symmetric tops).}$$

Typical values of B_v which give spectra in the easily accessible microwave regions range from 2,000 to 15,000 mc. D_J and D_{JK} usually have values of only a few kilocycles.

7. ELECTRIC QUADRUPOLE EFFECTS.

The nucleus in its normal state is assumed to have an intrinsic

angular momentum $\hbar$. At low values of electric field strength the nuclear and rotational angular momenta add together in the following way to give the total angular momentum, F. $F = J + I, J + I - 1, J + I - 2, \cdots |J - I|$. Different values of F are associated with different orientations of the nuclear spin with respect to the rotational angular momentum of the molecule; therefore, different average values of the interaction energy arising from the electric quadrupole moment possessed by the nucleus and the gradient of the electric field along the internuclear axis of the molecule occur. Casimir (12) has treated the shift of the energy levels as a perturbation problem; for a molecule with one quadrupolar nucleus and with a symmetry axis he obtains

$$\Delta\nu = -eQ \left\langle \frac{\partial^2 V}{\partial Z^2} \right\rangle_J \frac{3}{4} \times \frac{C(C+1) - I(I+1)J(J+1)}{2IJ(2I-1)(2J-1)}, \quad (7\text{-}1)$$

where the various quantities are defined as follows:

Q represents the departure of the nuclear charge from spherical symmetry and is called the quadrupole moment.

$\left\langle \frac{\partial^2 V}{\partial Z^2} \right\rangle_J$ is the second derivative of the potential due to electrons and other nuclei, taken along the space fixed Z axis, averaged over the rotational state J, and evaluated at the quadrupolar nucleus.

$$C = F(F+1) - I(I+1) - J(J+1).$$

The entire term $eQ \left\langle \frac{\partial^2 V}{\partial Z^2} \right\rangle_J$ may be regarded as a scale factor for

the splitting of an energy level. It varies from a fraction of a megacycle to several hundred megacycles according to the quadrupole moment of the nucleus and the particular electronic and nuclear configuration in the molecule. The spectral frequencies of absorptions are computed by applying the selection rule $\Delta F = 0, \pm 1$ to the energy levels obtained from equation (7-1).

This treatment is based on the assumption that only elements of the perturbation matrix are important that are diagonal in J. This is a first order treatment. If the hyperfine splittings are not small compared with the separation of the unperturbed levels, then second order correction terms must be computed, using the perturbation theory.

Townes and Dailey (13) have presented an argument that only the p electrons in the bonds adjacent to the quadrupolar nucleus are important contributors to $\left\langle \frac{\partial^2 V}{\partial z^2} \right\rangle$. This appears to be a useful concept leading to qualitative conclusions about the nature of the chemical bonding (14) in molecules for which the hyperfine structure can be resolved.

8. THE STARK EFFECT.

A. Linear Molecules.

In the presence of an electric field along the space fixed Z axis the energy levels of a linear molecule are shifted, and the degeneracy between states with different values of the quantum number M is removed. The perturbation operator is $-\mu E \cos\theta$, with μ the permanent dipole moment directed along the molecule fixed z axis, E the electric field, and θ the angle between the two axes. The perturbation operator is a matrix diagonal in M, hence the M degeneracy need not be taken into

account; instead, the problem may be solved by the usual first order treatment for each value of M. The first order correction to the energy is given by

$$W_{JM}^{(1)} = \int \Psi_{JM}^{*} (- \mu E \cos \theta) \Psi_{JM} \sin \theta \, d\theta \, d\phi . \qquad (8\text{-}1)$$

The properties of the associated Legendre functions which appear in the Ψ_{JM} require the integral to vanish.

Second order perturbation theory (15) gives for $W_{JM}^{(2)}$

$$W_{JM}^{(2)} = \sum_{J' \neq J} \frac{\left| \int \Psi_{JM}^{*} (-\mu E \cos \theta) \Psi_{J'M} \sin \theta \, d\theta \, d\phi \right|^2}{W_{J'M} - W_{JM}} . \qquad (8\text{-}2)$$

If the electric field is parallel to the electric vector of the microwave radiation the quantum number M does not change.

$$\Delta \nu_{J \rightarrow J+1} = \frac{3M^2(16J^2 + 32J + 10) - 8J(J+1)^2(J+2)}{J(J+2)(2J-1)(2J+1)(2J+3)(2J+5)} \frac{\mu^2 E^2}{h^2 \nu_0} . \qquad (8\text{-}3)$$

If μE, the product of dipole moment and electric field, and ν_0, the unperturbed frequency, are known in megacycles, then $\Delta \nu$, the shift in frequency of the spectral line, will also be given in mc. The conversion factor from the usual units is: μE (mc) = .5032 μE (Debye units) (volts/cm).

B. Symmetric Top Molecules.

Symmetric top molecules possess a dipole moment directed along the unique symmetry axis. The perturbation operator is again $- \mu E \cos \theta$, and on account of the form of the symmetric top wave functions it is a matrix diagonal in K and M. Therefore, the degeneracy of the energy levels with respect to K and M need not be taken into account. First order

perturbation theory (15) has yielded the result

$$W_{JKM}^{(1)} = -(\mu E)\ KM/J(J+1)\,. \qquad (8\text{-}4)$$

Coles (3) has given the result of the second order calculation.

$$W_{JKM}^{(2)} = \frac{E^2\mu^2}{2B}\left\{\frac{\left[\frac{3K^2}{J(J+1)}-1\right]\left[\frac{3M^2}{J(J+1)}-1\right]}{(2J-1)(2J+3)} - \frac{M^2K^2}{J^3(J+1)^3}\right\}. \qquad (8\text{-}5)$$

Levels with K or M equal to zero have no first order Stark effect.

C. Asymmetric top molecules.

A perturbation operator is defined in the following way.

$$H^{(1)} = -E\sum_g \Phi_{Zg}\,\mu_g\,.$$

E is the electric field along the space fixed Z axis; g refers to the molecule fixed inertial axes, x, y, z; μ_g are components of the dipole moment along the principal axes; Φ_{Zg} are the direction cosines between space fixed Z axis and molecule fixed inertial axes.

In the non-degenerate case, the wave functions of the asymmetric rotor belong to the representations of the Group V. The direction cosines belong to the representation B_x, B_y, B_z for g = x, y, and z respectively. Non-vanishing matrix elements are obtained only if the product of the direction cosine and the wave functions for the connected states belongs to representation A. Consequently, there can be no first order Stark effect unless there is accidental degeneracy between two or more levels.

From second order perturbation theory

$$W^{(2)}_{J\tau M} = E^2 \sum_{J',\tau',g}{}' \frac{\mu_g^2 \left[(\Phi_{Zg})_{J\tau M;J'\tau'M} \right]^2}{W^0_{J\tau} - W^0_{J'\tau'}},$$

where the prime on the summation indicates that it extends only over those values of $J'\ \tau'$ for which $W^0_{J\tau}$ is not near $W^0_{J'\tau'}$. Values of (Φ_{Zg}) may be obtained from Tables of Line Strengths, published by Cross, Hainer, and King (16).

If accidental degeneracy occurs, then the perturbation treatment will result in a simple second degree secular equation to be solved. Golden and Wilson (17) have examined the possible cases of degeneracy and given the form of the Stark shifts. For degeneracy between states of the same J (limiting symmetric rotor degeneracy) they find

$$\Delta\nu_M = \pm F|M|E .$$

Between states of different J

$$\Delta\nu_M = \pm \left\{ G\sqrt{J'^2 - M^2} \right\} E ,$$

where F and G are coefficients independent of M, J' is the larger of the J's involved, $\Delta\nu_M$ is the shift in the frequency of the M^{th} Stark component from the unperturbed frequency, and E is the electric field.

Stark splittings for the electric fields applied in microwave spectroscopy are usually less than 100 megacycles.

9. THE ZEEMAN EFFECT.

There are at least three sources of permanent magnetic moments in molecules. A large magnetic moment of one or two Bohr magnetons may arise in a small number of stable gaseous compounds and in free radicals, due to the presence of unpaired electrons. Moments measured in nuclear magnetons are generated by the rotation of the whole molecule or may

arise from the presence of nuclei with intrinsic magnetic moments.

Usually all electron spins are paired and the nuclear spins are coupled to the rotation of the molecule. For a single spinning nucleus we describe the molecule by the quantum numbers JIFM. The application of a weak magnetic field leads to the total Hamiltonian given by C. K. Jen (18).

$$\mathcal{H} = \mathcal{H}_0 - g_{mole}\,\mu_0\,\vec{J}\cdot\vec{H} - g_N\,\mu_0\,\vec{I}\cdot\vec{H}\ ,$$

where g_{mole} is the gyromagnetic ratio of the molecule along J, g_N is the g-factor of the nucleus, μ_0 is the nuclear magneton, $\vec{J}$, $\vec{I}$ are vector operators of J and I, and H is the external magnetic field. The similarity to Russell-Saunders coupling in atomic spectra permits us to take over the applicable equations and write for the interaction energy

$$W = -M\,\mu_0\,H\left\{\alpha_J\,g_{mole} + \alpha_I\,g_N\right\}, \qquad (9\text{-}1)$$

where

$$\alpha_J = F(F+1) + J(J+1) - I(I+1)\,/2F(F+1)\,,$$

$$\alpha_I = F(F+1) + I(I+1) - J(J+1)\,/2F(F+1)\,.$$

It is usually most convenient to apply the external field parallel to the E-vector of the radiation. This leads to σ-transitions for which the selection rule $\Delta M = \pm 1$ holds.

There are three different possible situations. These are: (1) $g_{mole} \ll g_N$ (2) $g_N \ll g_{mole}$ (3) $g_N \approx g_{mole}$. The first two cases lead to a symmetrical splitting or a simple doubling of the rotational levels. Quantitative measurements of the splitting yield values for the g-factors. Only a few substances have been examined; for $N^{15}H_3$ a representative splitting is about 1.2 mc for a field of 1700 oersteds. Since $g_N = 0$, this gives a value of 0.48 nuclear magnetons for $g_{mole}\cdot\mu_0$.

The third case leads to a complicated pattern from which, if either g_N or g_{mole} is known, it is possible to calculate the unknown g-factor.

The preceding equations hold only for fields which perturb the lines by an amount which is small compared to the original separation of the hyperfine components. Higher fields begin to uncouple the spin from the rotation of the molecule, and this leads to a Paschen-Back effect between 2000 and 10,000 oersteds in molecules with small (1 mc) quadrupole coupling.

10. LINE SHAPES AND INTENSITIES.

A. Line Shapes.

A truly isolated molecular system would possess definite and fixed energy levels, but certain unavoidable disturbances perturb the energy levels, giving a width to the spectral lines and varying their center frequencies. These are:

(1) Natural line width

(2) Doppler effect

(3) Pressure broadening

(4) Collisions with the walls

(5) Saturation broadening

Spontaneous emission is responsible for the natural width of spectral lines. Transition probability is proportional to the cube of the frequency, which, in the case of rotational transitions, is so low that the natural width of the lines is of the order of 10^{-7} cycles/sec.

If a molecule is moving with a component of velocity parallel to the direction of propagation of the radiation being absorbed, a frequency

shift of $\pm (\nu) v/v_p$ occurs, where ν is the resonant frequency at rest, v the molecular velocity, and v_p the phase velocity of the radiation. Usually $v_p \approx c$, the velocity of light in free space, and the fractional frequency shifts are simply v/c. The velocity distribution in gases is such that a symmetrical line with half width at half maximum of $\Delta\nu = \frac{\nu}{c}\sqrt{(2\ k\ T\ \log_e 2)/m}$ is obtained. For NH_3 at 300° K. this amounts to 70 kilocycles. Doppler broadening is smaller for heavier molecules and can be decreased by lowering the temperature. It is important because it may sometimes be the limiting factor in line width, and widths observed to be in excess of the Doppler width may indicate removal of degeneracies in the energy levels.

Van Vleck and Weisskopf (19) have derived an expression for the shape factor of a microwave absorption line due to collisions of the molecules with one another.

$$F(\nu, \nu_0) = \left\{ \frac{\frac{1}{2\pi\tau}}{(\nu - \nu_0)^2 + (\frac{1}{2\pi\tau})^2} + \frac{\frac{1}{2\pi\tau}}{(\nu + \nu_0)^2 + (\frac{1}{2\pi\tau})^2} \right\}, \qquad (10\text{-}1)$$

where ν_0 is the resonant frequency and τ is the average time between collisions for a molecule.

At atmospheric pressure the absorption lines can become several thousand megacycles wide. Accurate frequency measurements are impossible under these conditions; consequently, pressures below 1 mm of Hg are commonly employed. At these low pressures the time between collisions becomes large compared to the rotational frequency; then the second term in the brackets of (10-1) becomes negligible and the line shape becomes that

of a typical resonance curve.

$$F(\nu, \nu_o) = \frac{\Delta\nu}{(\nu - \nu_o)^2 + \Delta\nu^2} . \qquad (10\text{-}2)$$

The line half width, $\Delta\nu$, which is proportional to the number of collisions per second, is directly proportional to the gas pressure at a fixed temperature. A very rough value of $\Delta\nu$ for many gases is 15 mc/sec for a gas pressure of 1 mm of Hg. At pressures below 10^{-2} mm of Hg the pressure broadening becomes less than the Doppler broadening.

Collisions with the walls introduce a small but not negligible width to absorption lines. For NH_3 in K band waveguide (1 cm by 0.5 cm) at room temperature, the resulting half width is only 7 kilocycles.

If energy of suffieient intensity is absorbed by a gas, the molecules may be promoted from the lower state to the upper state more rapidly than they can be returned to the lower state by collisions. A consequent drop in the absorption must be expected. Such saturation occurs first at the resonant frequency since the absorption is highest at this frequency. The center of the line is depressed and the line appears broadened. Since the relaxation time increases at lower pressures, saturation effects set in at lower power levels as the pressure is reduced. At 10^{-2} mm of Hg, saturation can be avoided by keeping the radiation flux below about 1 milliwatt per square cm.

B. Line Intensities.

If the microwave power is kept low, the following law of absorption is valid.

$$I = I_o \exp(-\gamma x) . \qquad (10\text{-}3)$$

I_o is the intensity of the incident wave at a particular frequency, I is

the intensity of the transmitted wave, and γ is a constant called the absorption coefficient, which is a function of the frequency.

If one neglects the 2I + 1 degeneracy in the nuclear statistical weight factors, which is equivalent to the assumption that the hyperfine structure is not resolved, the following equation gives the absorption coefficient at the resonant frequency for a single Stark component of a microwave transition.

$$\gamma = \frac{8\pi^2 N \nu^2}{3ckT\,\Delta\nu} \sum_{F = XYZ} \sum_{g = abc} \mu_g^2 \left| (\Phi_{Fg})_{J\tau M;J'\tau'M} \right|^2 F_v g_I g_J \exp\frac{(-W_r)}{kT} / Q_r \qquad (10\text{-}4)$$

N = number of molecules per cc in absorbing path.

ν = frequency of rotational line in cycles/sec.

μ_g = component of the dipole moment along the principal axes a, b, and c.

$\left| (\Phi_{Fg})_{J\tau M;J'\tau'M} \right|^2$ = squared matrix element of the direction cosines between space fixed axes F = X, Y, Z and molecule fixed axes g = a, b, c.

$\Delta\nu$ = half width of line at half maximum points.

c,k,T = velocity of light, Boltzmann constant, and absolute temperature.

$F_v = g_v\{\exp(-W_v/kT)\} / Q_v$ = fraction of molecules in the particular vibrational state observed. W_v is the energy above the ground state, and Q_v is the vibrational partition function.

$g_I g_J\{\exp(-W_r/kT)\} / Q_r$ = fraction of molecules in the lower rotational state of the transition. $g_I g_J$ is the statistical weight of the state, and Q_r is the rotational partition function.

The total absorption coefficient of the transition in the absence of a field is often desired. This quantity is obtained by summing the squared matrix elements over all M values from -J to + J. The three directions X, Y, and Z are equivalent in the absence of an external field, hence the summation over X, Y, Z in (10-4) may be replaced by the factor 3.

Two very important conclusions can be drawn from equation (10-4). Since γ is proportional to ν^2, the intensity of absorption lines will increase rapidly for transitions between higher and higher J values. However, this advantage is partly offset by the difficulty of obtaining sufficient microwave power at these frequencies.

If the pressure is so adjusted that the line width is determined by pressure broadening, γ is independent of pressure, since both N and $\Delta\nu$ are directly proportional to pressure. In order to obtain the narrowest lines without sacrificing intensity, one should pump out the cell just to the point where the line width is determined by the Doppler effect and reduce the temperature as far as possible without condensing the sample.

II. DISCUSSION OF ERRORS IN MICROWAVE STRUCTURE DETERMINATIONS.

Several factors limit the ultimate accuracy of molecular structure parameters computed from microwave data.

(1) Uncertainty in Planck's constant.

(2) Uncertainty in atomic weights.

(3) Uncertainty in measured frequencies.

(4) Zero point vibrations.

A recent adjustment of the atomic constants (20) has yielded a value of $(6.623773 \pm .000180) \times 10^{-27}$ erg sec for Planck's constant. Any error from this source will not affect the structure parameters in a significant way.

Most atomic weights for the more common elements have been measured to one part in 10^5, but a small number are known only to one part in 10^4. The difference in the weights of various pairs of isotopes may be uncertain by 0.1 percent. Measurements of the frequency shift of a rotational line when one isotope is substituted for another may likewise be in error by 0.1 percent. In unfavorable cases these sources of error may introduce an uncertainty of 0.1 percent into the structure parameters.

A much more serious error is introduced by the zero point vibrations of molecular systems. Microwave measurements of the rotational constants for molecules in the ground state yield B_o rather than the equilibrium value, B_e, where

$$B_o = B_e - \sum_i \alpha_i^B d_i/2 \ .$$

In general, not all of the α_i^B are known; consequently, the equilibrium distances, r_e, cannot be computed. The quantity which is calculated is

r_o, the average distance the atoms would have to be separated in order to give the observed values of B_o. Unfortunately, making an isotopic substitution changes the α_i^B at the same time, so that the new B_o does not correspond to the original average configuration of atoms but represents a very slightly changed average configuration.

In any molecule with a figure axis, if an atom of mass m on the axis is replaced by an isotope of mass m', then the distance of these atoms from the center of mass of the original molecule is given by

$$z_o'^2 = (I_o' - I_o)(M + \Delta m)/M \Delta m . \qquad (1\text{-}1)$$

This equation is derived for a vibrating molecule in Appendix I. One or the other of the quantities I_o' and I_o may be regarded as being in error by the amount ΔI_o due to neglect of the change in zero point vibration amplitude. The error introduced in z_o' is given by

$$\Delta z_o' = \Delta I_o' (M + \Delta m)/2z_o'M \Delta m , \qquad (1\text{-}2)$$

obtained by differentiating the expression for z_o' with respect to I_o'. The error is largest for atoms which are located nearest the center of mass.

It is possible to solve for the bond distances directly if enough measurements of I_o have been made. The bond distances of the linear molecule OCS have been calculated (21) for several isotopic pairs. Serious lack of agreement between the different values obtained from different pairs indicates that before putting too much faith in the results of such calculations one should investigate them carefully. For this particularly simple molecule it is possible to write the following expressions for the OC and CS distances in terms of the moments of inertia.

For the pair OCS - OCS' only:

$$r_{OC}^2 = \left\{(M + \Delta m)I_o' - \frac{m_s'}{m_s} MI_o\right\} / m_o m_C \left(1 - \frac{m_S'}{m_S}\right). \quad (1\text{-}3)$$

For the pair OCS - O'CS only:

$$r_{SC}^2 = \left\{(M + \Delta m)I_o' - \frac{m_o'}{m_o} MI_o\right\} / m_S m_C \left(1 - \frac{m_o'}{m_o}\right). \quad (1\text{-}4)$$

Due to neglect of zero point errors, one or the other of the quantities I_o' and I_o is in error by ΔI_o. Differentiation with respect to I_o gives

$$\Delta r_{OC} = \Delta I_o (M + \Delta m)/2r_{OC}m_O m_C \left(1 - \frac{m_s'}{m_s}\right), \quad (1\text{-}5)$$

$$\Delta r_{CS} = \Delta I_o (M + \Delta m)/2r_{CS}m_S m_C \left(1 - \frac{m_o'}{m_o}\right). \quad (1\text{-}6)$$

An examination of equations (1-5) and (1-6) shows that for a ratio of isotopic masses m_s'/m_s or m_o'/m_o approaching unity, the bond distance becomes catastrophically sensitive to errors in measurement of I_o. Even for ratios of 34/32 or 18/16 it is easy to see that rather poor values for r_{OC} and r_{CS} are likely to be obtained if the change in α_i^B upon isotopic substitution shifts the absorption line as much as one megacycle. In this way, an error of one part in 20,000 in a moment of inertia measurement may show up as nearly a one percent error in a bond distance.

For molecules which are too complicated to analyze in this way, the application of equation (1-1) has much to recommend it. Even an underdetermined molecule, one for which there are fewer moment of inertia measurements than structural parameters, may permit calculation of some of the bond distances. A just determined molecule may be solved for some of the distances by equation (1-1), and the simultaneous equations for the remaining parameters will then be greatly simplified. The chance of

selecting a highly sensitive method (with respect to multiplication of errors) of solving the simultaneous equations is greatly reduced. Finally, an overdetermined molecule may be solved completely without the necessity of solving simultaneous equations.

No method of calculation is capable of yielding accurate bond distances for atoms which are very near the center of mass, since their contribution to the moment of inertia becomes negligible.

III. DESIGN, CONSTRUCTION, AND OPERATION OF THE MICROWAVE SPECTROSCOPE.

A microwave spectroscope is a device for detecting absorption of energy in the 1 mm to 2 cm region of the spectrum and for measuring the frequency of the absorption. The absorbing material is generally a gas, maintained at a low pressure and exposed to microwave radiation in an absorption cell capable of transmitting microwaves. The frequency of the monochromatic source is swept repeatedly through a small region of the spectrum in a linear way. Absorptions are displayed as deflections on a synchronized cathode ray oscilloscope trace.

In order to be suitable for the most general applications, a microwave spectroscope must possess the following qualities: high sensitivity, freedom from spurious responses, and ability to search smoothly over a large frequency range. It is the task of the designer to produce an instrument in which all of these qualities are compatible.

There are three fundamentally different designs: the superheterodyne, the crystal video, and the Stark modulated microwave spectroscope. The superheterodyne is extremely sensitive, but it is excessively complicated for use as a search instrument. The crystal video instrument is recommended only by its simplicity, since the sensitivity is limited by the low power handling capability, and, in addition, difficulties with spurious responses and tuning problems are almost overwhelming. Stark modulation eliminates most of the shortcomings of the other two systems, but it alters the shape of the absorption lines and introduces troubles with electrical pickup.

1. The Complete Instrument.

Figure 1 presents a complete block diagram of the spectroscope.

The instrument is a 50 kc Stark modulated spectroscope employing lock-in detection and either oscilloscope or recording meter presentation. Approximate frequency measurements are made with cavity wavemeters, and precise measurements are made by comparing the unknown absorption with the ammonia spectrum, using a crystal controlled secondary frequency standard. All units of the equipment except the oscilloscopes, radio receiver, klystron, and certain waveguide components were designed and constructed in this laboratory. Several striking metamorphoses occurred during the construction of the instrument, eventually leading to its present form.

2. Generation and Propagation of Microwaves.

Microwave energy is generated by a reflex klystron oscillator, the Western Electric 2K-50, which can be varied in frequency over a range of about 4000 mc about a center frequency of 23 kilomegacycles. The bending of a bimetallic strip flexes the resonant cavity and controls the frequency. This thermal element is heated by the plate current in a triode section of the 2K-50. Grid voltage for this triode is taken from a ten turn helipot which may be adjusted manually or driven slowly through the entire spectrum by a synchronous motor at a rate of 40 mc per minute. The beam voltage of the klystron is regulated electronically, and the reflector electrode and triode grid voltages are supplied from batteries. A circuit diagram is given in Fig. 2.

A series of high voltage, mechanically tuned, reflex klystrons manufactured by Raytheon Electronic Co. are on hand for use in investigations of absorption lines which fall outside of the range of the 2K-50. These

tubes, the QK-289, 2K-33, QK-142, QK-226, QK-227, and QK-306 cover a region of the spectrum from 17 to 30 kilomegacycles, and a second region from 36 to 50 kilomegacycles. An electronically regulated, high voltage power supply was constructed in order to operate this series of tubes. Figure 3 is a schematic circuit diagram of this power supply.

Microwaves are propagated along the one centimeter rectangular waveguide in a transverse electric mode, the TE_{01}. An attenuator (0-10 db) isolates the klystron and prevents reflections from discontinuities in the wave guide from disturbing the frequency of the klystron. No attempt is made to eliminate the standing waves set up by these discontinuities.

Approximately one percent of the microwave energy is abstracted by a 20 db directional coupler and diverted into the wavemeters and the harmonic frequency standard. The rest of the energy passes through a tapered horn into a standard ammonia cell (to be described later) and then into the main absorption cell.

3. Absorption Cell.

The absorption cell consists of a twelve foot length of three centimeter copper waveguide whose ends are sealed with thin (.010 inch) mica windows held in place by a hard wax. The cell is connected through a stopcock to a high vacuum system and can be evacuated to an estimated pressure of 10^{-6} mm. An R. C. A. thermocouple gauge on the absorption cell side of the stopcock permits a continuous approximate measurement of the sample pressure. This is very important, since large adsorption effects are often observed with the gaseous samples employed in microwave spectroscopy.

Provision is made for the introduction of an electric field parallel to the electric vector of the microwave radiation inside of the absorption cell. A 1/16" x 3/4" steel bus bar is supported in the exact center of the cell by slotted teflon strips and extends the entire length of the cell. A flexible electrical connection is made to this electrode through a glass to kovar seal. Considerable relative movement of electrode and cell must be expected due to expansion and contraction with changes of temperature. A cross section of the absorption cell is shown in Figure 4.

4. Mechanism of Stark Modulation.

Modulation of the absorption lines by the Stark effect was first introduced by Hughes and Wilson (22). If we imagine the source oscillator tuned to a fixed frequency and the position of the absorption line moved back and forth by a varying electric field, it is easy to see that amplitude modulation can be produced. Now, if the line is moved back and forth by a radiofrequency square voltage waveform impressed on the electrode and the klystron is swept over the absorption line at a rate which is slow compared to the molecular modulation, the absorption lines can be displayed on an oscilloscope by amplifying the modulation frequency, detecting it, and applying the absorption line envelope to the vertical deflection plates of the oscilloscope. The spot is swept horizontally across the face of the cathode ray tube by the same sawtooth waveform of voltage that is simultaneously sweeping the klystron over the absorption line. This sawtooth voltage is actually generated in the oscilloscope and is fed to the negatively charged reflector electrode of the klystron through an isolating capacitor.

The train of microwaves emerging from the absorption cell is modulated by the square wave frequency which, in turn, is modulated by the absorption line envelope. The microwaves are passed through a tapered reducing horn into a one centimeter section of waveguide provided with a tuning stub and a movable shorting plunger. A probe extends into this section and is connected to a 1N-26 silicon crystal rectifier. In practice, the shorting plunger and tuning stub are adjusted to yield a maximum standing wave of voltage at the pickup probe. The crystal rectifier passes on only the square wave, modulated by the absorption line envelope.

At this point one of the great advantages of Stark modulation becomes apparent. If some discontinuity in the waveguide introduces a frequency sensitive variation in microwave power, this merely shows up as a shift in the DC output level of the crystal. However, the modulated absorption signal is unaffected except for a small change in its amplitude. If no modulation were used, the change in power due to the discontinuity might completely mask the minute dip in power caused by molecular absorption.

5. The Modulation Waveform.

A square waveform was chosen for modulation purposes to avoid smearing the absorption lines. The square waveform is electronically clamped to a DC voltage which can be varied from zero to one thousand volts. Since there are only two different values the electric field can assume, modulation of the microwaves is introduced at only $2(J + 1)$ frequencies, corresponding to the splitting of the line into its $J + 1$ Stark components by the DC voltage and the appearance of each of these components at

two different positions corresponding to the top and bottom of the square wave. Had some other waveshape been employed, absorption would have occurred at all intermediate frequencies, leading to a hopeless smearing of the absorption line and its Stark components.

The modulation frequency is determined by three conflicting factors. The first is the difficulty of developing a voltage waveform with high frequency components across the low impedance presented by the .001 microfarad capacity of the waveguide and Stark electrode. This consideration dictates as low a modulation frequency as possible. The second factor is the dependence of the noise temperature of the silicon crystal rectifier upon frequency. A considerable amount of experimental data has been obtained by Miller, Greenblatt, and others (23) at the University of Pennsylvania which shows that the noise of a crystal rectifier is an inverse function of the frequency at power levels above a few microwatts. Since the limiting sensitivity of the microwave spectroscope is determined by the overall noise figure, and since the crystal contributes more noise than any of the other circuits, one would like to use as high a modulation frequency as possible, in order to reduce crystal noise to a minimum. The third factor is the effect of an uncertainty in the time on the energy levels of the molecules. If the energy levels are periodically shifted back and forth and remain in each state a time $t = \frac{1}{\nu}$, where ν is the repetition rate of the square wave, then to a first approximation the energy levels will be broadened by an amount ΔE given by the equation

$$\Delta E \; \Delta t \geq \hbar .$$

Therefore, the line acquires a width $\frac{h\nu}{2\pi}$. A rigorous calculation of

the dependence of line shape on ν has been given by Karplus (24), using time dependent perturbation theory. A modulation frequency of 50 kilocycles was finally chosen as a suitable compromise for all factors.

6. The Square Wave Generator.

Figures 5 and 6 represent schematic diagrams of the square wave generator and its power supply. The frequency is stabilized by a 100 kilocycle crystal oscillator which triggers a multivibrator every other cycle. The resulting waveform is clipped and amplified before it is applied to the grids of two parallel-connected cathode followers. A square wave with an amplitude of 350 volts and a rise time of about 1 microsecond is obtained on the electrode in the absorption cell.

7. Preamplification.

Modulated signals from the crystal detector are fed directly into the low noise preamplifier shown schematically in Figure 7. Rectified microwaves pass through a 0 - 150 microammeter which serves to monitor the power available from the klystron and also indicates whether the standing wave ratio in the waveguide possesses a maximum at the crystal. The 50 kc component corresponding to molecular absorption is isolated from the meter by an inductance and is capacitively coupled into the primary of a specially designed step-up transformer (1:15), which drives the grid of a low Q tuned amplifier, followed by a resistance coupled stage of amplification. The voltage gain of the combination is approximately 5×10^4.

8. Final Detection.

A heterodyne, or lock-in detector has been employed with marked success by Townes and co-workers at Columbia University. The advantages of

the circuit accrue from its narrow bandpass and its ability to differentiate between signals of opposite phase. Figure 8 shows the circuit diagram for the lock-in detector and associated circuits. Signals from the preamplifier are passed through one more tuned stage of amplification and are impressed on the control grid of a pentode. The suppressor grid of this pentode is modulated by a sine wave of sufficient amplitude to switch the pentode on and off at the exact frequency of the signal on the control grid. Exact coincidence in frequency is obtained by generating the sine wave from the same square wave which produces the modulation of the microwaves. A phase shifter is necessary in order to compensate for the different phase shifts which the two signals experience in passing through their respective circuits. Probably the simplest way to think of the operation of this detector is to consider the 50 kc signal modulated by the absorption line envelope as a carrier with the intelligence residing in side bands. When these side bands beat with the signal on the suppressor grid, the sum and difference frequencies appear in the current reaching the plate. A low pass filter eliminates the sum frequency, and the difference frequency is passed on to the indicator unit. It has previously been mentioned that each line is split into J + 1 components by the Stark effect and that each of these components appears at two frequencies corresponding to the top and bottom of the square wave. Since the top and bottom of the square wave differ in phase by 180 degrees, each Stark component will produce a positive and a negative deflection at the indicator unit. This is a result of the phase discriminating ability of the heterodyne detector. If the DC voltage is zero, the Stark components are

split only by the electric field corresponding to the top of the square wave, and when the field corresponds to the bottom of the square wave (ground) the line appears at its unperturbed frequency. Thus, the phase discriminating ability of the detector makes it possible to distinguish easily the unperturbed line from its Stark components.

If we assume that thermal noise is the limiting factor in the detection of weak signals, then we conclude that when the amplifier input is matched to the crystal, noise power equal to kTB watts is delivered, where k is the Boltzmann constant, T is the temperature in degrees Kelvin, and B is the bandwidth of the amplifier. The narrower the bandwidth, the less noise will appear at the output terminals of the amplifier. Now the noise will appear as side band frequencies around the 50 kc carrier frequency, and in the heterodyne detector will be converted to sum and difference frequencies. The sum frequencies are discarded, and only difference frequencies lower than the cut-off frequency of the low pass filter appear in the output. Therefore, the bandwidth of the amplifier is determined by the low pass filter cut-off.

A simple proportional detector does not show this effect when it is terminated with a low pass filter. The amount of noise power of a given frequency is the same in each increment of the band, and all increments are detected indiscriminately. If we terminate an amplifier with a 1000 cycle bandwidth in a 10 cycle low pass filter, there will be 100 times as much 10 cycle noise as there would be in a 10 cycle bandwidth amplifier similarly terminated. The heterodyne detector would, however, only detect noise within 10 cycles of the lock-in frequency in either case.

9. Indicating Units.

(a) Oscilloscope Presentation.

A Dumont 247 Oscillograph with a 5 inch cathode ray tube may be used to amplify the output of the lock-in detector and display it as a positive or negative vertical deflection. Horizontal sweep rates from one half cycle to 50 kilocycles per second are available. It is important to note that since the klystron sweeps through the absorption line each time the beam sweeps across the face of the cathode ray tube, the Fourier frequency components of the absorption envelope must be of the order of the repetition frequency or a little higher. In order to reduce noise to a minimum, the low pass filter is generally set for a bandwidth of a few cycles per second. To avoid distortion of the line envelope the sweep rate must be reduced to a point where the major Fourier components of the line fall within the bandwidth.

(b) Esterline-Angus Recording Meter Presentation.

A model AW Esterline Angus Graphic ammeter is available for obtaining permanent records of spectra and for attaining the very highest sensitivity. The bandwidth of the detector can be reduced indefinitely by lowering the cut-off of the filter. The klystron must be swept more and more slowly as this is done. Eventually, the tendency of the klystron to drift will set a practical limit for the sweep rate. The klystron power supply is equipped with a motor drive for sweeping through the spectrum as slowly as 40 mc per minute. This is about ten times as slow as the slowest sweep rate of the oscilloscope; as a consequence, lines ten times weaker may be studied.

10. Measurement of Absorption Frequencies.

Two cylindrical, reaction type, cavity wavemeters are arranged in series and connected to a directional coupler so that about one percent of the total klystron power passes through them and falls upon a probe connected to a 1N26 silicon crystal. These wavemeters have been calibrated against the accurately known absorption lines of NH_3 and the results plotted in Figure 9. One or the other of these meters will usually be resonant at the frequency of the line being studied. Frequencies are determined by bringing the wavemeter to resonance in two successive $TE_{11\,n}$ modes and measuring the change in length of the cavity. The indication of resonance is displayed as a dip in the plot of klystron power versus frequency on the monitor oscilloscope. The small amount of power available from the directional coupler necessitated the construction of a wavemeter signal amplifier, a simple, two stage, untuned amplifier shown schematically in Figure 10.

While careful work with a cavity wavemeter may yield frequency measurements accurate to 5 megacycles, it is often necessary to know relative frequencies to within one tenth of a megacycle. For this purpose, a secondary frequency standard has been constructed, following the general procedure outlined in the paper by Unterberger and Smith (25). Circuit diagrams of the standard and its power supply are given in Figures 11 and 12.

A 10 megacycle, temperature controlled, crystal oscillator provides a standard frequency which is successively tripled to 270 megacycles. A Sperry 2K47 klystron multiplier is driven by this 270 mc signal and

yields 2430 mc. Some of the power at 30, 90, and 270 mc is mixed with the 2430 mc power at a welded germanium crystal. A series of standard harmonics spaced 30 mc apart can be propagated down the one centimeter waveguide. The IN26 silicon crystal, which serves as a power indicator when wavemeter measurements are being made, now serves as a crystal mixer. The standard harmonic frequencies beat with the klystron as it is swept in frequency through the spectrum. Sum and difference frequencies appear on the crystal and are fed into a tunable receiver, the Signal Corps BC-348-O. The receiver output is fed into the vertical deflection amplifier of the Dumont 247 oscilloscope. Two "pips" appear on the oscilloscope for each setting of the receiver, separated by twice the receiver setting and centered about the standard harmonic frequencies. By tuning the receiver, one can always superimpose one of the "pips" on the absorption line. This constitutes a measurement of the frequency of the absorption line.

Many investigators monitor the 10 mc crystal frequency continuously by comparing it with radio station WWV. However, reception of WWV is not reliable. In addition, the crystal must be ground to a frequency slightly higher than 10 mc and brought back to a zero beat by shunting it with a small tuning capacitor. We avoided these difficulties by building a gas absorption cell one foot long, filling it with NH_3 to a pressure of 50 microns, and sealing it off permanently. Ammonia lines appear on the oscilloscope when the cell is connected to a source of square wave modulation. Whenever an unknown line is measured, one of the adjacent ammonia lines can also be measured as a reference. The difference in the frequencies can be determined to within a tenth of a megacycle.

Kisliuk and Townes (26) have published a complete table of observed line frequencies of ammonia.

11. Vacuum System.

The absorption cell is evacuated through a manifold provided with stopcocks at either end so that it can be closed off for gas handling operations or opened to either the vacuum pump or the gas cell. Gases are admitted to the manifold through two stopcocks terminating in standard taper joints. A freeze-out tube enables condensable materials to be freed from volatile impurities.

12. Cooling Arrangement.

Cooling the absorption cell can result in an improvement of the pure rotational spectrum by increasing the fraction of molecules in the lower quantum states and by reducing both Doppler and collision broadening effects. The absorption cell is surrounded by a sturdy trough which can be packed with dry ice.

13. Operation of the Spectroscope.

In order to investigate the spectrum of a substance, one must first allow the equipment to stabilize by waiting for the various units to come to operating temperature. The substance is introduced into the manifold and a small amount is condensed by immersing the freeze-out tube in liquid nitrogen. Both manifold and cell are evacuated, the stopcock to the pump closed, and the liquid nitrogen removed from the sample. As soon as the thermocouple gauge indicates a pressure of 50 microns in the cell, the stopcock between cell and manifold is closed. Several fillings may be required in order to compensate for adsorption effects. If absorption by molecules in the ground vibrational state is expected, the cell trough

is packed with dry ice.

The klystron is now adjusted to oscillate in the center of a "mode" by varying the potential on the reflector electrode. An R. C. A. 3 inch oscilloscope displays a plot of klystron power versus frequency; this should be a smooth, symmetrical curve. Power reaching the detector crystal is maximized by tuning the plunger and probe in the crystal holder. Crystal current should be limited to about 100 microamperes by inserting additional attenuation in series with the cell.

If the absorption lines are expected to have a first order Stark effect, the square wave voltage is set at 10 to 20 volts. If a second order effect is expected, the voltage is advanced to 350 volts. For searching, the D. C. voltage is set at zero.

A moderate sweep speed may be employed for searching, say, 30 cycles per second. The klystron cavity is varied slowly by changing the helipot setting controlling the cavity size. It is necessary to stop frequently and adjust the "mode". Less frequently, the tuning of the crystal holder requires attention.

Whenever a sharp fluctuation in the oscilloscope trace is observed, the D. C. potential of the Stark electrode is changed. Only an absorption line will broaden, split, or move under the influence of an electric field. Spurious responses are easily detected in this way. A more certain test is to pump the gas out of the cell and then readmit it.

After a line has been located, its position is determined with the cavity wavemeter. The sweep rate is then reduced to one cycle per second and the gain of the interpolation receiver is advanced until frequency

marker "pips" appear on the trace. One of these "pips" is superimposed on the absorption line by varying the receiver setting. If the sweep rate is not slow enough, the frequencies of the "pip" and the absorption line will be shifted relative to each other. The receiver setting, f, is recorded and the direction the "pip" moves with increasing frequency is noted. If it moves to higher frequencies with an increase in the receiver setting, it is f mc above the nearest standard harmonic frequency. If it moves to lower frequencies it is f mc below the nearest standard harmonic frequency.

Finally, the D. C. voltage on the electrode is raised until the line splits into some or all of its Stark components. In favorable cases these may be counted and the J value for the transition determined directly. Usually one will need to have additional spectral information, such as the position of other lines, in order to assign the transition.

IV. THE DETERMINATION OF THE STRUCTURE OF ISOCYANIC ACID IN THE VAPOR PHASE.

Conflicting chemical and physical evidence concerning the nature of the chemical bonds in cyanates and thiocyanates and the existence or non-existence of a tautomeric equilibrium between the normal and iso forms of cyanic and thiocyanic acids arouses great interest in these problems. Recently, Beard and Dailey (27, 29) have completed an investigation of the structure of thiocyanic acid in the vapor phase, using the technique of microwave spectroscopy. They found that this substance is at least 95 percent the iso acid, HNCS, and reported values for the molecular structure parameters. A complete structure determination of cyanic acid appeared to be desirable in order to clarify the situation still further.

1. Earlier Work on Cyanates and Isocyanates.

In 1920, Werner and Fearon (29) investigated the polymerization of the liquid obtained by condensing the gaseous decomposition product of heated cyanuric acid. This liquid can be shown to have the empirical formula HNCO. The polymerized cyanic acid always contained both cyamelide and cyanuric acid, the relative amounts depending upon the temperature at which the polymerization was carried out. Cyamelide was favored at low temperatures and cyanuric acid at high temperatures. Werner and Fearon postulated a keto-enol tautomerism to explain this behavior.

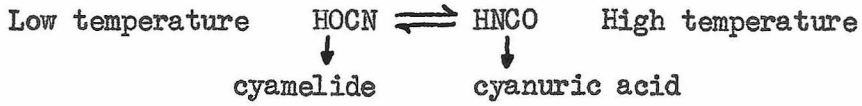

These investigators also carried out hydrolysis experiments in which they obtained different relative amounts of ammonium cyanate and urea. They explained this behavior on the basis of the same tautomeric equilibrium.

$$HOCN \rightleftharpoons HNCO + H_2O = CO_2 + NH_3$$

$$HNCO \rightleftharpoons HOCN + NH_3 = NH_4^+ + OCN^-$$

$$HOCN \rightleftharpoons HNCO + NH_3 = NH_2CONH_2$$

In 1940, Linhard and Betz (30) pointed out that the acid strength of cyanic acid is most easily explained for the structure HOCN, but that HNCO, like HN_3, would also be an acidic substance. They also showed that many of the reactions of cyanic acid could be interpreted in terms of addition to the double bond in the species HN=CO. For example,

$$HN{=}CO + NH_3 = NH_2\text{-}CO\text{-}NH_2 .$$

However, due to its acidic nature HNCO can also react with ammonia in a simple neutralization reaction.

$$H^+N^-CO + NH_3 = NH_4^+ + NCO^- .$$

Linhard and Betz finally concluded that the chemistry of isocyanic acid in solution can be explained on the basis of the structure HNCO alone.

Goubeau (31) investigated the Raman spectrum of liquid isocyanic acid and found the hydrogen stretching frequency to be 3320 cm^{-1}. From this he concluded that the hydrogen atom must be attached to the nitrogen atom and that HNCO must be the correct formula. More recently, Jones (32) has obtained from the infrared absorption spectrum a value of 3538 cm^{-1} for this stretching frequency for molecules in the gas phase. Goubeau's value of 3320 cm^{-1} in the liquid is not unreasonable, since association due to hydrogen bonding would tend to lower the frequency somewhat.

Herzberg and Verleger (33) investigated an infrared absorption band of HNCO at 9700 cm^{-1} and concluded that the complexity of this band

could only arise from a non-linear configuration of the NCO group. However, Eyster, Gillette, and Brockway (34) have pointed out that the band was probably a parallel-perpendicular band, and if the intensity of the perpendicular component is very great the observed band could be quite complex, even if the NCO group is linear.

Finally, Eyster, Gillette, and Brockway assumed that the stable form of cyanic acid is HNCO and interpreted their electron diffraction pictures in terms of this structure. They obtained 1.19 $\pm$ .03 Å for both the NC and CO distances and 2.38 $\pm$ .03 Å for the NO distance, which indicates that the NCO group cannot deviate more than a few degrees from linearity.

2. The Infrared Investigation by L. H. Jones.

The calculation of the structure of HNCO was greatly facilitated and improved by the infrared data communicated to us by L. H. Jones, who was carrying out an independent investigation of HNCO under Professor Richard M. Badger at the California Institute of Technology. Working with a vacuum grating spectrometer, he was able to resolve the first overtone of the N-H stretching vibration into its rotational structure, which enabled him to furnish us with a value for $A_o - \frac{1}{2}(B_o + C_o)$ for $HN^{14}C^{12}O^{16}$. This value, 30.30 $\pm$ .1 cm^{-1}, is very sensitive to the position of the hydrogen atom and made it possible for us to fix that position quite accurately. It also supports the assumption of a linear NCO group, since a non-linear configuration would lead to a much higher value for I_A.

Another important contribution of this infrared investigation was

the measurement of the fundamental and first overtone frequencies of the hydrogen stretching in both HNCO and HNCS. These are tabulated in Table IV, along with characteristic stretching frequencies for the various bonds which might be formed in these compounds.

Table IV. Hydrogen Stretching Frequencies.

Molecular Configuration	Fundamental (cm^{-1})	First Overtone (cm^{-1})
HNCO	3538	6915
HNCS	3530	6903
H-N	3350 *	
H-O	3680 *	
H-S	2750 *	

Although the hydrogen valence frequency in isocyanic acid is high in comparison with the value usually attributed to N-H vibrations, the practical identity of this frequency in HNCO and HNCS can leave little doubt but that in both cases it results from an N-H vibration and that isocyanic and isothiocyanic acids are predominantly, if not exclusively present in the vapor phase. The results of Beard and Dailey (27, 28) have thus been verified. On the basis of this work, the analysis of the microwave data which we obtained for isocyanic acid was carried out for a model with the sequence of atoms H-N-C-O.

3. Determination of the Structural Parameters.

A. Preparation of the Acid.

* See reference (5), page 195.

Isocyanic acid was prepared by heating powdered cyanuric acid in an evacuated tube until a vigorous evolution of gas was observed. This process was continued until the acid was thoroughly dried and freed from trapped air. The tube was then connected to the absorption cell, and a small amount of isocyanic acid was evolved. Finally, the pressure was reduced to approximately 50 microns in order to eliminate pressure broadening effects.

The cyanuric acid used in this investigation was obtained from the same lot that L. H. Jones was using in his infrared work. Although he condensed his isocyanic acid in a cold trap and distilled it into the absorption cell, this precaution was not necessary in the microwave work. Small amounts of impurities were not likely to cause serious difficulties, since the probability of their absorption lines having an appropriate Stark effect or forming a consistent set of B values was small. In this case, the most likely impurities which could absorb in the microwave region were H_2O and NH_3. No absorption due to either of these molecules was actually observed.

Deutero-cyanuric acid was prepared by letting 0.5 gm of cyanuric acid stand in 2 cc of heavy water for three days. After the exchange had occurred, the excess water was distilled out of the sample tube and deutero-isocyanic acid generated in the usual way. The conversion yield appeared to be approximately 50 percent.

B. The Observed Spectrum.

Microwave absorption spectra of isocyanic and deutero-isocyanic acid vapors were observed between 20,000 and 25,000 mc/sec under the

following conditions:

Pressure: 50 microns

Temperature: 300° K.

Modulation: 700 volts/cm square wave based on ground.

Five absorption lines were found and their frequencies measured relative to the $5_0 - 5_1$ transition in HDO at 22,307.67 mc. These frequencies are given in Table V.

Table V. Observed Spectrum of HNCO.

Molecule	Transition	ν mc.	Relative Intensity (300°K)
$HN^{14}C^{12}O^{16}$	$0_{0,0}-1_{0,1}$ (ground state)	21,981.7 ± .2	300
$HN^{14}C^{12}O^{16}$	$0_{0,0}-1_{0,1}$ ($v_6 = 1$)	21,993.0 ± .2	12
$HN^{14}C^{12}O^{16}$	$0_{0,0}-1_{0,1}$ ($v_5 = 1$)	22,017.3 ± .2	25
$HN^{15}C^{12}O^{16}$	$0_{0,0}-1_{0,1}$ (ground state)	21,323.5 ± .2	1
$DN^{14}C^{12}O^{16}$	$0_{0,0}-1_{0,1}$ (ground state)	20,394.7 ± .2	150

Each of these lines was examined while the electric field in the waveguide was varied from zero to 2300 volts/cm. In every case, only one component could be detected; therefore, the lines were all identified as corresponding to transitions in which J changes from 0 to 1. This agrees with the expectation that reasonable structure parameters in

HNCO would lead to a value of 2B between 20 and 25 kmc.

Each line was observed to disappear when the sample in the absorption cell was pumped out and to reappear when a fresh sample of isocyanic acid was admitted.

The line due to $HN^{15}C^{12}O^{16}$ molecules had to be identified by its proximity to the position predicted for it from the electron diffraction data of Eyster, Gillette, and Brockway (34), the fact that its relative intensity agrees well with the relative abundance of N^{14} and N^{15} isotopes, and its characteristic $J = 0 \rightarrow 1$ Stark pattern.

Two of the lines have been tentatively identified as arising from the $0_{0,0}$-$1_{0,1}$ rotational transition in molecules possessing one vibrational quantum of excitation in the modes of vibration ν_5 and ν_6, the in plane and out of plane bending vibrations. These two lines show a marked decrease in intensity relative to the ground state line in going from room temperature to dry ice temperature. Although relative intensity measurements were not very reproducible over a long period of time, the average of many measurements yielded the intensities given in Table V. The vibrational frequencies can be calculated with the aid of Boltzmann expression

$$N_\omega / N_0 = \exp(-\omega/kT)$$

to be 525 ± 50 cm^{-1} for ν_5 and 665 ± 50 cm^{-1} for ν_6. A recent measurement (35) of the fundamental frequencies of vibration in HNCO from its infrared absorption spectrum resulted in values of 572 cm^{-1} for ν_5 and 670 cm^{-1} for ν_6. The agreement in the frequencies makes the assignment reasonably convincing.

Careful measurements of the frequencies as a function of the applied electric field were made for all lines but the N^{15} line which was too weak. These measurements result in a value for the dipole moment of HNCO in each of these states. They will be discussed in detail in Part VI.

C. Calculation of Rotational Constants.

The expression for the energy levels of an asymmetric rotor is:

$$F(J, \tau) = \tfrac{1}{2}(B_o + C_o)J(J+1) + \left\{A_o - \tfrac{1}{2}(B_o + C_o)\right\} W_\tau ,$$

where W_τ takes on $2J + 1$ values which are roots of a secular determinant. This determinant can be factored to give algebraic equations for W_τ for each value of J. Nielsen (7) has given the following equations for W_τ

$$J = 0: \quad W_o = 0 ,$$

$$J = 1: \quad W_\tau = 0 ,$$

$$W_\tau^2 - 2W_\tau + (1 - b^2) = 0 ,$$

where $b = (C_o - B_o)/2\left\{A_o - \tfrac{1}{2}(B_o + C_o)\right\}$.

The transition which we have observed in HNCO is the $0_{0,0}$-$1_{0,1}$. The lower state is the state of no rotation; the upper state is a state in which the total angular momentum is shared between the two axes of large moment of inertia. Two other $J = 0 \rightarrow 1$ transitions exist, the $0_{0,0}$-$1_{1,1}$ and the $0_{0,0}$-$1_{1,0}$, but they lie 30 cm^{-1} above the microwave region, since the molecule gains angular momentum about the axis of smallest moment of inertia. Consequently, the $0_{0,0}$-$1_{0,1}$ transition is the one with the smallest value of W_τ ; $1 \pm b$ or zero. Since b lies between 0 and -1, the smallest value of W_τ is zero.

$$F(1_{0,1}) = \tfrac{1}{2}(B_o + C_o)\cdot(2) = B_o + C_o .$$

Therefore, the observed transitions yield directly the value of $B_o + C_o$ in mc/sec.

The average of the reciprocals of the two large moments of inertia is $\tfrac{1}{2}(B_o + C_o)$ which we shall henceforth call $\bar{B}_o$. For planar molecules,

$$I_c = I_a + I_b . \qquad (3\text{-}4)$$

This relation holds strictly only for planar non-vibrating molecules, but with very good approximation for the I_o. The following relation is easily found:

$$C_o = (A_o + \bar{B}_o) - (A_o^2 + \bar{B}_o^2)^{\frac{1}{2}} . \qquad (3\text{-}5)$$

By expanding the second term on the right and dropping terms higher than second order in $\bar{B}_o/A_o$ we obtain

$$C_o = \bar{B}_o - \bar{B}_o^2/2A_o + \cdots\cdots . \qquad (3\text{-}6)$$

There are four molecular structure parameters to be determined; therefore, four rotational constants will be required. The four which have been chosen to give the simplest computational problem are the following: I_c for $HN^{14}C^{12}O^{16}$, $HN^{15}C^{12}O^{16}$, $DN^{14}C^{12}O^{16}$, and I_a for $HN^{14}C^{12}O^{16}$. The value of $A_o - \bar{B}_o$ for $HN^{14}C^{12}O^{16}$ has been supplied by L. H. Jones from the infrared work mentioned in section 2 of this Part. From his value of $A_o - \bar{B}_o$ and the microwave value of $\bar{B}_o$ the value of A_o for $HN^{14}C^{12}O^{16}$ is immediately obtained. C_o for $HN^{14}C^{12}O^{16}$ can be calculated at once from equation (3-6). Since Jones did not measure $A_o - \bar{B}_o$ for $HN^{15}C^{12}O^{16}$ and $DN^{14}C^{12}O^{16}$, C_o for these species cannot be evaluated directly. However, by assuming a trial structure we can calculate values of A_o for each of these species. These values of A_o can be used

to calculate the small correction term, $\bar{B}_o^2/2A_o$, in equation (3-6). This term is about 1/165 of $\bar{B}_o$; consequently, if the trial structure gives A_o only to within 10 percent of its true value, the effect on the value of I_c from which we calculate the final structure will be only one part in 1650. These calculations have been carried out for the following trial structure* using the equations which will be developed in this section.

r_{N-H} : .9797 A.

r_{N-C} : 1.1887 A.

r_{C-O} : 1.1901 A.

Angle H-N-C : $127^{o}35'$.

Rotational constants for the various isotopic species are presented in Table VI.

Table VI. Rotational Constants for HNCO

Isotopic Species	$\bar{B}_o$ cm^{-1}	A_o cm^{-1}	C_o cm^{-1}	I_a a.m.u.A^{o2}	I_c a.m.u.A^{o2}
$HN^{14}C^{12}O^{16}$	.366636	30.67	.36444	.54960	46.2470
$HN^{15}C^{12}O^{16}$	.355657	<u>30.32</u>**	<u>.35357</u>	<u>.55583</u>	<u>47.6692</u>
$DN^{14}C^{12}O^{16}$	.340165	<u>16.77</u>	<u>.33677</u>	<u>1.00504</u>	<u>50.0557</u>

** Underlined values depend on trial structure calculation.

D. Moment of Inertia Equations.

A set of parameters, x, y, z, and α have been assigned to HNCO; their values determine the moments of inertia of the molecule. Figure 13 illustrates the relationship of these parameters to the interatomic distances and bond angle and also shows the principal axes. The center

* This trial structure is the result of a preliminary iteration calculation which failed to converge rapidly enough.

of mass is given in the XY coordinate system by

$$a = m_O z - m_N y - m_H(y + x\cos\alpha) / W , \quad (3\text{-}7)$$

$$b = m_H x \sin\alpha / W , \quad (3\text{-}8)$$

where W is the molecular weight and m_O, m_N, and m_H are the atomic weights of the oxygen, nitrogen, and hydrogen atoms. The moment of inertia about the axis perpendicular to the plane of the molecule may be written

$$I_c = (a^2 + b^2)m_C + \left\{b^2 + (z - a)^2\right\}m_O + \left\{b^2 + (y + a)^2\right\}m_N + \left\{(y + x\cos\alpha + a)^2 + (x\sin\alpha - b)^2\right\}m_H . \quad (3\text{-}9)$$

The moment of inertia about the axis which is nearly parallel to the NCO axis may be written

$$I_a = m_O\left\{(z - a)\sin\theta - b\cos\theta\right\}^2 + m_C\left\{a\sin\theta + b\cos\theta\right\}^2 + m_N\left\{(y + a)\sin\theta + b\cos\theta\right\}^2 + m_H\left\{x\sin(\alpha - \theta) - (y + a)\sin\theta - b\cos\theta\right\}^2 . \quad (3\text{-}10)$$

When a and b from equations (3-7) and (3-8) are substituted in equations (3-9) and (3-10), the following equations are obtained:

$$I_c = (m_o - m_O^2/W)z^2 + \left\{m_N + m_H - \frac{(m_N + m_H)^2}{W}\right\} y^2 + (m_H - m_H^2/W)x^2 + \frac{2m_O(m_H + m_N)}{W} yz + 2m_O m_H xz\cos\alpha /W + \left\{2m_H - \frac{2m_H(m_N + m_H)}{W}\right\}xy\cos\alpha , \quad (3\text{-}11)$$

and

$$WI_a = m_O(W - m_O)z^2\sin^2\theta + (W - m_N - m_H)(m_N + m_H)\, y^2\sin^2\theta +$$

$$+ m_H(W - m_H)x^2 \sin^2(\alpha - \theta) + 2m_O(m_O + m_N)yz \sin^2\theta \quad (3\text{-}12)$$

$$-2m_O m_H xz \sin\theta \sin(\alpha - \theta) + \{2m_H(m_H + m_N - W)xy\} \cdot$$

$$\cdot\{\sin\theta \sin(\alpha - \theta)\}.$$

The angle θ is itself a function of the parameters which is too complicated to be introduced explicitly. However, we can calculate θ for a trial structure, insert it in the equations for I_a and I_c, and solve for the structure parameters. These parameters may be used to calculate a new value of θ and the iterative process can be repeated until the output θ equals the input θ.

For a set of principal axes, the products of inertia equal zero. We have, therefore, an equation for calculating the angle θ.

$$\sum_i m_i X_i' Y_i' = 0. \quad (3\text{-}13)$$

Equation (3-13) gives the following equation for θ.

$$m_O(z - a)\{(z - a)\sin\theta - b\} + m_C ab +$$
$$+ m_N(y + a)\{(y + a)\sin\theta + b\} - \quad (3\text{-}14)^*$$
$$- m_H\{x \sin(\alpha - \theta) - (y + a)\sin\theta - b\} \cdot$$
$$\cdot\{x\cos\alpha + (y + a) + x\sin\alpha \sin\theta\} = 0.$$

The same trial structure used in evaluating I_c for $HN^{15}C^{12}O^{16}$ and $DN^{14}C^{12}O^{16}$ has been used to calculate θ for all three isotopic species. These values appear in Table VII.

---

* In equation (3-14) $\cos\theta$ has been taken to be unity, although Table VII shows that it is really slightly less.

Table VII. Sin θ and θ for HNCO

Isotopic Species	Sin θ	Cos θ	θ
$HN^{14}C^{12}O^{16}$	.03135	.9995	$1^{\circ}48'$
$HN^{15}C^{12}O^{16}$	.02996	.9995	$1^{\circ}43'$
$DN^{14}C^{12}O^{16}$	.05814	.9983	$3^{\circ}20'$

Values for the atomic weights of the various isotopes and for sin θ were substituted into equations (3-11) and (3-12) in order to obtain the following four equations whose solution yields the structure parameters for HNCO. The atomic weights used were: O^{16}, 16.00000; C^{12}, 12.00389; N^{14}, 14.00751; N^{15}, 15.00493; H^{1}, 1.00813; and H^{2}, 2.01473.

$$\Phi : 10.0492\, z^2 + 9.7745\, y^2 + 11.1693\, zy + .9845\, x^2 + .7499\, xz \cos\alpha + 1.3125\, xy \cos\alpha = 46.2470.$$

$$\Psi : 10.1841\, z^2 + 10.1876\, y^2 + 11.6413\, zy + .9850\, x^2 + .7329\, zx \cos\alpha + 1.2827\, xy \cos\alpha = 47.6692.$$

$$\Pi : 10.1853\, z^2 + 10.1914\, y^2 + 1.9225\, x^2 + 11.6456\, zy + 1.4644\, xz \cos\alpha + 2.5630\, xy \cos\alpha = 50.0557.$$

$$\Gamma : .4250\, z + .4133\, y + 42.3102\, x^2 \sin^2\alpha - 2.6541\, x^2 \sin\alpha \cos\alpha + .0416\, x^2 \cos^2\alpha + .4723\, yz - 1.0108\, xz \sin\alpha + .0317\, xz \cos\alpha - 1.7692\, xy \sin\alpha + .0555\, xy \cos\alpha = 23.6435.$$

E. Solution of the Moment of Inertia Equations.

The method used to solve these equations is due to Newton. The equations can be written in the form

$$\Phi(x,y,z,\alpha) = 0 \quad ; \quad \Pi(x,y,z,\alpha) = 0 \; ;$$

$$\Psi(x,y,z,\alpha) = 0 \quad ; \quad \Gamma(x,y,z,\alpha) = 0 \; .$$

and approximate values x_o, y_o, z_o, and α_o assumed for the roots. True values of the roots are obtained by adding small correction terms.

$$x = x_o + h \; ; \; y = y_o + k \; ; \; z = z_o + m \; ; \; \alpha = \alpha_o + n .$$

Then
$$\Phi (x_o + h, y_o + k, z_o + m, \alpha_o + n) = 0 ,$$
$$\Psi (x_o + h, y_o + k, z_o + m, \alpha_o + n) = 0 ,$$
$$\Pi (x_o + h, y_o + k, z_o + m, \alpha_o + n) = 0 ,$$
$$\Gamma (x_o + h, y_o + k, z_o + m, \alpha_o + n) = 0 .$$

Expand by Taylor's Theorem.

$$\Phi (x_o + h, y_o + k, z_o + m, \alpha_o + n) = \Phi (x_o, y_o, z_o, \alpha_o) + h\left(\frac{\partial \Phi}{\partial x}\right)_o + k\left(\frac{\partial \Phi}{\partial y}\right)_o + m\left(\frac{\partial \Phi}{\partial z}\right)_o + n\left(\frac{\partial \Phi}{\partial \alpha}\right)_o = 0 ,$$

where all second order terms in h,k,m,n have been neglected. Similar equations can be written for Ψ, Π, and Γ. The set of four equations is solved by the method of determinants. For example,

$$h = \frac{\begin{vmatrix} -\Phi_o & \left(\frac{\partial \Phi}{\partial y}\right)_o & \left(\frac{\partial \Phi}{\partial z}\right)_o & \left(\frac{\partial \Phi}{\partial \alpha}\right)_o \\ -\Psi_o & \left(\frac{\partial \Psi}{\partial y}\right)_o & \left(\frac{\partial \Psi}{\partial z}\right)_o & \left(\frac{\partial \Psi}{\partial \alpha}\right)_o \\ -\Pi_o & \left(\frac{\partial \Pi}{\partial y}\right)_o & \left(\frac{\partial \Pi}{\partial z}\right)_o & \left(\frac{\partial \Pi}{\partial \alpha}\right)_o \\ -\Gamma_o & \left(\frac{\partial \Gamma}{\partial y}\right)_o & \left(\frac{\partial \Gamma}{\partial z}\right)_o & \left(\frac{\partial \Gamma}{\partial \alpha}\right)_o \end{vmatrix}}{\begin{vmatrix} \left(\frac{\partial \Phi}{\partial x}\right)_o & \left(\frac{\partial \Phi}{\partial y}\right)_o & \left(\frac{\partial \Phi}{\partial z}\right)_o & \left(\frac{\partial \Phi}{\partial \alpha}\right)_o \\ \left(\frac{\partial \Psi}{\partial x}\right)_o & \left(\frac{\partial \Psi}{\partial y}\right)_o & \left(\frac{\partial \Psi}{\partial z}\right)_o & \left(\frac{\partial \Psi}{\partial \alpha}\right)_o \\ \left(\frac{\partial \Pi}{\partial x}\right)_o & \left(\frac{\partial \Pi}{\partial y}\right)_o & \left(\frac{\partial \Pi}{\partial z}\right)_o & \left(\frac{\partial \Pi}{\partial \alpha}\right)_o \\ \left(\frac{\partial \Gamma}{\partial x}\right)_o & \left(\frac{\partial \Gamma}{\partial y}\right)_o & \left(\frac{\partial \Gamma}{\partial z}\right)_o & \left(\frac{\partial \Gamma}{\partial \alpha}\right)_o \end{vmatrix}} .$$

Similar equations can be written for k, m, and n.

The values assumed for the roots in the zero approximation were: $x_o = .9797$ Å, $y_o = 1.207$ Å, $z_o = 1.172$ Å, and $\alpha_o = 52^\circ 26'$. These yielded the following values for the first approximation roots: $x_1 = .9872$ Å, $y_1 = 1.2065$ Å, $z_1 = 1.1707$ Å, and $\alpha_1 = 51^\circ 55'$.

At this point, minor changes in the I_c and I_a values were made, using the first approximation for a trial structure. The Newton approximation was carried out once again, leading to the final result: $x_2 = .9873$ Å, $y_2 = 1.2068$ Å, $z_2 = 1.1710$ Å, and $\alpha_2 = 51^\circ 55'$.

The structure of HNCO as determined from the combined data of microwave and infrared investigations and with an estimate of the limits of error is:

r_{N-H}	$.987 \pm .01$ Å,
r_{N-C}	$1.207 \pm .01$ Å,
r_{C-O}	$1.171 \pm .01$ Å,
r_{N-O}	$2.378 \pm .002$ Å,
Angle H-N-C	$128^\circ 5' \pm 1^\circ$.

F. Discussion of Errors.

Zero point errors discussed in Section II account for most of the uncertainty in the structure determination, although the measurement of I_a by Jones to one part in three hundred lacks the precision required to fix the position of the hydrogen atom more closely than within about .002 Å of its true position. All microwave measurements are sufficiently precise that uncertainties from this source are negligible.

The magnitude of zero point errors is extremely difficult to estimate. The presence of both stretching and bending vibrations complicates the problem. Rotation-vibration interaction constants, α_i^B, for the effect of the normal modes of vibration on the intermediate moment of inertia have been measured for all six of the normal modes, α_1^B to α_4^B by infrared techniques (35), and α_5^B and α_6^B by microwave measurements of the excited vibrational states given in Table V of this thesis. Numerical values for the α_i^B are such that the effect of the two N-C-O bending vibrations nearly cancels that of the hydrogen stretching vibration. The effect of the N-H rocking against the N-C-O group, about 9 mc/sec, is small and of opposite sign to the effect of the remaining two vibrations which correspond to the symmetric and antisymmetric stretching vibrations in a molecule like CO_2. The anharmonicity of these vibrations is apparently fairly high. B_0 in HNCO is shifted about 50 mc/sec away from B_e.

Substitution of deuterium for hydrogen will no doubt change the α_i^B enough to introduce a considerable error in the measurement of B_0 for DNCO relative to B_0 for HNCO. Since the isotopic shift, $I' - I$, is 1587 mc/sec, we can stand a fairly large absolute error without incurring a serious percentage error. The distance of the hydrogen from the center of mass will be roughly proportional to the square root of $I' - I$. Consequently, the percentage error in the distance will be half of the percentage error in the measurement of $I' - I$. If the effect of the α_i^B for HNCO and DNCO differs by as much as, say, 30 percent in going from the one isotopic molecule to the other, we incur an error of only one percent in $I' - I$, and only 0.5 percent in the distance of the

hydrogen from the center of mass. This is equivalent to an absolute error of 0.01 Å in the position of either the hydrogen atom or the center of mass of the molecule.

The contribution to the large moment of inertia, I_c, of the N and O atoms together is a very slowly changing function of the position of the center of mass, because as the contribution from one increases, the contribution from the other decreases as we move the center of mass along the line joining the two atoms. The carbon atom is so near the center of mass that its contribution to the moment of inertia is negligible; consequently, its position is not known any more accurately than that of the center of mass. Thus, although the data fix the position of the hydrogen atom with respect to the N-C-O group, they would be satisfied by locating the center of mass (and the carbon atom with it) anywhere along the N-C-O axis within 0.01 Å of the place where we have now located it. The N-H, N-C, and C-O distances must accordingly be considered uncertain by this amount.

The N and O atoms contribute so much to the moment of inertia that their position relative to one another is determined quite accurately, probably to within .002 Å.

Uncertainty in the H-N-C angle equivalent to .01 Å in the N-H distance is approximately one degree.

4. Electric Quadrupole Effects.

Examination of the $0_{0,0}-1_{0,1}$ transition of $HN^{14}C^{12}O^{16}$ under conditions resulting in highest resolving power revealed a triplet structure. This is due to the interaction of the electric quadrupole moment of the nitrogen nucleus with the molecular electric field.

Nitrogen possesses a nuclear spin of $I = 1$. Its nuclear angular momentum is then

$$\hbar \sqrt{I(I+1)} \text{ erg sec}.$$

This nuclear angular momentum vector, I, adds to the rotational angular momentum vector, J, according to the general rules for vector addition to give the total angular momentum vector

$$F = (J + I),\ (J + I-1),\ (J + I-2),\ \cdots\cdots |J - I|.$$

Bragg (36) has given an expression for the interaction energy of a single nuclear electric quadrupole moment with the gradient of the electric field in an asymmetric molecule. For a molecule like HNCO which is very nearly linear, this expression reduces to that for a linear molecule for the levels $0_{0,0}$ and $1_{0,1}$.

$$W = -eQ\left(\frac{\partial^2 V}{\partial z^2}\right) \frac{\frac{3}{4}C(C+1) - I(I+1)J(J+1)}{2I(2I-1)(2J-1)(2J+3)}, \tag{4-1}$$

where $$C = F(F+1) - I(I+1) - J(J+1),$$

and $eQ\left(\frac{\partial^2 V}{\partial z^2}\right)$ is a scale factor for the splitting of the energy levels described in Part I,7, where $\left(\frac{\partial^2 V}{\partial z^2}\right)$ is now the second derivative of the electric potential along the molecule fixed z axis, the principal axis of least moment of inertia. The quantity $\left(\frac{\partial^2 V}{\partial z^2}\right)$ will hencefforth be referred to as q.

Selection rules which apply for transitions between the split levels are: $\Delta J = +1$, $\Delta F = 0, \pm 1$.

In order to resolve lines which are as close together as 0.35 mc/sec it was necessary to modify the usual experimental technique.

Line widths were reduced to a minimum by lowering the pressure to 10^{-4} mm of Hg and the temperature to 195° K. Collision and Doppler broadening were thereby minimized. Sweep rates as low as 2 cycles per second were required to avoid broadening of the lines by distortion in the amplifier circuits when oscilloscope presentation was used.

A special gear train was installed on the frequency control of the 2K-50 klystron so that the frequency of the source could be varied as slowly as 6 mc/min. With the Esterline Angus recording meter running at 12" per minute, a scale of two inches per megacycle was obtained.

The $0_{0,0} - 1_{0,1}$ transition in $HN^{14}C^{12}O^{16}$ is shown under high resolution in Figure 14. This recording meter trace establishes the sign of eQq as positive, since the highest frequency component is less widely split and is of higher intensity than the lowest frequency component. Frequency measurements were made on the cathode ray oscilloscope by superimposing a "pip" from the harmonic frequency standard on one of the lines, reading the receiver frequency, tuning the receiver until the "pip" was superimposed on another of the lines, and repeating this process until all three of the lines had been measured relative to one another. Receiver frequency readings and relative intensities for the three components of the triplet are recorded in Table VIII.

Table VIII. Hyperfine components of $0_{0,0} - 1_{0,1}$ Transition in $HN^{14}C^{12}O^{16}$

Transition J = 0 → 1	Receiver Frequency (mc)	Observed Rel. Int.	Theoretical (37) Rel. Int.
F = 1 → 0	-6.75 ± .02	1	1
F = 1 → 2	-5.85 ± .05	5	5
F = 1 → 1	-5.25 ± .02	3	3

Figure 14 shows an energy level diagram and a comparison of the observed and theoretical spectra. Evaluation of the coefficient of eQq in equation (4-1) makes it possible to calculate this quantity from the measured separation of the hyperfine components. The two most widely separated lines are calculated to lie 0.75 eQq mc apart, which requires that eQq be 2.00 $\pm$ .05 mc in this molecule. Since the principal axis and the molecular N-C-O axis nearly coincide, this value is the quadrupole coupling constant along the N-C-O axis.

It appeared to be desirable to measure the value of eQq in HNCS in order to determine if the molecular fields in HNCO and HNCS are similar as we would predict from a consideration of the bonding in the two compounds. Accordingly, frequency measurements under high resolution were made for the $1_{1,1}$-$2_{1,2}$ transition in $HN^{14}C^{12}S^{32}$ at 23,499.5 mc. The HNCS was generated by heating a mixture of thoroughly dried KSCN and $NaHSO_4$ and passing the evolved gas directly into the waveguide.

The $1_{1,1}$-$2_{1,2}$ transition in HNCS is a $\Delta J = +1$, $\Delta K = 0$, $K = 1$ transition. In a symmetric top, such a transition would be degenerate with two others; here, however, the three lines appear at slightly different frequencies. The quadrupole interaction energy for each of the energy levels involved in this transition reduces to that for the limiting symmetric top.

$$\Delta W = eQq\left\{\frac{3K^2}{J(J+1)} - 1\right\}\frac{\frac{3}{4}C(C+1) - I(I+1)J(J+1)}{2I(2I-1)(2J-1)(2J+3)}. \qquad (4\text{-}2)$$

The symbols in this expression have the same significance as in the expression for a linear molecule except that the rotational quantum number

K modifies the rotational dependence.

A recording meter trace was obtained which establishes the sign of eQq in HNCS as positive; this is verified by comparison with the theoretical pattern calculated for a positive coupling constant in Figure 15.

Frequency measurements made on the cathode ray oscilloscope with the harmonic frequency standard are given in Table IX.

Table IX. Hyperfine Components of $1_{1,1}-2_{1,2}$ Transition in $HN^{14}C^{12}S^{32}$

Transition $J = 1 \rightarrow 2$	Receiver Frequency(mc)	Observed Rel. Int.	Theoretical(37) Rel. Int.
$F = 1 \rightarrow 2$	$+11.85 \pm .05$	43	50
$F = 2 \rightarrow 3$	$+11.50 \pm .02$	100	100
$F = 0 \rightarrow 1$	$+11.00 \pm .20$	15	24

In order to fit the theoretical pattern to the observed separation of the two strongest lines in the multiplet, the $F = 1 \rightarrow 2$ and the $F = 2 \rightarrow 3$ lines, a value for eQq of $1.2 \pm .20$ mc for HNCS is required.

In Table X the values of eQq are given for various compounds containing nitrogen on the molecular axis.

All of the compounds in which nitrogen has an unshared pair of electrons on the molecular axis have coupling constants of the order of - 4 mc. On the other hand, isocyanic and isothiocyanic acids possess small positive coupling constants. The similarity of these values in the two molecules and the difference between these and the values in

Table X. N^{14} Nuclear Quadrupole Coupling Constants

Molecule	eQq (mc)
HCN	- 4.58[a]
CH_3CN	- 4.67[b]
ClCN	- 3.67[c]
BrCN	- 3.83[c]
ICN	- 3.80[c]
HNCS	+ 1.2
HNCO	+ 2.00

[a] See reference (38). [b] See reference (26). [c] See references (39) and (21)

the various cyanides listed in Table X lead to two qualitative conclusions: 1. Bonds to nitrogen in isocyanic acid are similar to those in isothiocyanic acid, and 2. These bonds are in both cases quite dissimilar to the -C≡N bond which would be formed if the molecules were HOCN and HSCN. Therefore, the alternative structures HNCO and HNCS are indicated.

5. Discussion of the Structure of HNCO.

The order of atoms, H-N-C-O, determined by comparison of HNCO and HNCS hydrogen stretching frequencies, has been shown to be consistent with the observed hyperfine structure. In order to calculate accurate values for the bond distances and bond angle it was necessary to assume that the NCO group does not depart appreciably from linearity. This has been demonstrated by infrared and electron diffraction studies

and is consistent with the fact that the three important structures contributing to resonance in this molecule should be linear. Following the procedure outlined by Pauling (40), the approximate contributions of each of these structures to the hybrid structure in order to satisfy the observed bond distances are:

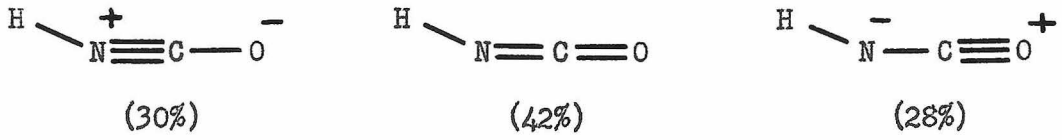

(30%) (42%) (28%)

It is interesting to note that Badger's rule accurately predicts a value of .987 Å for the N-H bond length from the N-H stretching frequency in HNCO, if the stretching frequency and bond length in NH_3 are taken as reference values.

The absorption line presently attributed to molecules in the excited vibrational state $v_6 = 1$ possesses a Stark effect with a slightly different magnitude than the rest of the observed lines. This line could conceivably be due to absorption by the molecular species HOCN. Relative intensity measurements place an upper limit of 4 percent upon the abundance of HOCN.

V. THE STRUCTURE OF CF_3-C≡C-H FROM MICROWAVE AND ELECTRON DIFFRACTION STUDIES.

Recent microwave studies (41, 42, 43) of linear acetylenes show a pronounced shortening of the C-C single bonds adjacent to the triple bonds. Carbon compounds containing fluorine often show anomalously short C-F bonds. Trifluoromethyl acetylene represents an interesting case in which both of these influences are at work.

A sample of trifluoromethyl acetylene was obtained from Professor

A. L. Henne of Ohio State University. Some of this material was converted into CF_3CCD by condensing several cubic centimeters of the vapor (s. t. p.) into a tube containing one cc of a 50 percent solution of NaOH in D_2O. Approximately 50 percent conversion was obtained overnight. Isotopic species in which C^{13} is substituted for one of the C^{12} atoms are present in 1.1 percent natural abundance.

1. The Microwave Spectrum.

Trifluoromethyl acetylene is expected to be a symmetric top similar to methyl acetylene (41). Observation of a simple microwave spectrum indicates that this is indeed the case. The $J = 3 \longrightarrow 4$ rotational transitions of several isotopic species were found with the Stark modulated spectroscope and their frequencies were measured with the harmonic frequency standard. These are given in Table XI. A recording meter trace of the absorption for the species CF_3CCH appears in Figure 16. A complicated excited vibrational state structure can be seen quite clearly. Although the recording meter trace makes the lines appear to be quite narrow, they are several megacycles wide when viewed under high resolution. Lines of the same J and different K values should appear at slightly different frequencies, but are not resolved. This results in a broadening of the lines and limits the accuracy of the frequency measurements.

2. Identification of Lines.

Most of the measurements were made with the square wave amplitude set at 10 to 20 volts and with the bottom of the square wave based on ground. A first order Stark effect was observed. However, the rotational transition of CF_3CCH in the ground vibrational state was resolved

Table XI. Measured Frequencies for the J = 3 → 4 Transition in Several Isotopic Species of CF_3CCH

Species	Transition	Frequency* (mc/sec)
CF_3CCH	J = 3 → 4 Ground state	23,023.4
	J = 3 → 4 Excited state	23,053.5
	v_{10} = 1	23,067.7
	(-C-C≡C- bending)	23,082.4
	J = 3 → 4 Excited state	23,111.2
	v_{10} = 2	
	J = 3 → 4 Excited state	23,153.0
	v^{10} = 3	
$CF_3C^{13}CH$	J = 3 → 4 Ground state	22,839.9
$CF_3CC^{13}H$	J = 3 → 4 Ground state	22,301.0
CF_3CCD	J = 3 → 4 Ground state	21,568.2

* Absolute frequencies are measured to ± 0.3 mc. Relative frequencies are measured to ± 0.1 mc.

into its four second order Stark components by the application of 700 volts D C to the Stark electrode in addition to the square wave modulation. This identifies it as the $J = 3 \rightarrow 4$ transition. The corresponding transitions in the isotopic species $CF_3C^{13}CH$ and $CF_3CC^{13}H$ were identified by their appearance near the predicted frequencies, possession of first order Stark components, and the presence of excited vibrational state absorptions at slightly higher frequencies. These excited vibrational lines can be seen clearly in Figure 17.

From relative intensity measurements at room and dry ice temperatures the five lines between 23,053.5 and 23,152.9 mc are shown to arise from $J = 3 \rightarrow 4$ rotational transitions in CF_3CCH molecules with the degenerate bending vibration ν_{10} excited. Assignments are given in Table XI.

3. Rotational Constants.

Rotational constants and moments of inertia for the ground vibrational state of four different isotopic species of CF_3CCH are given in Table XII.

Table XII. Rotational Constants for Various Isotopic Species of CF_3CCH in the Ground Vibrational State

Species	B_o (mc/sec)	I_B (a.m.u.-$\AA^2$)
CF_3CCH	2877.93 ± .04	175.61_3
$CF_3C^{13}CH$	2854.99 ± .04	177.02_4
$CF_3CC^{13}H$	2787.63 ± .04	181.30_2
CF_3CCD	2696.02 ± .04	187.46_4

Centrifugal stretching at low values of J and K is not appreciable except in very light molecules which are rotating at high frequencies. Values of B_o in Table XII were calculated from the following equation in which centrifugal stretching terms have been omitted:

$$\nu = 2B_o J'.$$

J' is the higher of the two J values involved in the transition.

4. Microwave Contribution to the Determination of the Molecular Structure.

A derivation given in Appendix I shows that for a molecule with a figure axis the distance of a particular atom on that axis from the center of gravity of the unsubstituted molecule is given by

$$z = \left\{(I' - I)(M + \Delta m)/ M \Delta m\right\}^{\frac{1}{2}}, \qquad (4\text{-}1)$$

where I' - I is the difference in the moments of inertia for the unsubstituted molecule and one in which the particular atom has been replaced by a different isotope, M is the original molecular weight, and Δ m is the increase in mass as a result of the substitution.

The total moment of inertia of the symmetric top

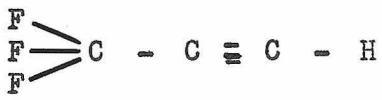

may be written

$$I_B = \frac{3}{2} m_F X_F^2 + 3m_F Z_F^2 + m_C Z_C^2 + m_C Z_{C'}^2 + m_{C''} Z_{C''}^2 + m_H Z_H^2, \qquad (4\text{-}2)$$

where X_F is the perpendicular distance of the F atoms from the figure axis, and the Z's are the components of the distance of each atom from the center of mass measured along the figure axis.

Interatomic distances were computed using the following atomic weights: H, 1.00813; D, 2.01471; C, 12.00382; C^{13}, 13.00761; and

F, 19.00450. From equation (4-1) and the data of Table XII the distances from the center of mass of the reference molecule $CF_3C^{12}C^{12}H$ for each of the atoms C', C", and H were obtained. These are: $Z_{C'}$, 1.192 Å; $Z_{C''}$, 2.393 Å; Z_H, 3.449 Å. One can immediately obtain the C≡C and C-H bond lengths by the process of subtraction.

$$r_{C\equiv C} = 1.201 \pm .002 \text{ Å};$$

$$r_{C-H} = 1.056 \pm .005 \text{ Å}.$$

In estimating these limits of error, the equation for the uncertainty in Z as a function of the uncertainty in the moment of inertia has been used. (Section II, equation 1-2) The uncertainty in the moment of inertia that we are interested in is that which arises from neglect of the change of zero point vibration amplitude with change of isotope. In the case of a light hydrogen atom attached to a massive molecule as we have here, the effect of a deuterium substitution should be similar to that in the case of HCl and DCl, for which an actual shift of .002Å in the average internuclear distance was observed (p. 397, ref. 5). In order to get an order of magnitude estimate of the error in CF_3CCH we assume an actual shift of .002A in the average length of the C-H bond, even though the force constants and anharmonicities are not exactly the same for the H-C≡ and H-Cl bonds. The error in the moment of inertia introduced by neglecting such a shift is .028 a.m.u. Å^2, which is equivalent to a computational error of .004 Å in the distance of the hydrogen atom from the center of mass. The carbon atoms are much more massive, hence a substitution which changes their mass by one part in 12 will have much less effect than the substitution of deuterium for hydrogen. However, the carbon atoms do enter into a

larger number of normal vibrations, all of which affect the moment of inertia. Fortunately, the effects of the bending and stretching vibrations tend to oppose one another. A reasonable estimate of the uncertainty of the distance of the carbon atoms from the center of mass is .001 Å. These estimates lead to the limits of error in the bond distances listed above.

There are five structural parameters in CF_3CCH, but moment of inertia measurements have been made for only four isotopic species. The structural determination cannot be completed without additional information. However, no infrared moment of inertia measurements have been made for this compound. In order to solve this problem, the following procedure was devised, based on the fact that electron diffraction photographs of this compound had been taken. Since the C-H and C≡C distances have already been eliminated, the problem is reduced to one of calculating two of the remaining three parameters as a function of the third. This relationship would be expected to reduce the region of parameter space which must be investigated in the electron diffraction study so that a rapid and accurate completion of the structural determination could be brought about.

By assuming a series of values for the F-C-F angle, the C-C and C-F distances can be calculated for each assumed value, and a functional relationship between the three can be displayed graphically. This calculation has been carried out with the aid of equation (4-2), using the value of I_B for the species $CF_3C^{12}C^{12}H$. The results are plotted in Figure 18. Each and every set of three parameters obtained by intersecting the two curves and the horizontal coordinate axis of Figure 18

by a vertical line is consistent with the measured moments of inertia for CF_3CCH.

A detailed account of the electron diffraction technique will not be given here. The suggested procedure was to calculate from the data of Figure 18 and the C≡C and C-H distances a series of electron diffraction intensity curves for different values of the F-C-F angle. There should be only a small range of F-C-F angles which give theoretical curves closely resembling the observed visual curve. Mr. William F. Sheehan, Jr., calculated the necessary theoretical curves and compared them with the visual curve. His results are given in Table XIII.

Table XIII. Structure of Trifluoromethyl Acetylene

Parameter	Value	Sum of covalent radii
C-F	1.335 ± .01 Å	1.375 Å
C-C	1.464 ± .02 Å	1.540 Å
FCF angle	107.5° ± 1°	
C≡C	1.201 ± .002 Å	1.204 Å
C-H	1.056 ± .005 Å	1.10 Å

The C-F and C-C distances are more uncertain than the distances determined solely by microwave methods because the electron diffraction data only restrict the other parameters to a region of parameter space large enough to introduce the stated uncertainties.

5. Discussion of the Structure.

All of the bonds are shortened somewhat from the normal sum of the covalent radii. The C-H shortening is probably due to more s and

less p character in the C-H bond, since the multiple bond requires extra p character. This same effect could also account for .05 Å of the C-C bond shortening. The other .03 Å shortening is probably due to double bond character arising from structures like

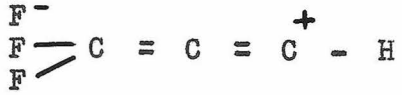

The high force constant of the triple bond prevents it from being lengthened a like amount. On the other hand, structures of the type

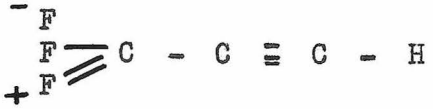

contribute to the shortening of the C-F bond.

An interesting property of the CF_3CCH molecule is its extremely low frequency bending vibration, ν_{10}. From the frequencies of the absorption lines given in Table XI for the excited state $v_{10} = 1$ and Gordy's (44) solution of Neilsen's (45) secular equation for ℓ-type doubling of excited vibrational states it was possible to conclude that the bending vibration, ν_{10}, must be around 170 cm^{-1}. Relative intensity measurements at 300° K. of the $v_{10} = 2$ and $v_{10} = 0$ (ground state) absorption lines at 23,153.0 and 23, 023.4 mc show that the populations of these states are in the ratio 24/40. If we assume a Boltzmann distribution of vibrational states, the value 170 cm^{-1} is again obtained for ω_{10}.

VI. ELECTRIC DIPOLE MOMENTS FROM STARK EFFECT MEASUREMENTS.

Detailed studies of the Stark effect on the rotational energy levels of molecules as a function of the applied electric field lead to a determination of their electric dipole moments. These dipole moments have somewhat more significance than those which are determined by the usual method of measuring the dielectric constant as a function of the temperature. There are two reasons for this: 1. The dipole moment is measured for a particular state of the molecule, and 2. Impurities have absolutely no effect upon the result of the measurement.

In the course of the structural determinations of HNCO and CF_3CCH it was important to resolve the second order Stark structure of the spectrum. Quantitative measurements of the shift of the rotational absorption lines were made while a D C electric field parallel to the E-vector of the radiation was applied between the central Stark electrode and the walls of the absorption cell. Additional experimental techniques were employed and will be described briefly.

1. Experimental Technique.

It has been pointed out in an earlier section that the steel Stark electrode is carefully centered in the waveguide by slotted teflon strips. Special attention was given to the problem of maintaining a uniform electrode spacing. If variations in spacing of as much as a few thousandths of an inch occur, the electric field will be non-uniform and the absorption lines will be broadened and even doubled. A small amount of broadening does no harm since the center frequency is not greatly shifted, but doubling of the lines results in a reduction in intensity and inaccuracy in frequency measurements. The teflon strips

were grooved precisely in the center and were machined to a press fit in the narrow dimension of the waveguide. A piano wire served to pull the entire electrode assembly into place.

No electronic clamping is employed when Stark effect measurements are being made; instead, the 50 kc square wave is allowed to center itself about the d.c. potential. The displacement of the absorption line is taken as the average of the displacements caused by the top and bottom of the square wave. This introduces a small second order error which can be corrected. We measure a displacement which equals

$$\tfrac{1}{2}K \left\{ (E_o + E)^2 + (E_o - E)^2 \right\}$$

and call it KE_o^2, where E_o is the d.c. voltage and E is the square wave amplitude. The difference is KE^2. Fractionally, this is a small quantity, E^2/E_o^2, which makes the true values of the displacements smaller than measured values by 0.11 percent for the usual value of $E/E_o \approx 1/30$.

Measurements of the d.c. field were made by connecting a 10,000:1 precision (.01%) voltage divider from the Stark electrode to ground. A Leeds and Northrup type 8662 portable precision potentiometer was employed to determine the voltage across the small arm of the divider. The accuracy of this measurement was around .02 percent and errors from this source are negligible.

A determination of the spacing in the waveguide may be made by direct measurement of the electrode thickness and inside dimensions of the waveguide. The narrow dimension of the waveguide is claimed by the manufacturer not to vary more than .001 inch from .400 inch. In the present absorption cell, the electrode is spaced .432 $\pm$ .025 cm from the cell walls on either side.

Shulman (46) has considered errors arising from inhomogeneities in the electric field due to curvature near the edges of the electrode. He points out that the intensity of microwave radiation in the TE_{01} mode varies with y, the distance from the longitudinal axis, as $\sin^2 \pi y/a$, where a is the width of the waveguide. Therefore, most of the microwave absorption takes place in a region of uniform field. He calculated the integrated effect of the inhomogeneity and found that in a waveguide and electrode assembly similar to that used here the true values of dipole moments will be 0.6 percent lower than the measured values.

Stark effects have been studied for six different molecular species. This work was done with two different spectroscopes, the instrument at the California Institute, and one which the author built during the summer of 1950 at the General Electric Research Laboratory in Schenectady, New York. Since all of the absorption lines studied are well identified transitions, the purity of the samples need not be discussed, although in no case were any unexplained lines observed. All measurements were made with the absorption cells packed in dry ice and with gas pressures in the vicinity of 50 microns.

At the time of taking the data, all frequencies were reduced to values of $\Delta \nu_M$, the displacement of the M^{th} Stark component, and all voltage measurements were reduced to the corresponding field strengths in the waveguide and recorded as the square of the field strength in $(ESU/cm)^2$. These data are tabulated separately for the six molecular species studied; namely, HNCO, DNCO, H_2CO, CHF_3, OCS, and CF_3CCH.

2. Calculations.

In all of the following cases the selection rule $\Delta M = 0$ applies.

A. OCS.

Carbon oxysulfide is a linear molecule for which the Stark splitting is given by equation (I, 8-3). When appropriate numerical factors are inserted, we have for the M = 0 and M = 1 components of the J = 1 → 2 transition

$$\mu^2 = -3.502 \quad \Delta\nu_0/E^2 \quad (M = 0, J = 1);$$
$$\mu^2 = +4.311 \quad \Delta\nu_1/E^2 \quad (M = 1, J = 1).$$

B. HNCO.

Isocyanic acid is a slightly asymmetric rotor. However, the matrix elements connecting the initial and final states of the $0_{0,0}$-$1_{0,1}$ transition with other allowed states through the component of the dipole moment perpendicular to the N-C-O axis involve energy changes of about 30 cm^{-1} corresponding to the acquisition of angular momentum about the principal axis of least moment of inertia. Rough calculations show the effect of these matrix elements to be about one thousandth as large as for those corresponding to the second order change in energy due to the component of the dipole moment along the N-C-O axis. Equation (I, 8-3) for a linear molecule is again applicable and, taking account of slight differences in frequency, we have for the three observed vibrational states the component of μ parallel to the N-C-O axis:

Ground state: $\mu^2 = 1.8085 \quad \Delta\nu_0/E^2$, (J 0,M 0)

Excited state: (v_5 1) $\mu^2 = 1.8120 \quad \Delta\nu_0/E^2$, (J 0,M 0)

Excited state: (v_6 1) $\mu^2 = 1.8095 \quad \Delta\nu_0/E^2$, (J 0,M 0).

C. DNCO.

The perpendicular component of the dipole moment in deutero-isocyanic acid makes a contribution to the Stark effect which is twice as

large as that in HNCO. It may still be safely neglected and the component of the dipole moment parallel to the principal axis of least moment of inertia is obtained from the following equation:

Ground state: $\mu^2 = 1.6780 \ \Delta\nu_o / E^2$, $(J = 0, M = 0)$.

D. H_2CO.

Formaldehyde, like HNCO, is a slightly asymmetric rotor. In order to calculate the Stark effect for this molecule it is necessary to determine the squared direction cosine matrix elements, $\left| (\Phi_{Zg})_{J\tau M, J'\tau' M} \right|^2$, appearing in equation (I, 8-6). For the transition $9_{2,8}$-$9_{2,7}$, only the two states involved in the transition lie close enough together in energy to contribute appreciably to the second order Stark effect.

The computation of the direction cosine matrix elements requires the asymmetric rotor eigenfunctions for the states involved. These eigenfunctions are linear combinations of the eigenfunctions for the limiting symmetric rotor.

$$\Psi^A_{J\tau M} = \sum_{JKM} a_{JKM} \Psi^S_{JKM} .$$

It has already been shown in Section I, Part 3, that the asymmetric rotor energy levels are the solutions of secular equations of order $2J + 1$ for a given J. King, Hainer, and Cross (47) have shown how to find the roots of this secular equation. When the roots corresponding to the levels $9_{2,8}$ and $9_{2,7}$ have been calculated, they may be put back into the set of simultaneous equations

$$\sum_K a_K \left(H_{K';K} - E \ \delta_{K';K} \right) = 0 ,$$

where J and M have been dropped because the energy is diagonal in J and does not depend upon M. The solution of this set of equations gives

the coefficients in the symmetric rotor expansion of the asymmetric rotor eigenfunctions for the levels $9_{2,8}$ and $9_{2,7}$. Because of symmetry considerations, only symmetric rotor eigenfunctions with even K values can contribute to these levels.

Energy terms E($\varkappa$) of reference (47) have been calculated for the levels $9_{2,8}$ and $9_{2,7}$ using the methods outlined therein. These are: $9_{2,8}$, -80.35752; $9_{2,7}$, -80.17328. The asymmetric rotor expansion coefficients were then evaluated.

$$\Psi^{A}(9_{2,8}) = .9994\, S_2^- - .0330\, S_4^- \;;$$

$$\Psi^{A}(9_{2,7}) = .1493\, S_0 + .9882\, S_2^+ - .0329\, S_4^+ .$$

The $S_K^{\pm}$ are the Wang (47) functions for the limiting symmetric rotor.

Table I of reference (16) gives the matrix elements of the direction cosines for symmetric top functions from which the matrix element

$$\left| \int \Psi^{A*}(9_{2,8}) \cos\theta\, \Psi^{A}(9_{2,7})\, d\tau \right|^2 = \frac{K_{eff}^2\, M^2}{J^2(J+1)^2}$$

is evaluated. K_{eff} is determined by the expansion coefficients given above for the asymmetric rotor eigenfunctions and has the value $(3.92)^{\frac{1}{2}}$ for the levels $9_{2,8}$ and $9_{2,7}$.

The $9_{2,8}$ and $9_{2,7}$ levels move equal distances in opposite directions under an applied field, giving a total Stark shift of

$$\Delta\nu = \frac{2\mu^2 E^2}{\nu_0} \frac{K_{eff}^2\, M^2}{J^2(J+1)^2} .$$

Insertion of appropriate numerical factors gives

$$\mu^2 = 16.30\ \Delta\nu_8/E^2 , \quad (M = 8 \text{ component}) ;$$

$$\mu^2 = 12.88\ \Delta\nu_9/E^2 , \quad (M = 9 \text{ component}) .$$

E. CHF_3.

Fluoroform is a symmetric top molecule for which the Stark splitting is given by equation (I, 8-5). For the J = 0 → 1 transition at 20,697 mc ,

$$\mu^2 = 1.7027\ \Delta\nu/E^2 \qquad (J = 0, M = 0) .$$

F. $CF_3C{\equiv}CH$.

The J = 3 → 4 rotational transition was observed for trifluoromethyl acetylene. This transition possesses both first and second order Stark effect; however, when either K or M equals zero, only a second order effect is observed. Instead of measuring the displacements for the various values of the quantum number M, one may equally well measure the difference in the displacements for different values of M. Equation (I, 8-5) with appropriate numerical factors gives

$$\mu^2 = 8.76\ (\nu_3 - \nu_1)/E^2 , \quad (M = 3 \text{ and } M = 1 \text{ components});$$

$$\mu^2 = 14.0\ (\nu_3 - \nu_2)/E^2 , \quad (M = 3 \text{ and } M = 2 \text{ components}) .$$

3. Results.

Tables XIV through XXII list the observed shifts in frequency at several different field strengths for each of the compounds studied. The quantity $\Delta\nu/E^2$ was tabulated and averaged before the dipole moments were calculated, which tends to weight the higher values for the dipole moments more heavily than the lower values, but not significantly.

Table XXIII presents the final values of the dipole moments obtained for each compound. The error quoted is the sum of the precision error of the particular measurement and the systematic errors. These are: Electrode spacing, ± 0.2 percent (G. E.), ± 0.6 percent (Cal. Tech.); Voltage divider, ± 0.06 percent (G. E.), ± 0.01 percent

(Cal. Tech.); Error in the displacement due to error in the measurement of the undisplaced frequency of the absorption line, ± 0.1 percent. The precision error is taken as the average deviation from the mean divided by the square root of the number of measurements.

A reduction of 0.7 percent has been applied to the calculated dipole moments to account for field inhomogeneities and other small errors discussed under experimental technique.

4. Discussion.

A number of dipole moments have been measured considerably more accurately than it is possible to do with conventional techniques. When our understanding of the electric charge distribution in molecules has advanced to the point where we can compute theoretical values for their dipole moments, it is hoped that these measurements will serve as a check on the theory. The measurement of OCS agrees within experimental error with that obtained earlier by Shulman (46). Carbonyl sulfide should prove to be a convenient compound for calibrating a microwave spectroscope in which the systematic errors have not been determined by direct measurement.

Isocyanic acid was investigated in several vibrational states. The vibrational state $v_5 = 1$ appears to have very nearly the same dipole moment as the ground state. The state $v_6 = 1$ has a radically different electric moment, so different that doubt is cast on the assignment of the line and the possibility of 4 percent abundance of the molecular species HOCN must be considered. If the vibrational assignment be assumed correct, then the higher energy of this mode of bending in

HNCO (out of the plane of the molecule) must be associated with a small change in the electric charge distribution, possibly interpretable in terms of a change in the resonance hybrid structure.

Table XIV. Stark Effect for OCS in Ground State. (G.E.)

$\Delta\nu_0$ (mc)	$\Delta\nu_1$ (mc)	$(ESU/cm)^2$	$\Delta\nu_0/E^2$	$\Delta\nu_1/E^2$
-1.22	1.00	8.335	-.1463	.1200
-1.44	1.17	9.803	-.1469	.1194
-1.84	1.52	12.698	-.1450	.1198
-2.20	1.80	15.039	-.1463	.1197
-2.63	2.13	17.978	-.1463	.1185
-3.05	2.52	20.940	-.1457	.1203
-3.58	2.92	24.354	-.1470	.1199
-4.06	3.38	27.826	-.1459	.1215
	4.10	34.152		.1200
	4.70	39.263	———	.1197
		Average	-.1462 ± .0005	.1199 ± .0005

Table XV. Stark Effect for HNCO in Ground State. (Cal. Tech.)

$\Delta\nu$ (mc)	$(ESU/cm)^2$	$\Delta\nu/E^2$
8.96	6.60	1.358
9.04	6.53	1.383
25.74	18.62	1.382
25.63	18.90	1.357
19.04	13.75	1.386
9.83	7.18	1.369
15.84	11.57	1.370
	Average	1.372 ± .003

Table XVI. Stark Effect for HNCO in Ground State. (G.E.)

$\Delta\nu$ (mc)	$(ESU/cm)^2$	$\Delta\nu/E^2$
12.90	9.237	1.3965
16.48	11.506	1.4323
20.74	14.565	1.4239
23.04	16.218	1.4207
27.45	19.285	1.4234
31.75	22.330	1.4218
36.59	25.828	1.4167
41.84	29.749	1.4064
47.00	33.360	1.4089
55.42	39.456	1.4046
66.92	47.403	1.4117
59.64	42.259	1.4113
52.89	37.148	1.4238
46.19	32.571	1.4181
40.22	28.494	1.4115
34.79	24.366	1.4278
29.68	20.623	1.4391
24.28	17.078	1.4217
19.58	13.766	1.4223
	Average	1.4180 $\pm$ .0016

Table XVII. Stark Effect for HNCO, $v_5 = 1$. (Cal. Tech.)

$\Delta\nu$ (mc)	$(ESU/cm)^2$		$\Delta\nu/E^2$
6.92	4.71	(omit)	1.470
13.58	9.58		1.418
25.59	18.61		1.374
20.10	14.46		1.390
16.35	11.70		1.398
		Average	1.395 ± .006

Table XVIII. Stark Effect for HNCO, $v_6 = 1$. (Cal. Tech.)

$\Delta\nu$ (mc)	$(ESU/cm)^2$		$\Delta\nu/E^2$
20.28	12.15		1.670
13.14	7.88		1.668
12.79	7.67		1.667
29.37	17.82		1.646
15.15	9.18		1.651
26.51	15.82		1.674
11.82	7.01		1.688
13.36	7.87		1.697
16.62	9.94		1.672
		Average	1.670 ± .003

Table XIX. Stark Effect for DNCO in Ground State. (Cal. Tech.)

$\Delta\nu$ (mc)	$(ESU/cm)^2$		$\Delta\nu/E^2$
18.16	11.10		1.635
24.85	16.40		1.515
11.15	6.47	(omit)	1.722
20.89	13.94		1.500
16.05	10.40		1.542
		Average	1.548 ± .021

Table XX. Stark Effect for H_2CO in Ground State. (G.E.)

$\Delta\nu_8$ (mc)	$\Delta\nu_9$ (mc)	$(ESU/cm)^2$	$\Delta\nu_8/E^2$	$\Delta\nu_9/E^2$
13.38	16.86	39.38	.3398	.4282
11.41	14.49	33.72	.3383	.4297
10.09	12.77	29.73	.3394	.4295
8.79	11.10	25.87	.3398	.4291
7.74	9.79	22.66	.3415	.4320
6.67	8.44	19.48	.3424	.4333
5.69	7.13	16.48	.3453	.4327
4.78	6.01	13.81	.3462	.4353
		Average	.3416 ± .0008	.4310 ± .0007

Table XXI. Stark Effect for CHF_3 in Ground State. (G.E.)

$\Delta\nu$ (mc)	$(ESU/cm)^2$	$\Delta\nu/E^2$
12.16	7.59	1.6021
17.12	10.68	1.6049
25.84	16.10	1.6054
32.10	19.80	1.6209
39.48	24.46	1.6138
47.94	29.69	1.6103
	Average	1.6096 ± .0022

Table XXII. Stark Effect for $CF_3C{\equiv}CH$ in Ground State. (C.I.T.)

(mc) $\nu_3 - \nu_2$	(mc) $\nu_3 - \nu_1$	$(ESU/cm)^2$	$\frac{\nu_{M=3} - \nu_{M=2}}{E^2}$	$\frac{\nu_{M=3} - \nu_{M=1}}{E^2}$
12.39	19.82	32.40	.382	.612
9.49	14.77	22.85	.415	.646
7.92	12.47	19.82	.399	.628
6.45	10.30	16.24	.397	.634
		Average	.398 ± .004	.630 ± .004

Table XXIII. Final Values for Dipole Moments

Compound	Vib. State	Rot. Trans.	Freq. (mc)	Dipole Moment (Debye)	Inst.
OCS	Ground	$J = 1 \rightarrow 2$	24,325.9	.712 ± .004	(G.E.)
HNCO	Ground	$J = 0 \rightarrow 1$	21,981.7	1.592 ± .01	(G.E.)
HNCO	Ground	$J = 0 \rightarrow 1$	21,981.7	1.563 ± .02	(C.I.T.)
HNCO	$v_5 = 1$	$J = 0 \rightarrow 1$	22,017.3	1.579 ± .02	(C.I.T.)
HNCO	$v_6 = 1$	$J = 0 \rightarrow 1$	21,993.0	1.726 ± .02	(C.I.T.)
DNCO	Ground	$J = 0 \rightarrow 1$	20,394.7	1.600 ± .04	(C.I.T.)
H_2CO	Ground	$9_{2,8}-9_{2,7}$	22,965.7	2.339 ± .013	(G.E.)
CHF_3	Ground	$J = 0 \rightarrow 1$	20,697	1.645 ± .009	(G.E.)
$CF_3C{\equiv}CH$	Ground	$J = 3 \rightarrow 4$	23,023.4	2.36 ± .04	(C.I.T)

VII. OTHER SUBSTANCES WHICH WERE STUDIED.

Attempts were made to observe the microwave spectra of $(CO)_3CoNO$, $(CH_3)_3N$, and $(HF)_2$ in the hope of obtaining structural information. The procedure and probable reasons for failure will be discussed briefly in each case.

1. $(CO)_3CoNO$.

Cobalt-nitroso-tricarbonyl was prepared after the method of Blanchard, Rafter, and Adams (48). Transitions were expected in the 20,000 to 25,000 mc region for $J = 10 \rightarrow 11$ or $J = 11 \rightarrow 12$. At least one transition should fall in the range covered by the spectroscope. Since the compound is probably a symmetric top, first and second order Stark effects should be observed. Actually, no transitions were found which were attributable to this molecular species. Possible reasons for this are that the compound has such a small dipole moment that the intensity of each transition is small, that the large number of Stark components so splits up the transition that the useful intensity is still further reduced, and that so many vibrational modes are possible that the fraction of molecules in the ground state is small.

2. $(CH_3)_3N$.

Trimethylamine is probably a symmetric top with hindered internal rotation. A search from 20,000 to 25,000 mc revealed no absorption lines due to this compound. The search was complicated by the presence of a very strong NH_3 spectrum, arising entirely from a small amount of ammonia present as an impurity in the $(CH_3)_3N$. The much weaker absorption of $(CH_3)_3N$ was either masked by the strong ammonia spectrum or may possibly fall in the regions adjacent to the region studied.

3. $(HF)_2$.

According to vapor density measurements, HF forms a series of polymers. The dimer may be present in appreciable amount under the most favorable conditions; namely, low temperature and the highest pressure consistent with satisfactory line widths. To test this idea and to obtain structural information about the dimer, a sample of HF was prepared by heating KHF_2 and condensing the HF vapor in equilibrium with it. This sample was placed in a copper bulb and small amounts were admitted into the absorption cell. A very thorough search revealed no absorption lines of any kind. It soon became apparent that difficulties in handling the HF and in monitoring the pressure dictated extensive modifications of the apparatus. Since the heat of dimerization of HF is not accurately known, the prediction concerning the concentration of $(HF)_2$ to be expected may be greatly in error. Consequently, the project was reluctantly abandoned.

VIII. REFERENCES.

(1) C. E. Cleeton and N. H. Williams, Phys. Rev. 45, 234, (1934)

(2) W. Gordy, Rev. Mod. Phys. 20, 668, (1948)

(3) D. K. Coles, Advances in Electronics, II, 299, (1950)

(4) Pauling and Wilson, Introduction to Quantum Mechanics, (McGraw-Hill, 1935)

(5) G. Herzberg, Infrared and Raman Spectra of Polyatomic Molecules, (Van Nostrand, New York, 1945)

(6) S. C. Wang, Phys. Rev. 34, 243, (1929)

(7) H. H. Nielsen, Phys. Rev. 38, 1432, (1931)

(8) R. S. Mulliken, Phys. Rev. 59, 873, (1941)

(9) P. M. Morse, Phys. Rev. 34, 57, (1929)

(10) Z. I. Slawsky and D. M. Dennison, J. Chem. Phys. 7, 509, (1939)

(11) E. B. Wilson, Jr., J. Chem. Phys. 4, 526, (1936)

(12) H. B. G. Casimir, On the Interaction Between Atomic Nuclei and Electrons, (E. F. Bohn, Haarlem, Netherlands, 1936)

(13) C. H. Townes and B. P. Dailey, J. Chem. Phys. 17, 782, (1949)

(14) J. N. Shoolery, R. G. Shulman, and Don M. Yost, J. Chem. Phys. 19, 250, (1951)

(15) R. de L. Kronig, Proc. Nat. Acad. Sci. 12, 608, (1926)

(16) P. C. Cross, R. M. Hainer, and G. W. King, J. Chem. Phys. 12, 210, (1944)

(17) S. Golden and E. B. Wilson, Jr., J. Chem. Phys. 16, 669, (1948)

(18) C. K. Jen, Phys. Rev. 74, 1396, (1948)

(19) J. H. Van Vleck and V. F. Weisskopf, Rev. Mod. Phys. 17, 227, (1945)

(20) J. W. M. Dumond and E. R. Cohen, Report to Nat. Research Council, Dec. (1950)

(21) C. H. Townes, A. H. Holden, and F. R. Merritt, Phys. Rev. 74, 1113, (1948)

(22) R. H. Hughes and E. B. Wilson, Jr., Phys. Rev. 71, 562, (1947)

(23) Miller and Greenblatt, N. D. R. C. Report

(24) R. Karplus, Phys. Rev. 73, 1027, (1948)

(25) R. Unterberger and W. V. Smith, Rev. Sci. Inst. 19, 580, (1948)

(26) P. Kisliuk and C. H. Townes, J. Res. Nat. Bur. Stand. 44, 611, (1950)

(27) C. I. Beard and B. P. Dailey, J. Chem. Phys. 15, 762, (1947)

(28) C. I. Beard and B. P. Dailey, J. Chem. Phys. 18, 1437, (1950)

(29) Werner and Fearon, J. Chem. Soc. 117, 1356, (1920)

(30) Linhard and Betz, Ber. 73B, 177, (1940)

(31) J. Goubeau, Ber. 68, 912, (1939)

(32) L. H. Jones, J. N. Shoolery, R. G. Shulman, and Don M. Yost, J. Chem. Phys. 18, 990, (1950)

(33) G. Herzberg and Verleger, Phys. Z. 37, 444, (1936)

(34) Eyster, Gillette, and Brockway, J. Am. Chem. Soc. 62, 3236, (1940)

(35) C. Reid, J.Chem. Phys. 18, 1544, (1950)

(36) J. K. Bragg, Phys. Rev. 74, 533, (1948)

(37) H. E. White, Introduction to Atomic Spectra (McGraw-Hill, New York, 1934) p. 439

(38) J. W. Simmons, W. E. Anderson, and W. Gordy, Phys. Rev. 77, 77, (1950)

(39) A. V. Smith, H. Ring, W. V. Smith, and W. Gordy, Phys. Rev. 74, 310, (1948)

(40) L. Pauling, The Nature of the Chemical Bond, (Cornell University Press, Second edition, 1945)

(41) R. Trambarulo and W. Gordy, J. Chem. Phys. 18, 1613, (1950)

(42) Westenberg and Wilson, J. Am. Chem. Soc. 72, 199, (1950)

(43) Westenberg, Goldstein, and Wilson, J. Chem. Phys. 17, 1319, (1949)

(44) W. E. Anderson, R. Trambarulo, J. Sheridan, and W. Gordy, Phys. Rev. 82, 58, (1951)

(45) H. H. Nielsen, Phys. Rev. 77, 130, (1950)

(46) R. G. Shulman and C. H. Townes, Phys. Rev. 77, 500, (1950)

(47) G. W. King, R. M. Hainer, and P. C. Cross, J. Chem. Phys. 11, 27, (1943)

(48) Blanchard, Rafter, and Adams, J. Am. Chem. Soc. 56, 16, (1934)

APPENDIX I.

Consider a molecule of mass M with a figure axis Y. Change mass A to A', allowing no other changes except the change in zero point vibrations resulting in a small change of all effective distances.

If the molecule were not vibrating, $z_o = z_o' = z_e$, where z_e is the equilibrium distance. The isotopic substitution would result in the expression

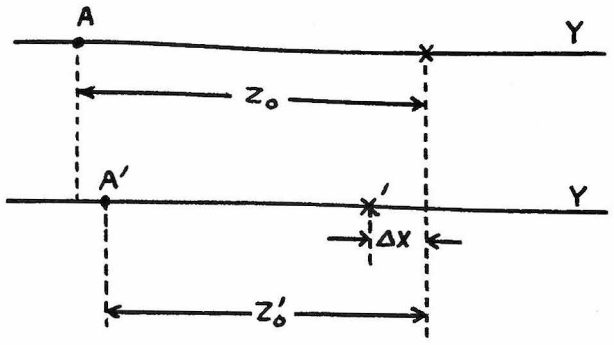

$$\Delta m z_e = (M + \Delta m)\,\Delta x . \quad (1)$$

Conservation of linear momentum requires that this expression hold for the vibrating molecule as well.

Let ΔI be the difference between I measured for the original molecule and I for the original if it had the zero point amplitude of the substituted molecule.

The moment of inertia, I', of the new molecule about x', the new center of mass, is equal to the moment of the new molecule about the old center of mass minus $(M + \Delta m)\,\Delta x^2$.

$$I' = I + \Delta I + \Delta m z_o'^2 - (M + \Delta m)\,\Delta m^2 z_e^2/(M + \Delta m)^2 .$$

$$(M + \Delta m)(I' - I - \Delta I) = M\,\Delta m z_o'^2 + \Delta m^2 (z_o'^2 - z_e^2) .$$

If $z_o' = z_e + \Delta z$, (Δz is generally less than .01 A)

$$z_o'^2 = \left\{ I' - I - \Delta I - \frac{\Delta m^2 (2 z_e \Delta z + \Delta z^2)}{M + \Delta m} \right\} (M + \Delta m)/M\,\Delta m .$$

In the case of OCS, neglect of the fourth term in brackets would introduce an error of only .0003 Å in the distance of the sulfur atom from the center of mass. It is an order of magnitude smaller than the

Δ I term, hence we write

$$z_o' = (I' - I - \Delta I)(M + \Delta m)/M \Delta m \ .$$

BLOCK DIAGRAM OF MICROWAVE SPECTROMETER

FIGURE 1

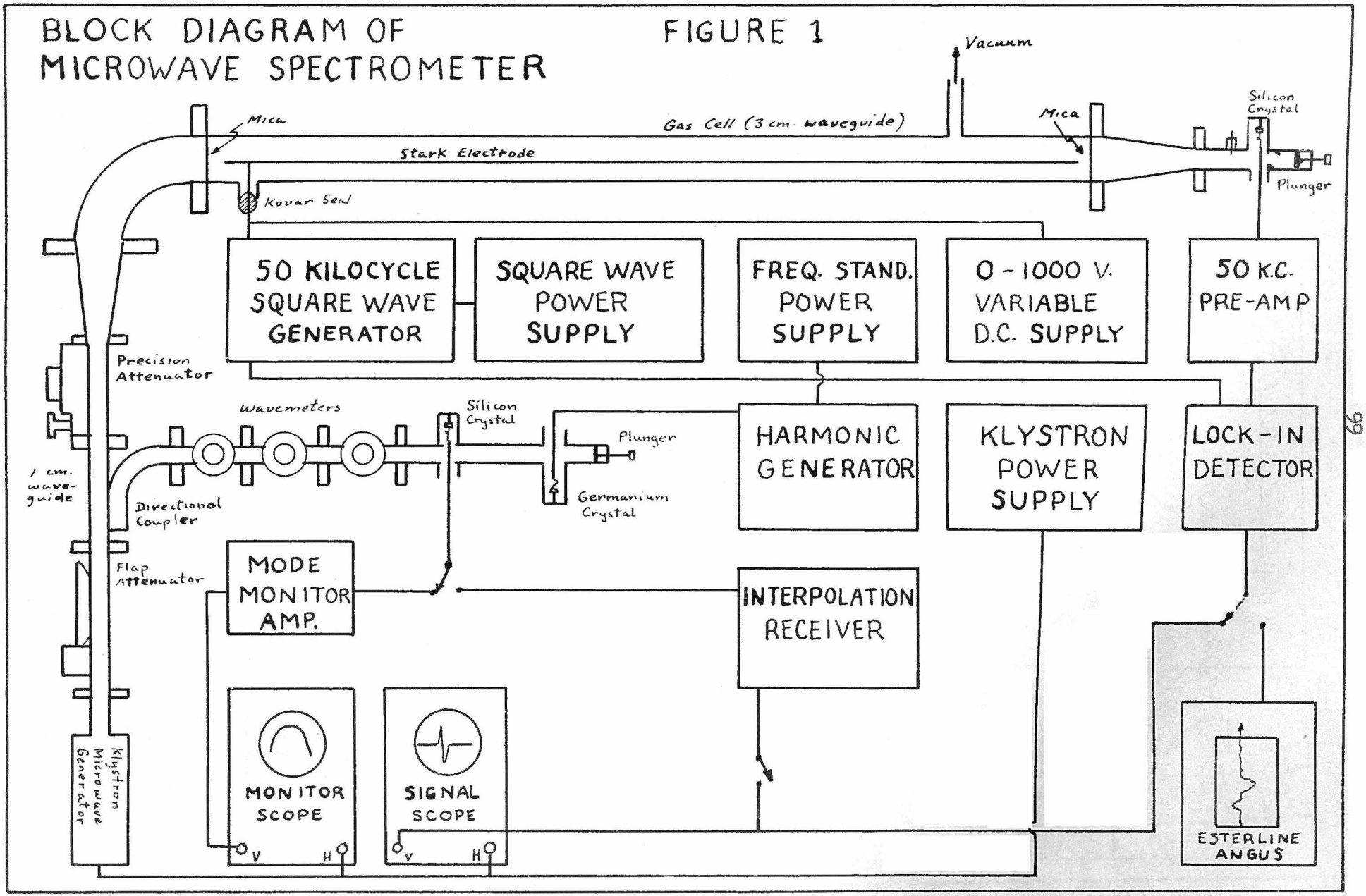

LOW VOLTAGE KLYSTRON POWER SUPPLY

FIGURE 2

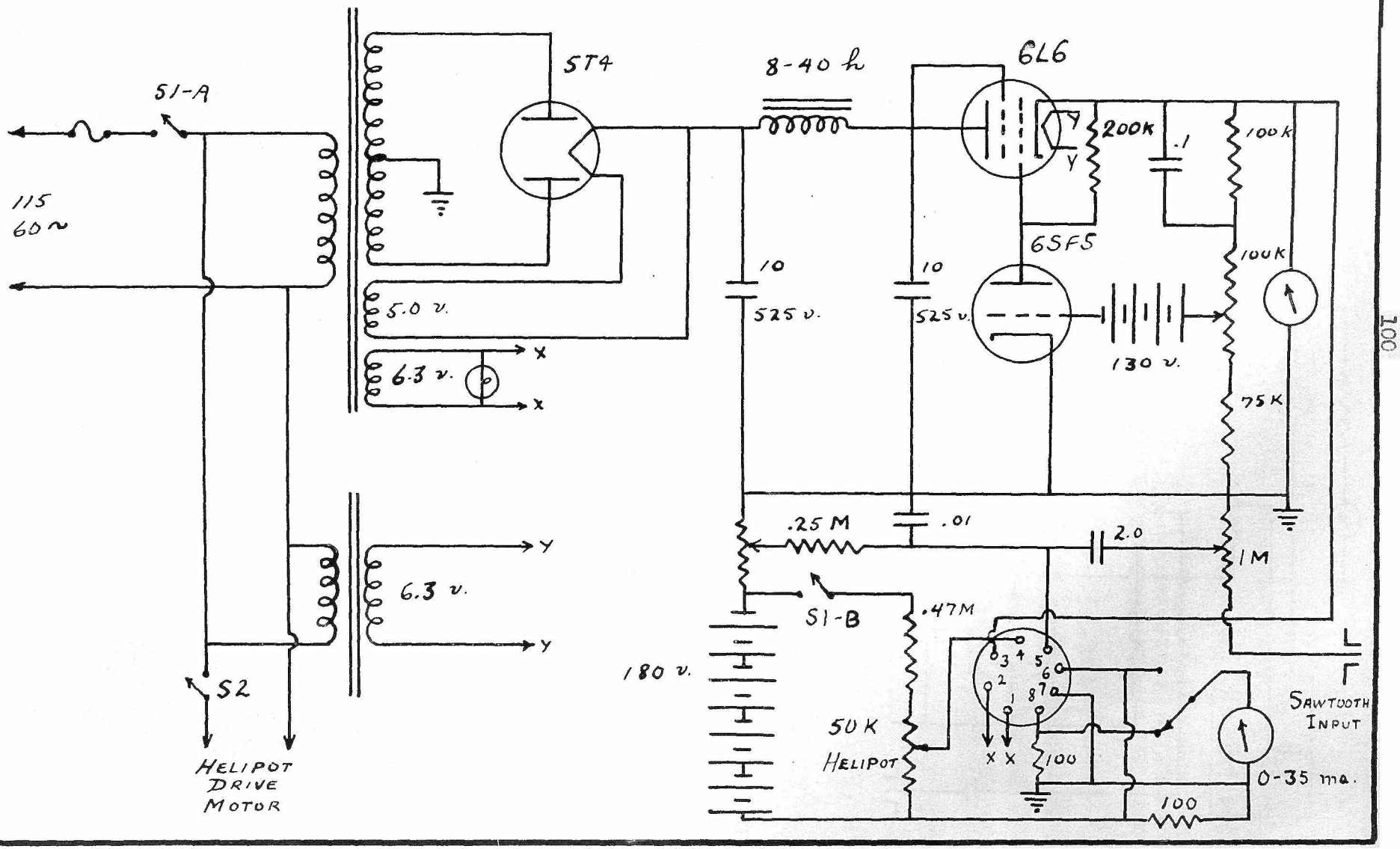

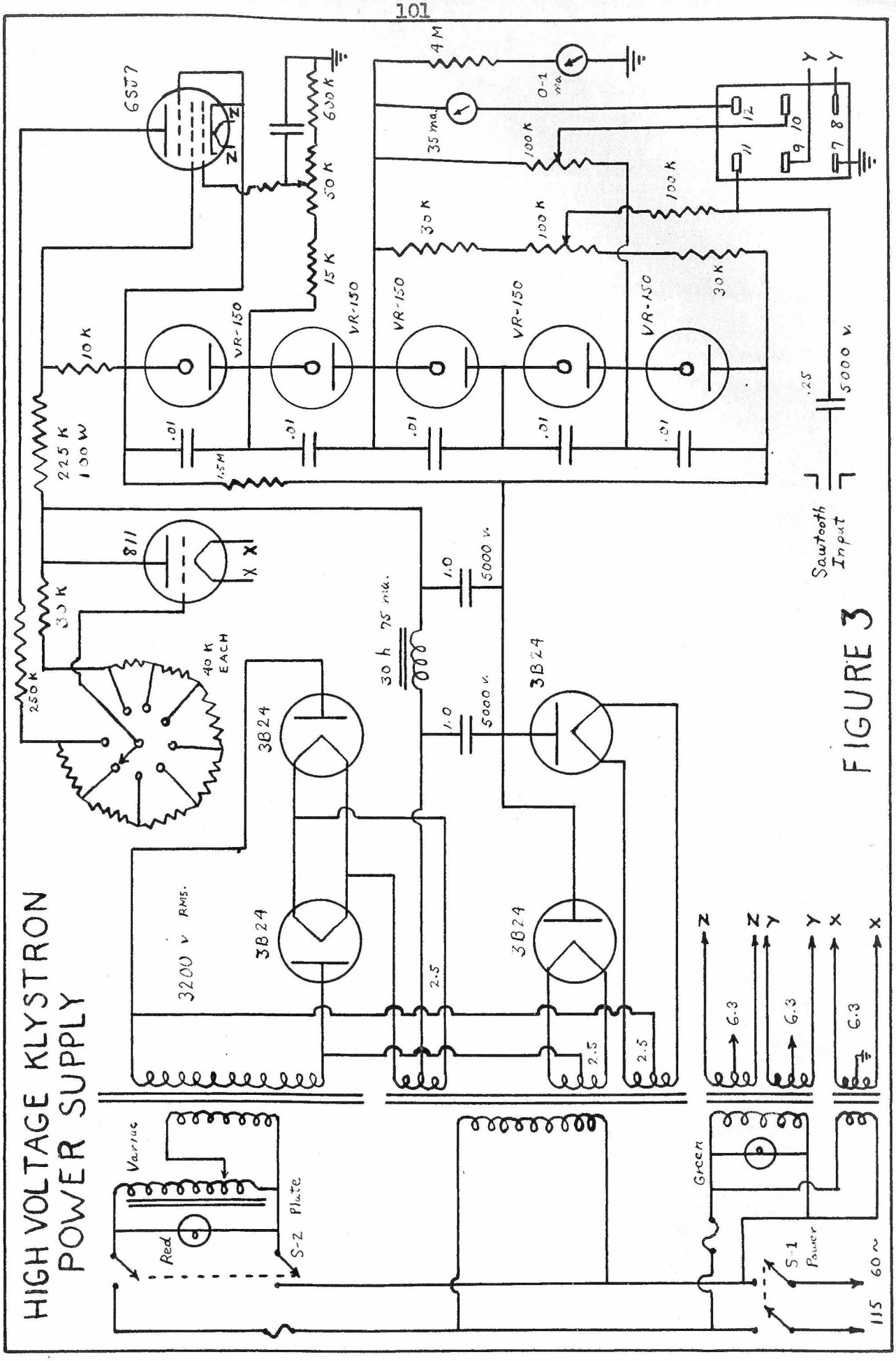
HIGH VOLTAGE KLYSTRON
POWER SUPPLY
6SJ7
811
VR-150
VR-150
VR-150
VR-150
VR-150
10 K
225 K
100 W
15 K
50 K
600 K
30 K
100 K
100 K
30 K
4 M
0-1 ma
35 ma.
.01
.01
.01
.01
.01
1.5 M
.25
5000 v.
Sawtooth
Input
230 K
30 K
40 K
EACH
30 h 75 ma.
1.0
5000 v.
1.0
5000 v.
3B24
3B24
3B24
3B24
3200 v RMS.
2.5
2.5
2.5
6.3
6.3
6.3
Variac
Red
S-2 Plate
Green
S-1
Power
115 60~

FIGURE 3

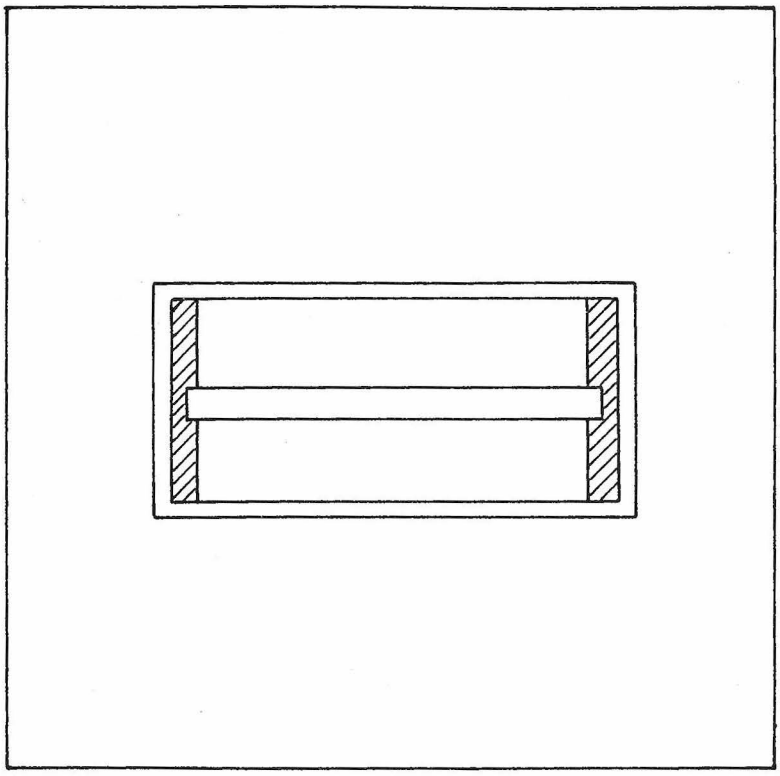

CROSS SECTION OF CELL

FIGURE 4

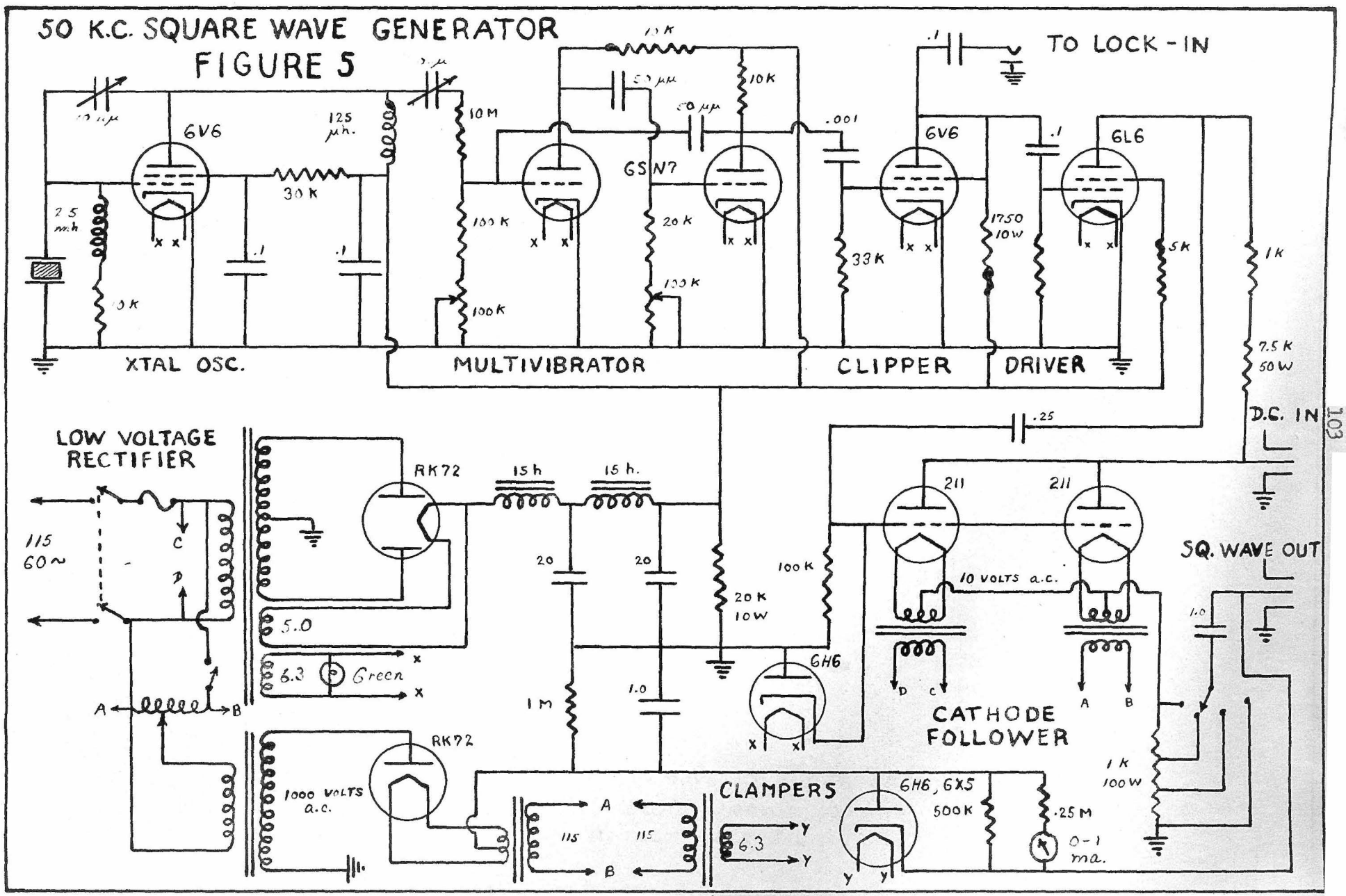
50 K.C. SQUARE WAVE GENERATOR
FIGURE 5
TO LOCK-IN
6V6
125 μh.
30 K
10 M
100 K
100K
6SN7
50 μμ
10K
.001
33K
6V6
.1
6L6
1750 10W
5K
1K
7.5 K 50W
D.C. IN
XTAL OSC.
MULTIVIBRATOR
CLIPPER
DRIVER
LOW VOLTAGE RECTIFIER
115 60~
RK72
15 h
15 h.
20
20
5.0
6.3
Green
1 M
1.0
20 K 10W
100 K
6H6
.25
211
211
10 VOLTS a.c.
SQ. WAVE OUT
CATHODE FOLLOWER
1.0
1 K 100W
RK72
1000 VOLTS a.c.
CLAMPERS
6H6, 6X5
500K
.25 M
0-1 ma.
115
6.3

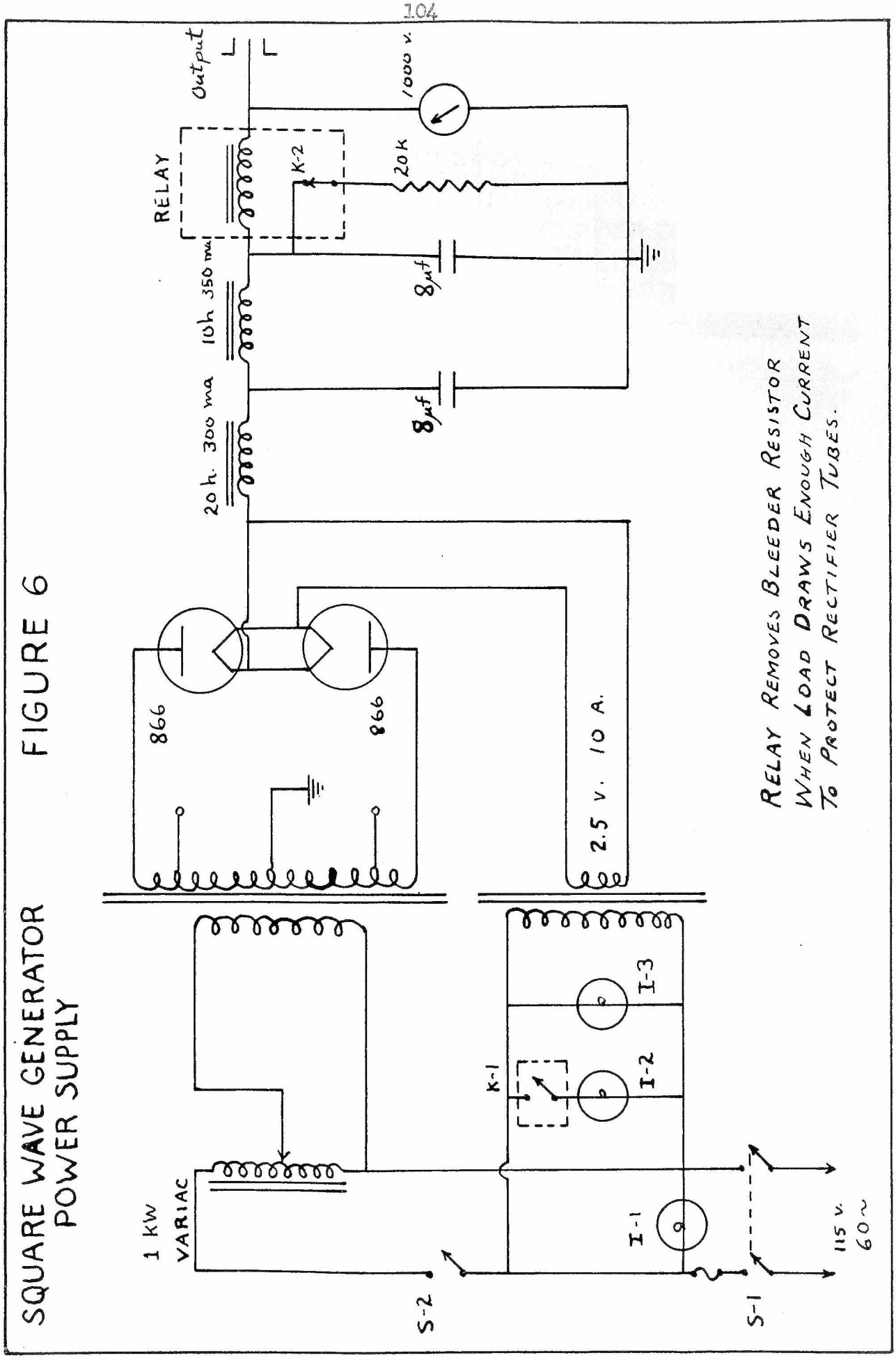
SQUARE WAVE GENERATOR
POWER SUPPLY
FIGURE 6
Output
1000 v.
RELAY
K-2
20 K
10h 350 ma
8 µf
20 h. 300 ma
8 µf
866
866
2.5 v. 10 A.
1 KW
VARIAC
K-1
I-3
I-2
I-1
S-2
S-1
115 v.
60 ~
RELAY REMOVES BLEEDER RESISTOR
WHEN LOAD DRAWS ENOUGH CURRENT
TO PROTECT RECTIFIER TUBES.

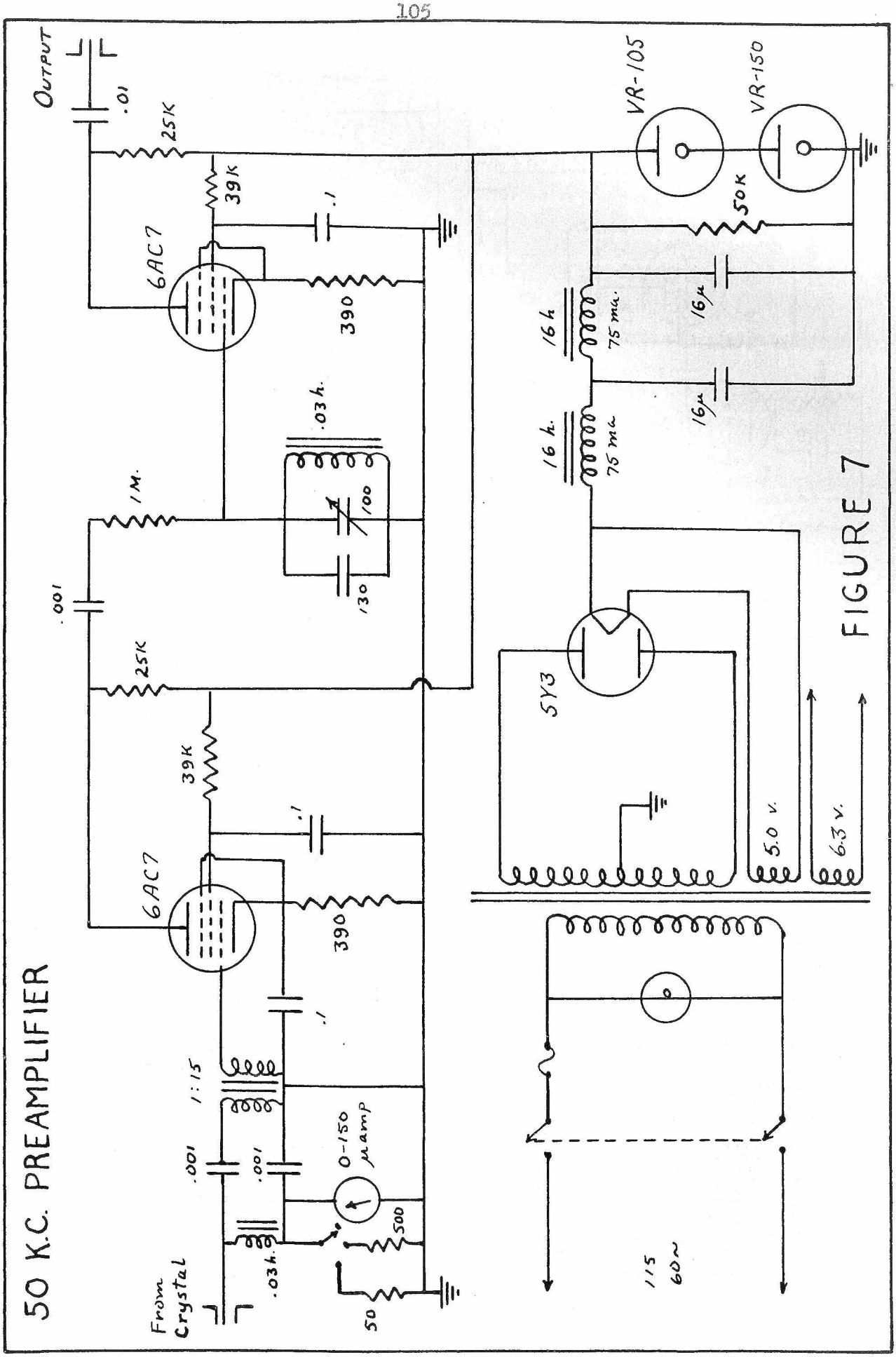
50 K.C. PREAMPLIFIER
From Crystal
.034.
.001
.001
1:15
.1
.001
25K
1M.
6AC7
390
.1
39K
.03 h.
100
130
.01
Output
25K
39K
6AC7
390
.1
50
500
0-150 μamp
VR-105
VR-150
50K
16 h.
75 ma.
16 h.
75 ma
16μ
16μ
5Y3
5.0 v.
6.3 v.
115
60~

FIGURE 7

LOCK-IN DETECTOR AND PHASE SHIFTER

FIGURE 8

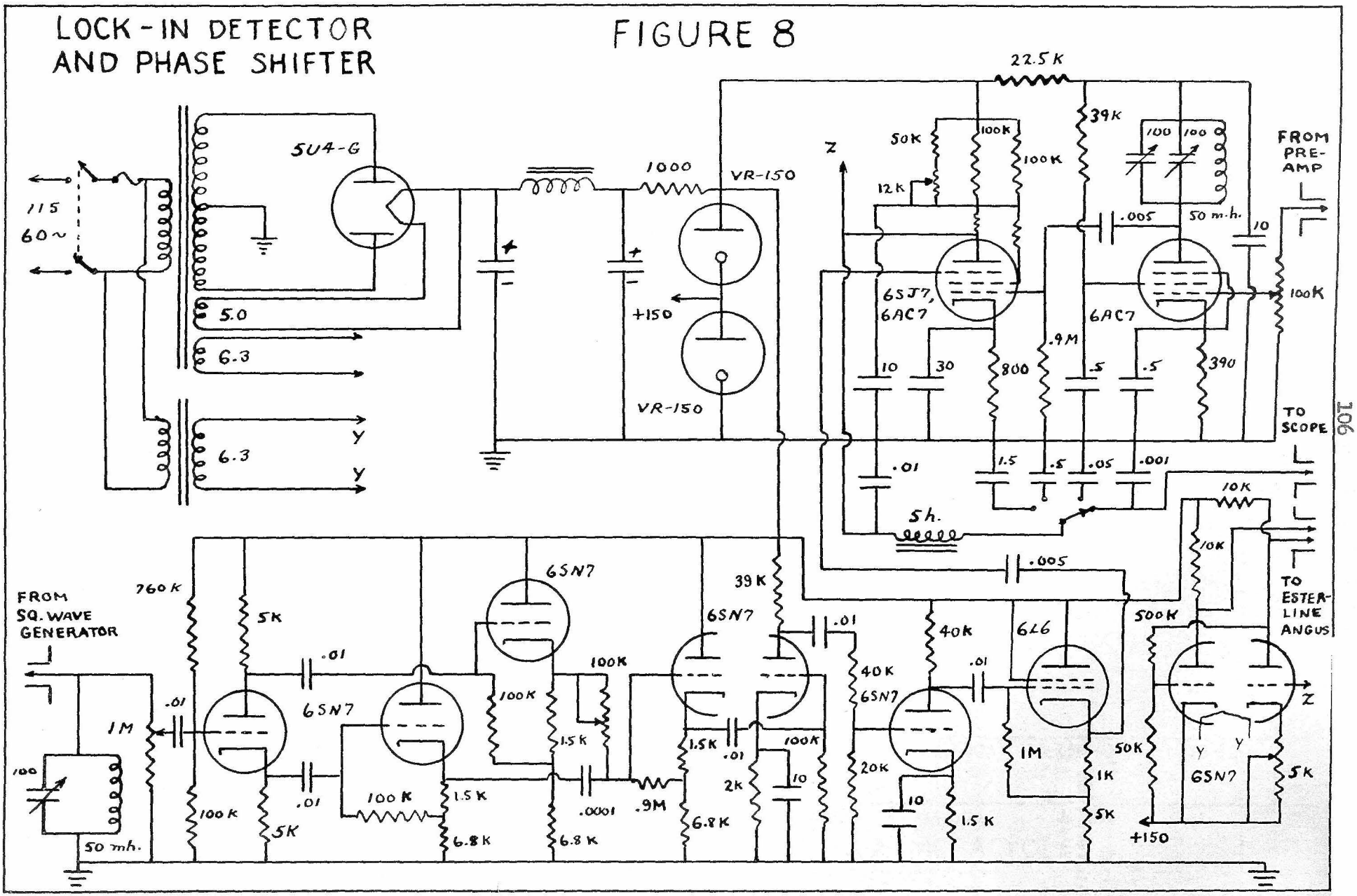

FIGURE 9

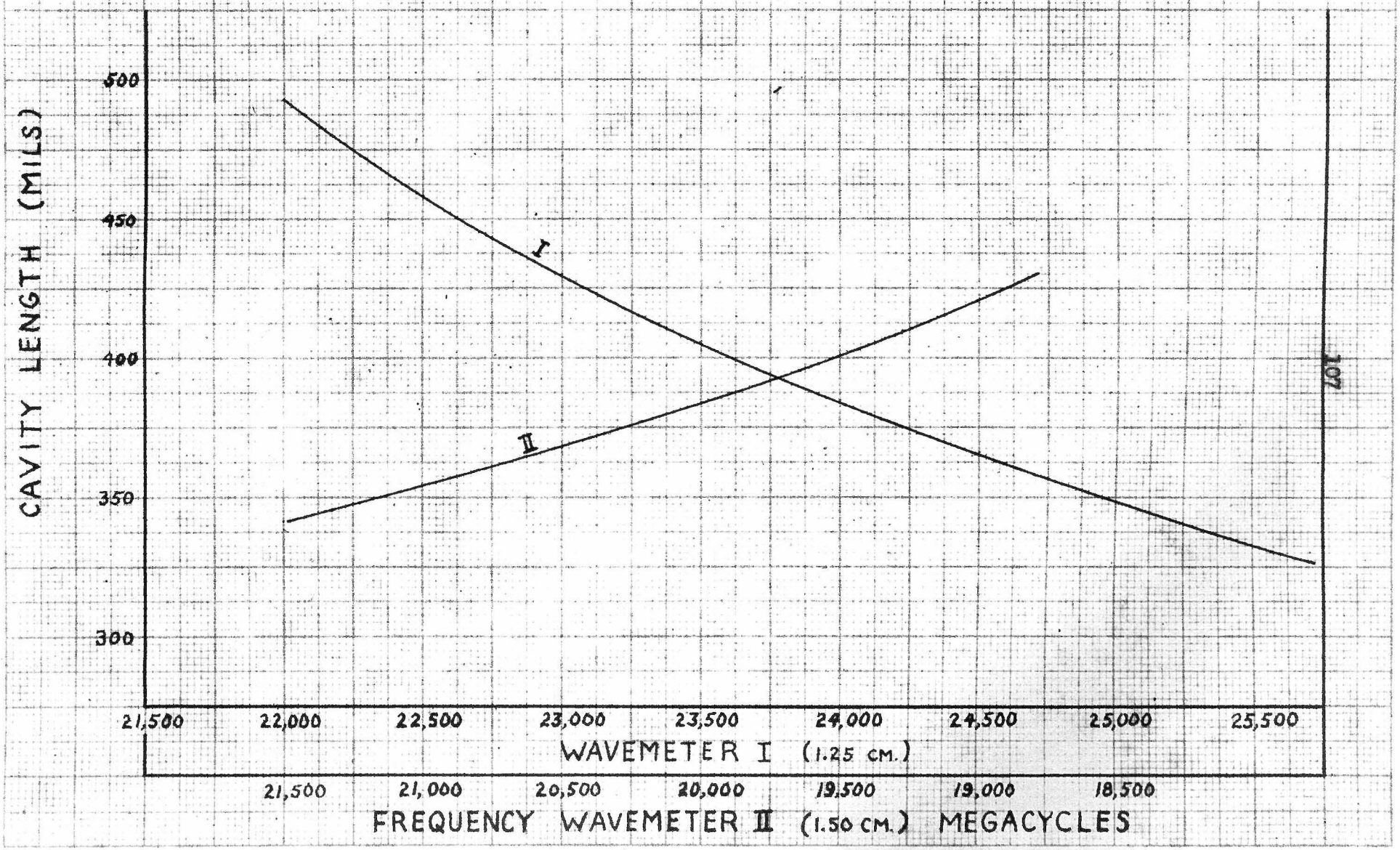
CAVITY LENGTH (MILS)
500
450
400
350
300
I
II
107
21,500
22,000
22,500
23,000
23,500
24,000
24,500
25,000
25,500
WAVEMETER I (1.25 CM.)
21,500
21,000
20,500
20,000
19,500
19,000
18,500
FREQUENCY WAVEMETER II (1.50 CM.) MEGACYCLES

MODE MONITOR AMPLIFIER

FIGURE 10

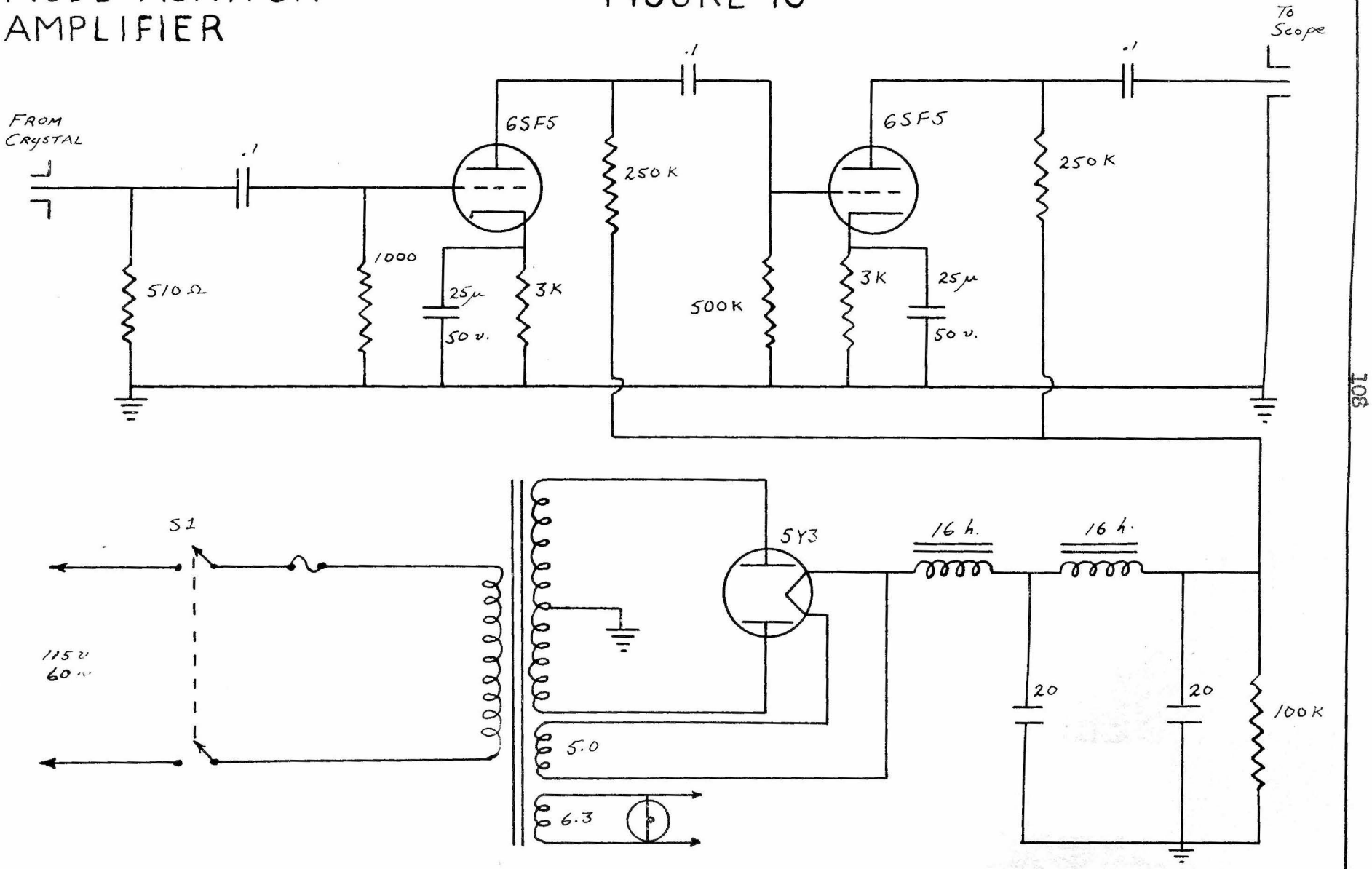

STANDARD FREQUENCY MULTIPLIER FIGURE 11

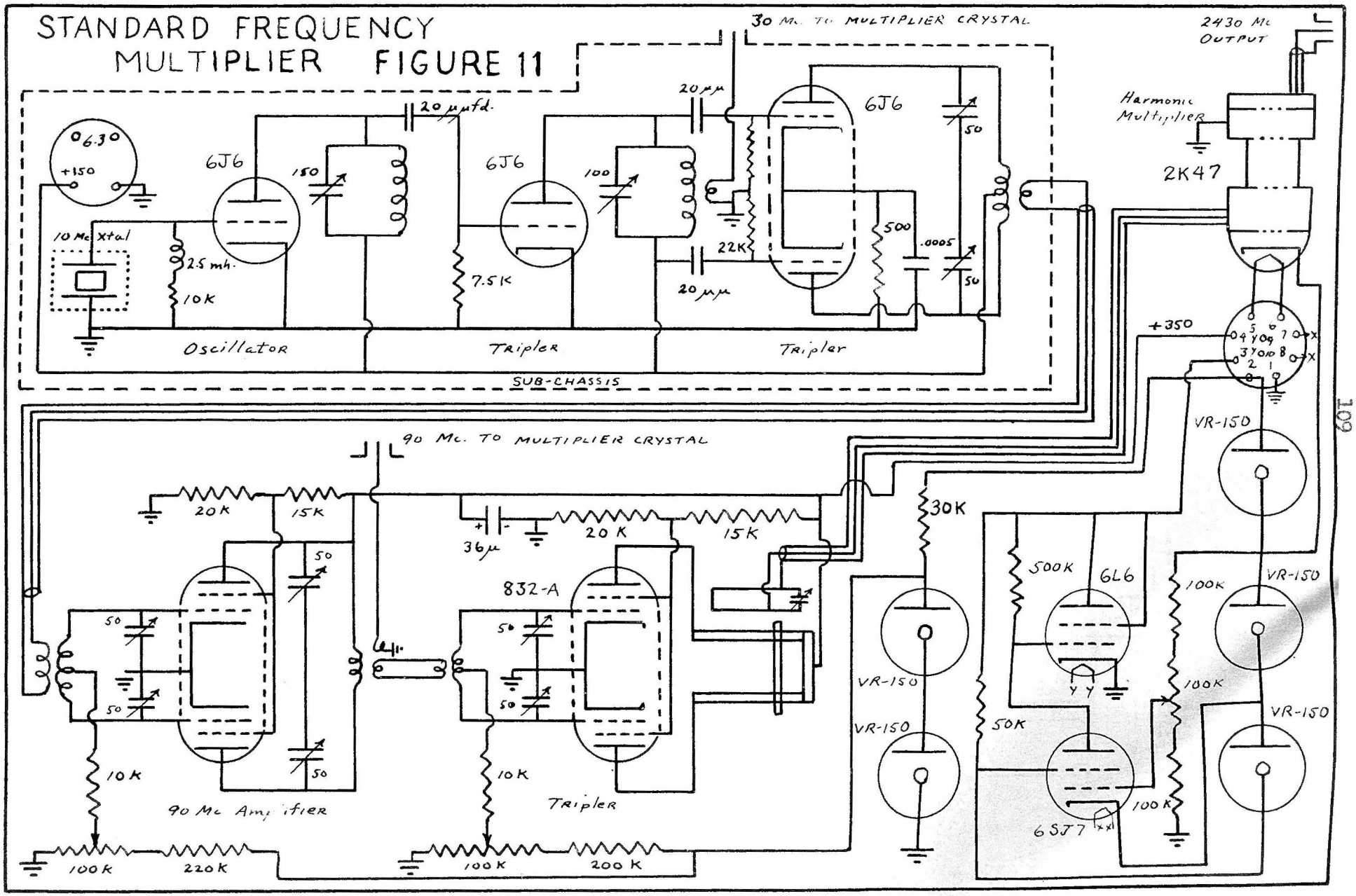

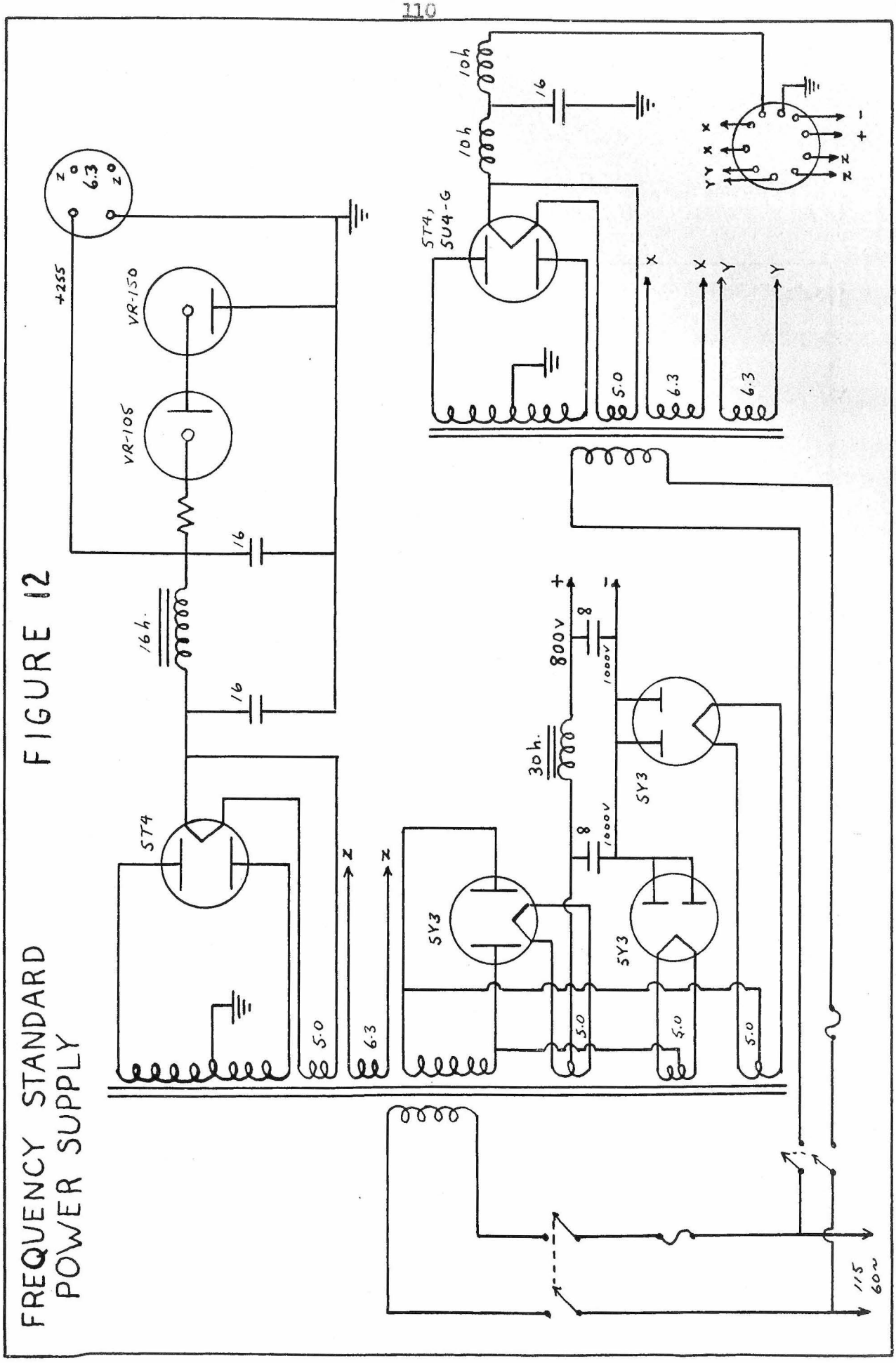
FREQUENCY STANDARD
POWER SUPPLY
FIGURE 12
115
60~
ST4
ST4,
SU4-G
SY3
VR-150
VR-105
+255
800v
1000v
16
8
10h.
16h.
30h.
5.0
6.3
X
Y
Z

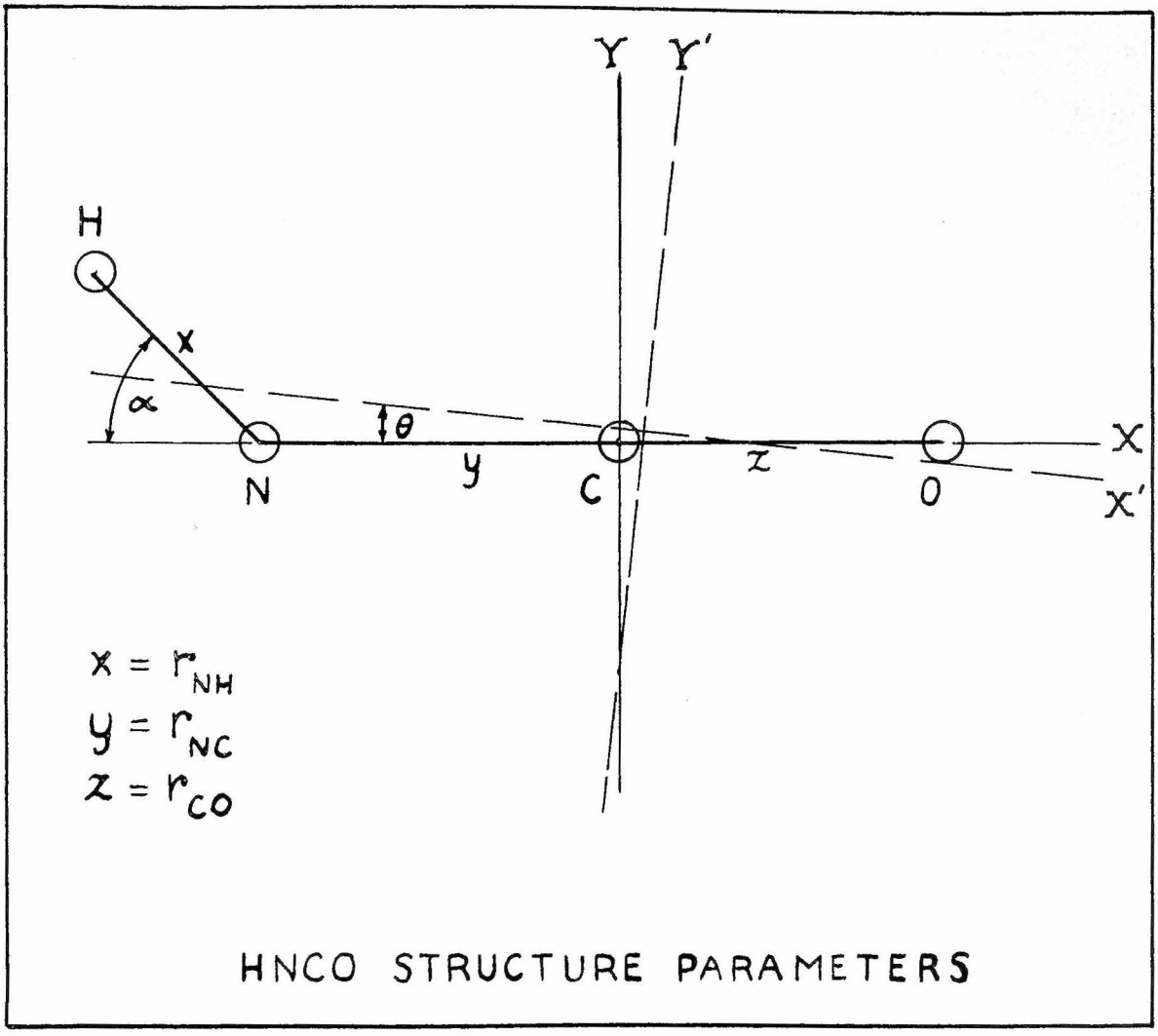

FIGURE 13

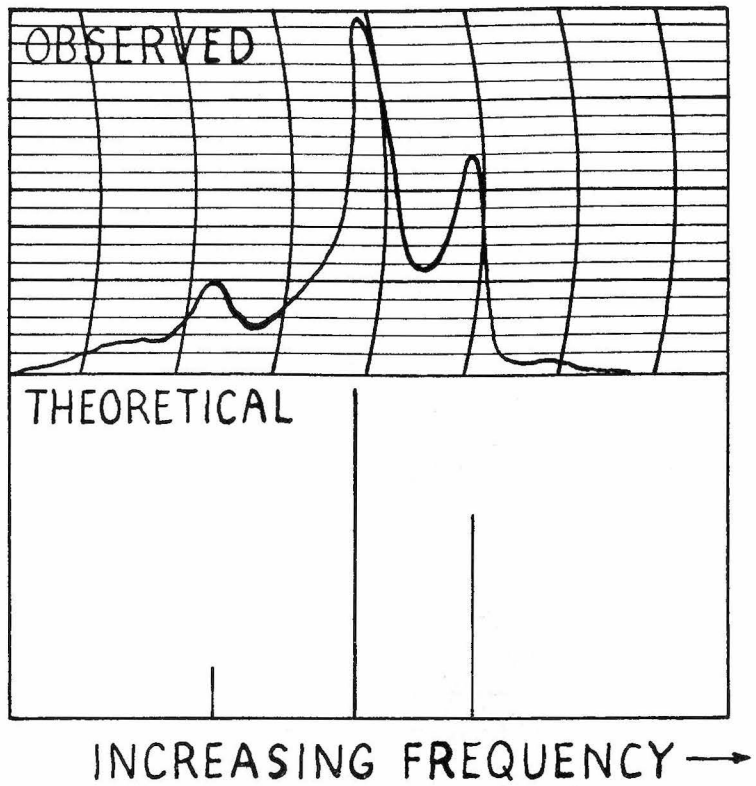
OBSERVED
THEORETICAL
INCREASING FREQUENCY →

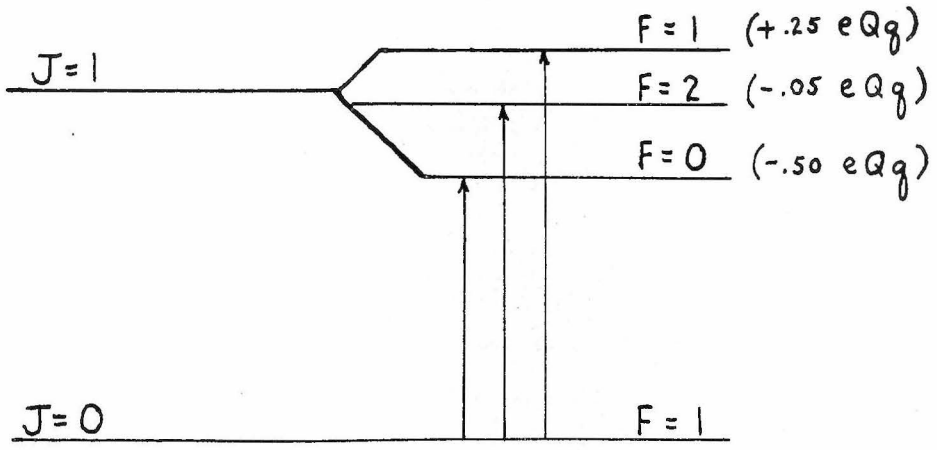
J = 1
J = 0
F = 1 (+.25 eQq)
F = 2 (-.05 eQq)
F = 0 (-.50 eQq)
F = 1

FIGURE 14

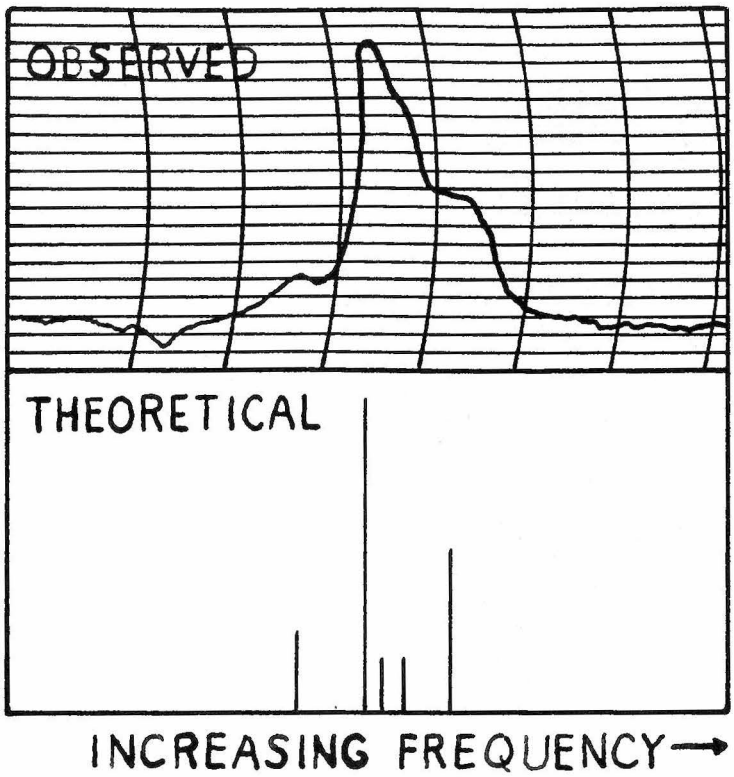
OBSERVED
THEORETICAL
INCREASING FREQUENCY

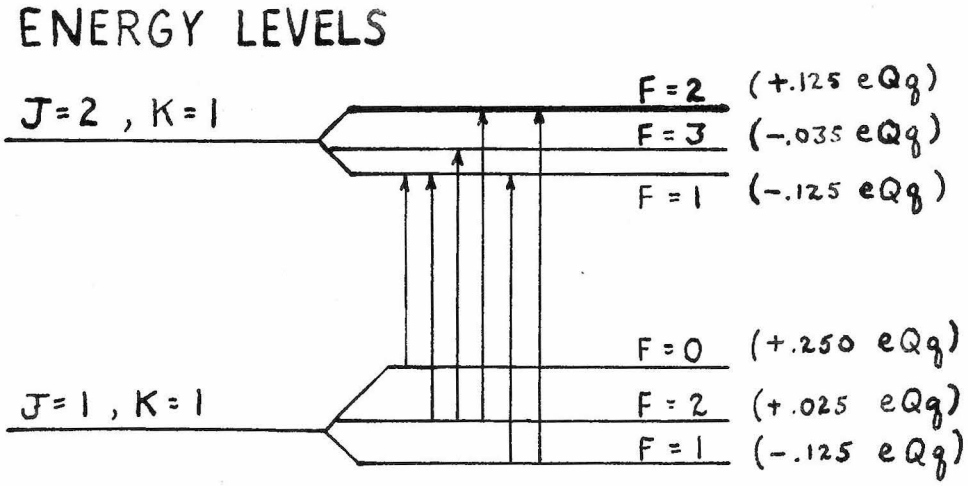
ENERGY LEVELS
J=2 , K=1
F=2 (+.125 eQq)
F=3 (-.035 eQq)
F=1 (-.125 eQq)
F=0 (+.250 eQq)
J=1 , K=1
F=2 (+.025 eQq)
F=1 (-.125 eQq)

FIGURE 15

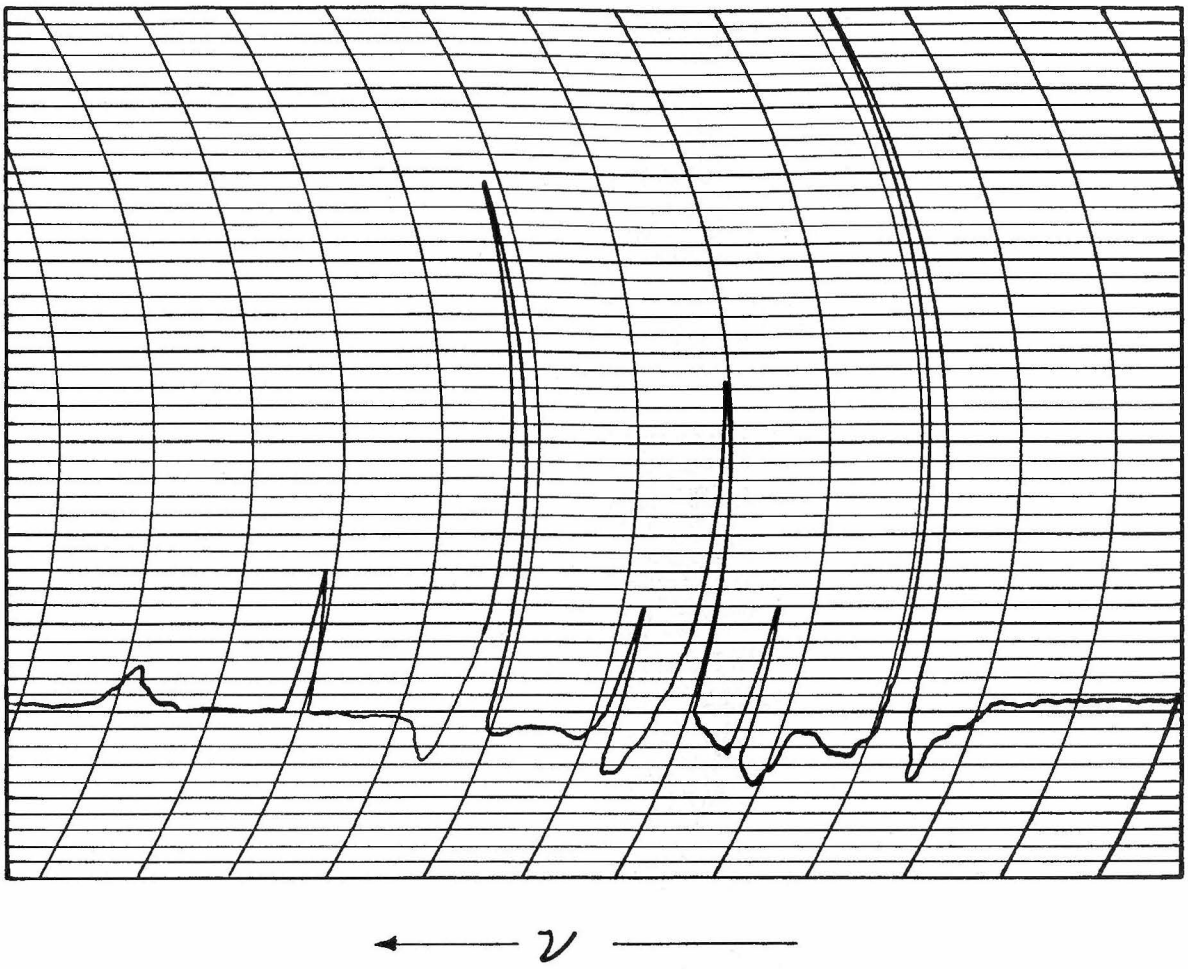

FIGURE 16

FIGURE 17

$-C \equiv C-$	1.201 A°
$-C-H$	1.056 A°

FIGURE 18

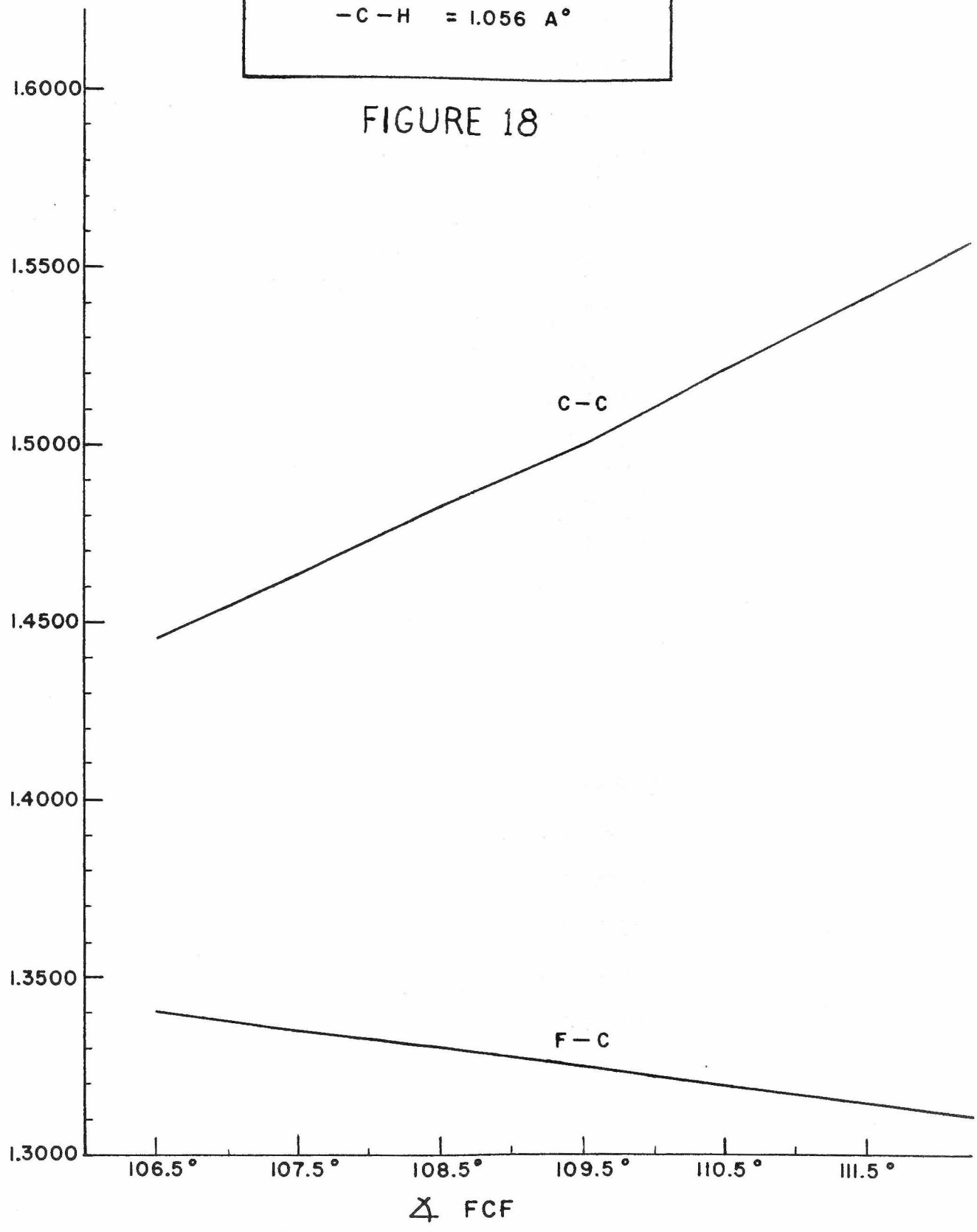

Propositions

1. G. Groetzinger (1) claims that the thermal conductivity of a dielectric material increases by as much as 70 percent when it is made into an electret. He suggests that the inhomogeneous fields employed partially resolve a mixture such as beeswax into components with different dielectric constants and thermal conductivities. I propose that application of the thermodynamic equations for a system in an electric field will show an insignificant amount of sorting for components whose dielectric constants differ by any reasonable amount for fields attainable in such experiments.

2. The non-existence of HOCN (2) in the vapor phase, even at low temperatures, casts some doubt on the keto-enol tautomerism proposed by Werner (3) to account for the fact that the liquid obtained by depolymerizing cyanuric acid polymerizes to a mixture of cyamelide and cyanuric acid, cyamelide being the main product (60%) at 0° C, and cyanuric acid predominating (60%) at 20° C. I propose that this experimental fact may be explained by assuming that the single species HNCO may engage in either of two reactions:

$$\text{I. } 3\text{HNCO} \longrightarrow \text{cyanuric acid}$$

$$\text{II. } 3\ \text{HNCO} \longrightarrow \text{cyamelide}$$

for which the activation energy would be required to be 6.5 Kcal higher for I than II, but the probability of being in a configuration capable of reacting would be 10^5 less for II than I.

3. The component of the dipole moment along the principal axis of least moment of inertia for HNCO and HNCS has been measured (4,5) and found to be 1.59 and 1.72 Debye units respectively. Since oxygen

is much more electronegative than sulfur, one would expect HNCO to have the larger electric dipole moment on the basis of electronegativities alone. I propose that the additional charge separation in HNCS may be considered to arise from a predominance of one formal resonating structure over another, whereas in HNCO the contributions of such structures cancel each other.

4. A recent structure determination for OCSe (6) by microwave spectroscopy lists the probable error in the bond distances as .0001 Å. This figure was obtained from the consistency of the OC and CSe distances computed from moment of inertia measurements for two separate pairs of molecules containing the isotopes

$$O^{16}C^{12}Se^{78} \quad O^{16}C^{13}Se^{78}$$

and

$$O^{16}C^{12}Se^{80} \quad O^{16}C^{13}Se^{80}$$

It is proposed that

a. These pairs represent a particularly unfortunate choice for comparison because they would result in large but similar computational errors.

b. Comparison with distances computed from the isotopic pair $O^{16}C^{12}Se^{78}$ - $O^{16}C^{12}Se^{80}$ would bring to light a discrepancy considerably in excess of the error quoted.

5. Certain experimental investigations, e.g., nuclear magnetic resonance absorption experiments, call for a gradual linear change in a magnetic field. I propose the following circuit for this application.

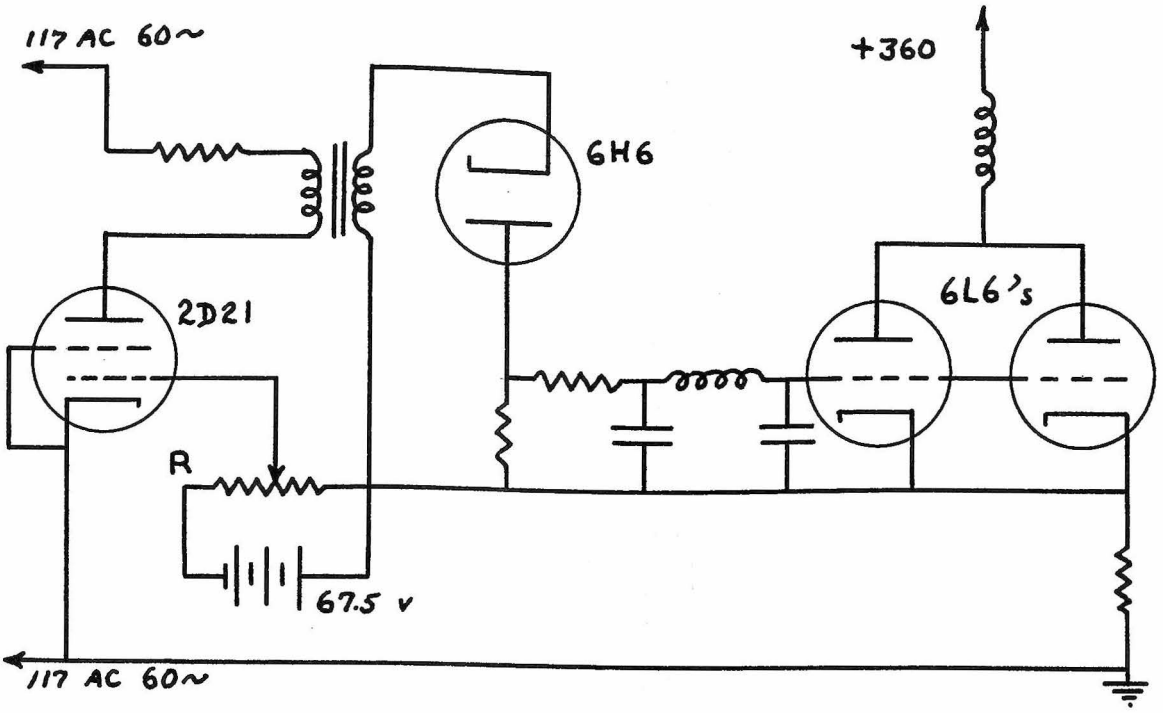

R is a motor driven helical potentiometer.

6. a. Formyl chloride has often been proposed as an intermediate in various reactions involving mixtures of CO and HCl. It appears to form a stable addition compound with $AlCl_3$. At low temperatures there may conceivably be a small concentration of HCOCl in equilibrium with CO and HCl. One might test this hypothesis by putting pure CO and HCl (observed to give no absorption below 100 kmc) into a waveguide and looking for absorption lines of the asymmetric rotor HCOCl.

b. A similar experiment could be performed with BF_3 and HF in order to test for the existence of fluoboric acid, HBF_4, in the vapor phase.

7. Microwave studies of the symmetric top $CF_3-C\equiv C-CH_3$ would be interesting because of the almost completely unhindered rotation about the figure axis of the CF_3 and CH_3 groups relative to one another. This would permit independent quantization of the angular momentum for each

of these groups along the figure axis and could be observed through the effect of centrifugal stretching on the large moment of inertia.

8. The reaction between isocyanates and diazomethane should be investigated. It is suggested that triazolones could be prepared in this way.

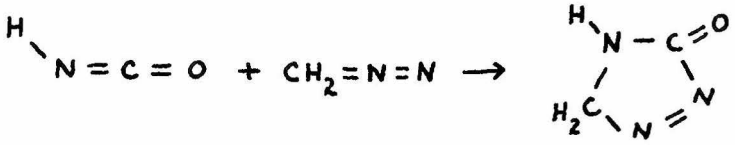

The reaction could be generalized to include substituted triazolones.

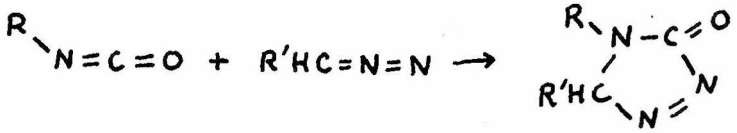

9. A method of removing the last traces of water from NH_3 gas is proposed. The very efficient drying agents P_2O_5 and $Mg(ClO_4)_2$ would not be satisfactory for this purpose since P_2O_5 is acidic and $Mg(ClO_4)_2$ absorbs NH_3. The free energy of the reaction

$$NaNH_2 + H_2O = NaOH + NH_3 \qquad \Delta F \approx -20 \text{ Kcal}$$

is large enough that the equilibrium would lie almost completely to the right; consequently, sodamide would serve as a satisfactory drying agent.

10. The structure of nitryl chloride is unknown. Two types of bonding may be proposed, leading to the following structures.

A. 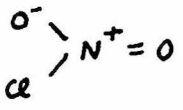

B. 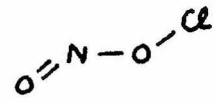

a. The microwave spectrum of this substance should be obtained and analyzed.

b. Measurements of the nitrogen quadrupole coupling constant would probably allow a choice between structures A and B to be made.

References

(1) G. Groetzinger, Phys. Zeit. 37, 589, (1936)

(2) L. H. Jones, J. N. Shoolery, R. G. Shulman, and Don M. Yost, J. Chem. Phys. 18, 990, (1950)

(3) Werner, J. Chem. Soc. 103, 1010, (1913)

(4) J. N. Shoolery, R. G. Shulman, and Don M. Yost, J. Chem. Phys., 19, 250, (1951)

(5) C. I. Beard and B. P. Dailey, J. Chem. Phys. 15, 762, (1947)

(6) Strandberg, Wentink, and Hill, Phys. Rev. 75, 827, (1949)